INFORMATION TO USERS

This manuscript has been reproduced from the microfilm master. UMI films the text directly from the original or copy submitted. Thus, some thesis and dissertation copies are in typewriter face, while others may be from any type of computer printer.

The quality of this reproduction is dependent upon the quality of the copy submitted. Broken or indistinct print, colored or poor quality illustrations and photographs, print bleedthrough, substandard margins, and improper alignment can adversely affect reproduction.

In the unlikely event that the author did not send UMI a complete manuscript and there are missing pages, these will be noted. Also, if unauthorized copyright material had to be removed, a note will indicate the deletion.

Oversize materials (e.g., maps, drawings, charts) are reproduced by sectioning the original, beginning at the upper left-hand corner and continuing from left to right in equal sections with small overlaps.

Photographs included in the original manuscript have been reproduced xerographically in this copy. Higher quality 6" x 9" black and white photographic prints are available for any photographs or illustrations appearing in this copy for an additional charge. Contact UMI directly to order.

Bell & Howell Information and Learning
300 North Zeeb Road, Ann Arbor, MI 48106-1346 USA
800-521-0600

Adrenergic Modulation of Neurotransmission in the Intracardiac Nervous System of the Guinea-Pig

by

James P. Leger

Submitted in partial fulfilment of the requirements for the degree of Doctor of Philosophy in Anatomy and Neurobiology/Neuroscience

at

Dalhousie University

Halifax, Nova Scotia

September, 1999

DALHOUSIE UNIVERSITY

FACULTY OF GRADUATE STUDIES

The undersigned hereby certify that they have read and recommend to the Faculty of Graduate Studies for acceptance a thesis entitled "Adrenergic Modulation of Neurotransmission in the Intracardiac Nervous System of the Guinea-Pig"

by James Leger

in partial fulfillment of the requirements for the degree of Doctor of Philosophy.

Dated: August 24, 1999

External Examiner

Research Supervisor

Examining Committee

Copyright Agreement

Dalhousie University

DATE: September 6, 1999

AUTHOR: James P. Leger

TITLE: Adrenergic modulation of neurotransmission in the intracardiac nervous system of the guinea-pig.

DEPARTMENT OR SCHOOL: Department of Anatomy and Neurobiology

DEGREE: Doctor of Phylosophy CONVOCATION: October YEAR: 1999

Permission is herewith granted to Dalhousie University to circulate and have copied for non-commercial purposes, at its discretion, the above title upon request of individuals or institutions.

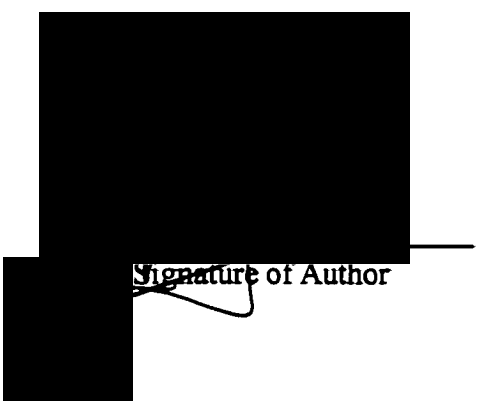

The author reserves other publication rights, and neither the thesis nor extensive extracts from it may be printed or otherwise reproduced without the author's written permission.

The author attests that permission has been obtained for the use of any copyrighted material appearing in this thesis (other than brief excerpts requiring only proper acknowledgement in scholarly writing), and that all such use is clearly acknowledged.

I dedicate this thesis to my family: to my mother, Sharron, who often referred to me as "the little professor" or more often as "the absent minded professor", I have lived up to both names intentionally or otherwise; to my brother, Bern, whose good nature tolerated the experiments involving his toys which I could never reassemble; and to my grandmother, Margarete Smith, who like a second mother, was always concerned for my education and taught me an important lesson, "that a job worth doing, was worth doing right". Their support and encouragement have lead me to this point in my life. I also would like to dedicate this thesis to the newest member of my family, my wife Andrea, whose wit and charm encouraged me to continue on those days when no experiment worked.

Table of Contents

List of Figures

List of Tables

Abstract

Neurons within the mammalian heart are connected into a neural network which functions in regional and global control of cardiodynamics. There is anatomical and functional evidence for the presence of adrenergic terminals surrounding some intracardiac neurons but the function of these terminals is not clear. The focus of this thesis is to investigate the anatomical distribution of adrenergic elements within the intracardiac nervous system, and determining the influence of adrenergic agents on neurotransmission in this system in the guinea-pig heart. Immunohistochemical processing for tyrosine hydroxylase (TH) and histochemistry for aldehyde-induced fluorescence showed that no neuronal somata contained TH or detectable levels of amines. Amine-containing terminals and small cells (less than 11 μm diameter) were found throughout the atria; many of these elements were associated with ganglionic neurons. The presence of adrenergic terminals in intracardiac ganglia is hypothesized to represent potential sites for adrenergic modulation of ganglionic neurotransmission.

To evaluate the effects of adrenergic agents on ganglionic neurotransmission, an *in vitro* preparation of guinea-pig atria including attached extrinsic innervation was developed and its viability confirmed. This preparation was then used in intracellular electrophysiological studies of the properties of intracardiac neurons and the influence of adrenergic agents on these properties. Local application of the α-adrenergic agonist phenylephrine or the ß-adrenergic agonist isoproteronol modified properties of some intracardaic neurons, and both agonists were capable of facilitating or inhibiting neurotransmission to these neurons. These effects were blocked by the α- and ß-adrenoceptor specific antagonists prazosin and timolol, respectively. These studies suggest that endogenous catecholamines, released from adrenergic nerve terminals within intracardiac ganglia, can have powerful effects on the functions of individual neurons in these ganglia. Taken together, the results of the studies in this thesis provide evidence of an anatomical and physiological substrate for potential modulation of intracardiac ganglionic neurotransmission by the sympathetic nervous system.

List of Abbreviations and Symbols

α	alpha
ACh	acetylcholine
AChE	acetylcholine esterase
AHP	afterhyperpolarization
ANOVA	analysis of variance
AO	aorta
AP	action potential
ASC	ascending limb
AV	atrioventricular
AZV	azygos vein
β	beta
bpm	beats per minute
BS	brain stem
°C	degrees Celsius
Ca^{++}	calcium ion
ChAT	choline acetyltransferase
CNS	central nervous system
CPN	cardiopulmonary nerve
EPSP	excitatory postsynaptic potential
Fig.	figure
FITC	fluorescein thyocianin
GCV	great cardiac vein
Hex	hexamethonium
IR	immunoreactivity
ISO	isoproteronol
IVC	inferior vena cava
K^{+}	potassium
kg	kilogram

LA	left atrium
LAA	left atrial appendage
L CPN	left cardiopulmonary nerve
L MCG	left middle cervical ganglion
L SG	left stellate ganglion
L SIV	left superior intercostal vein
L VN	left vagus nerve
MΩ	megohm
μM	micromolar
mA	milliampere
Mec	mecamylamine
min	minute
Mg^{++}	magnesium ion
ms	milliseconds
mV	millivolt
nm	nanometer
n	number sampled
NE	norepinephrine
NIC	nicotine
OBL V	oblique vein
PGP 9.5	protein gene product 9.5
PHEN	phenylephrine
PV	pulmonary vein
RA	right atrium
RAA	right atrial appendage
RCPN	right cardiopulmonary nerve
Rhod	rhodamine
R MCG	right middle cervical ganglion
R SG	right stellate ganglion
R VN	right vagus nerve

S	septum
SA	sinoatrial
SC	spinal cord
SE	standard error
STIM	electrical stimulus
SVC	superior vena cava
τ	time constant
T_2	second thoracic ganglion
TH	tyrosine hydroxylase
TMR	tetramethyl rhodamine dextran (3000 m.w.)

Acknowledgements

My sincere thanks go to Dr. Frank M. Smith for his insightful supervision and for providing a pleasant environment in which to carry out my graduate research training. Thanks to Helen Sauveur, Janette Nason and Kathleen McCleave for their technical expertise and assistance. I would also like to thank the lab members of Dr. Richard Wassersug, Dr. William Currie, and Dr. David Hopkins for their helpful discussions, advise and encouragement. This study was supported by the Heart and Stroke Foundation of Canada.

Chapter 1: Introduction and Background

Introduction

The general anatomy of the autonomic innervation of the viscera has been known for centuries, however the functional roles of this innervation in terms of specific autonomic control of visceral processes are still unclear. In fact, it has recently been speculated that so little is known of the information processing mechanisms in peripheral autonomic ganglia in general that it appears that there would be no difference in control of effector organs if they were innervated by preganglionic axons directly from the central nervous system (Adams & Koch, 1990). Nevertheless, there is great deal of evidence that peripheral ganglionic neurons are in a position to play important roles in integrating and co-ordinating visceral motor and sensory information, and to provide flexibility in the regulation of specific visceral processes. In this thesis, I present studies that investigated the anatomical and functional characteristics of elements within the intracardiac nervous system which could be responsible for sympathetic modulation of intraganglionic neurotransmission. The thesis is organized into five parts. In Chapter 1, the objectives and overall hypothesis for the studies are stated, the classical model for neural control of cardiac function is presented, and a proposed revision of this model incorporating recent evidence for intracardiac mechanisms of sympathetic and parasympathetic interaction is developed. An analysis of previous work in this area is presented and the rationale for the experiments is described. In Chapters 2-4, I have described in detail the experiments designed to test the proposed hypothesis. Chapter 5 is a general discussion summarizing the implications of this work for neural control of the heart.

Objectives

The objectives of this thesis are to determine:

1) the regional distribution of cholinergic and adrenergic cells and nerve fibres within the atria of the guinea-pig;
2) the anatomical and functional relationships of amine-containing and amine-synthesizing cells and terminals to intracardiac neurons;
3) the basic membrane and firing properties and morphology of different classes of intracardiac neurons, and their patterns of synaptic input.
4) whether exogenous application of adrenergic agonists can affect the properties of intracardiac neurons and can directly modulate neurotransmission within the intracardiac nervous system.

Hypothesis

The overall hypothesis for this thesis is that some intracardiac neurons receiving cholinergic synaptic inputs are also targeted by extrinsic sympathetic nerve terminals. These sympathetic terminals could modulate vagal excitation of intracardiac neurons through both excitatory and inhibitory postsynaptic potentials, mediated by the adrenergic neurotransmitter norepinephrine.

Background

Anatomical and functional organization of the intracardiac nervous system:

In the classical model of autonomic regulation of the heart, summarized in Fig. 1, extrinsic sympathetic postganglionic terminals provide the only capability for autonomic

augmentation of cardiac function: norepinephrine (NE) released from these terminals activates ß-adrenergic receptors on the myocardium. The cell bodies of these sympathetic neurons are located within the thoracic ganglia and are innervated by terminals of preganglionic neurons with their somata in the spinal cord (Fig 1). Preganglionic terminals in the thoracic ganglia release acetylcholine (ACh) which acts at nicotinic receptors on the postganglionic neurons. The parasympathetic limb of the autonomic nervous system inhibits cardiac activity; postganglionic parasympathetic neurons within the heart release ACh which activates muscarinic receptors on the myocardium. Preganglionic drive reaches the intracardiac postganglionic parasympathetic neurons via the terminals of axons in the vagus nerves; these preganglionic terminals also release ACh, activating postsynaptic nicotinic receptors (Fig.1). Therefore, in the classical model, sympathetic and parasympathetic pathways to the heart differ in: a) the location of their postganglionic cell bodies, b) the transmitter released at the postganglionic terminal and c) their respective effects on cardiac output. Functionally, sympathetic and parasympathetic control of cardiac output works in a reciprocal fashion in the classical model. That is, when vagal cardiodepressant activity is low, sympathetic cardioaugmentatory activity is high, and vice versa (Cannon, 1939). However, recent evidence has shown that this model is incomplete: a mechanism exists within the heart which allows for co-activation and integration of extrinsic sympathetic and parasympathetic inputs. Simultaneous recordings *in vivo* from vagal and cardiopulmonary nerves have shown that both inputs to the mammalian heart can be co-activated under a wide range of physiological conditions (Koizumi *et al.*, 1982; Koizumi and Kollai, 1992), as for example, during periods of increased atrial filling.

The two primary sites for vago-sympathetic interactions are at present considered to be: 1) at the autonomic neuroeffector junctions on the myocardium (Furukawa *et al.*, 1990; Levy, 1990; Loffelholz and Pappano, 1985; Pirola and Potter, 1990; Potter and Ulman, 1994); and 2) prejunctional neuromodulatory mechanisms at the neuroeffector terminals (Levy, 1990; Potter and Ulman, 1994). These mechanisms of potential interactions are illustrated by the dashed lines in Figure 1. This model incorporates presynaptic inhibition at both types of neuroeffector junction as a major modulatory mechanism. Collaterals from sympathetic postganglionic axons have been proposed to synapse on postganglionic parasympathetic terminals so that sympathetic input can reduce vagally mediated cardiomotor effects, and vice versa (Fig 1, reviewed by Berne and Levy, 1983). However, recent anatomical reports, summarized below, have demonstrated the presence of adrenergic terminals within intracardiac ganglia, suggesting the possibility of direct sympathetic influences on ganglionic neurotransmission in the heart.

In mammals, histochemical techniques have been used to demonstrate the existence of catecholamine-containing terminals associated with intracardiac ganglia (Ellison and Hibbs, 1974 and 1976; Moravec and Moravec, 1987; Moravec *et al.*, 1990). Glyoxylic acid histochemistry, for example, revealed catecholamine-containing fibres and terminals surrounding "principal" neurons (Neel and Parsons, 1986) in the rat heart. The formaldehyde-induced fluorescence technique for catecholamine detection demonstrated a similar intracardiac pattern of adrenergic nerve terminal distribution (Ehinger *et al.*, 1968) to that shown by the glyoxylic acid technique. Immunocytochemistry for tyrosine

Figure 1. Classical model of the autonomic innervation of the heart (refer to text for details). (ACh, acetylcholine; BS, brain stem; N, nicotinic receptor; NE, norepinephrine; SC, spinal cord; +, excitatory; -, inhibitory)

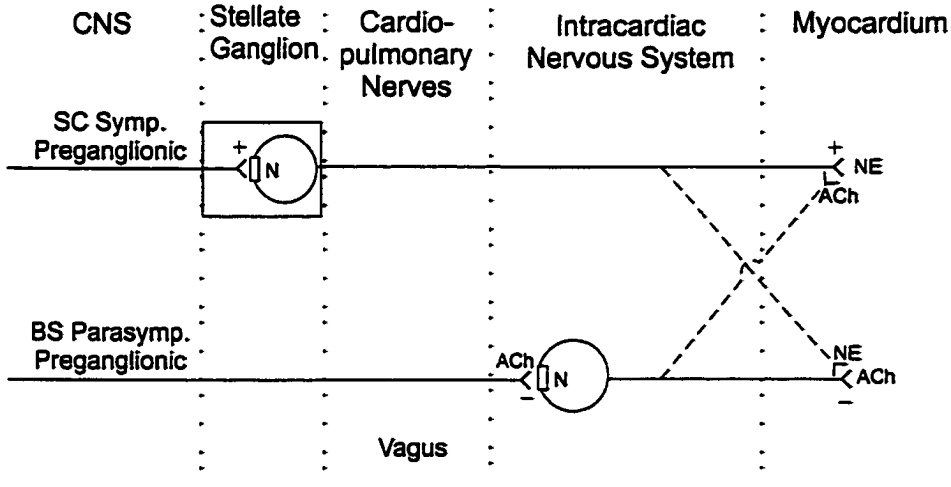
CNS
Stellate Ganglion
Cardio-pulmonary Nerves
Intracardiac Nervous System
Myocardium
SC Symp. Preganglionic
+
N
+
NE
ACh
BS Parasymp. Preganglionic
ACh
N
NE
ACh
−
−
Vagus

Figure 1

hydroxylase (TH), a rate-limiting enzyme involved in the synthesis of catecholamines, labelled terminals which formed basket-like patterns around "principal" intracardiac neurons (Slavikova *et al.*, 1993; Steele *et al.*, 1994) in guinea-pigs. These authors proposed that such terminals were of extrinsic sympathetic origin. Therefore, based on anatomical evidence, it is possible that sympathetic and parasympathetic inputs converge on single intracardiac neurons.

A precedent for this pattern of innervation has been established in other visceral organs. Abdominal and pelvic neurons were once considered to belong exclusively in the parasympathetic pathway to enteric and pelvic organs but there is a growing body of persuasive anatomical evidence for sympathetic innervation of some of these neurons. Hamberger and Norberg (1965a,b), using formaldehyde induced fluorescence, described basket-like terminals reactive for catecholamines on cell bodies of putative cholinergic neurons within the bladder ganglia of the cat. These authors also described a subpopulation of somata reactive for catecholamines within the heart. In a later review, Janig and McLachlan (1992) confirmed by ultrastructural examination in the transmission electron microscope that catecholamine-containing terminals made synaptic contact with putative cholinergic neurons within the pelvic ganglia.

In the context of integrated sympathetic and parasympathetic control of viscera, innervation of the gall bladder appears to have a unique pattern, compared with the innervation of other visceral organs. In the gall bladder, axons from extrinsic sympathetic postganglionic neurons do not innervate the muscularis directly; instead there is abundant sympathetic innervation of neurons in the gall bladder ganglia (Baumgarten and Lange, 1969; Cai and Gabella, 1989). This would suggest that the

primary mode of influence of the sympathetic nervous system on the gall bladder would be indirect, mediated through the ganglia. The somata of the adrenergic axons innervating gall bladder ganglia were located within the coeliac ganglion (Mawe and Gershan, 1989). Additionally, in the pancreas, TH-positive terminals of axons originate from neurons in the prevertebral ganglia, and have been shown to colocalize the peptide galanin (Ahrén *et al.*, 1990). In an ultrastructural study of pancreatic ganglia, synaptic specialization was observed between terminals containing the large dense-core vesicles typical of adrenergic neurons and the cytoplasmic membranes of "principal" neurons (King, Love and Szurszewski, 1989). These observations in the gall bladder and pancreas provide anatomical evidence that adrenergic terminals, possibly postganglionic sympathetic terminals, could potentially modulate the activity of "principal" ganglionic neurons.

Functional roles of identified neuron types within the peripheral autonomic nervous system

The overall function of the neural network in control of the heart depends on the properties and characteristics of the individual neuronal elements within the network. The properties of intracardiac neurons have not been well established, but the concept of functionally distinct neuron types within the autonomic nervous system has received increasing support in recent years. Functional neuron types within the heart may include: sensory or afferent neurons responding to chemical or mechanical stimuli, and motor or efferent neurons which control musculature, vasculature and pacemaker cells. In addition, interneurons or "local circuit neurons" may be present, providing the means for

interactions making up local reflex links among neurons in afferent and efferent pathways. Such reflex interactions would enable the intrinsic nervous system to process information received from a number of local sources to govern organ function. In the peripheral autonomic nervous system in general, the best evidence for the existence of function-specific neuron types has been collected from immunohistochemical, physiological and pharmacological experiments in the guinea-pig small intestine. It was proposed that identified neurons of functionally distinct types had different roles and distinctive morphological, neurochemical and pharmacological properties specific to their roles within control pathways (Furness and Bornstein, 1995; Wood, 1981,1994; Janig and McLachlan, 1992).

An example of a function-specific pathway with its elements entirely within the gut, involves the pathway that integrates motor reflexes over relatively short lengths of intestine. This pathway has been examined in isolated intestine preparations which eliminate the influences of the central nervous system and circulating hormones. A number of studies have shown that these reflexes do not need the participation of neurons in the central nervous system or prevertebral ganglia. In studies on gut segments *in vitro*, mechanical or chemical stimulation of the mucosa resulted in contraction of the gut tissue orad to the site of stimulation (Hirst and McKirdy, 1974; Hirst *et al.*, 1975). Neurons in the myenteric plexus appeared to be crucial to the propagation of the reflex response with distension of the intestinal wall, while an intact mucosa was important for the response to chemical stimulation (Smith *et al.*, 1990; Smith and Furness, 1988). These results suggested that separate populations of sensory neurons driving this reflex may exist in the

submucosal and myenteric plexus although to date no definitive anatomical evidence exists in support of this hypothesis (Smith *et al.*, 1991).

Several authors suggested that Dogiel Type II neurons (Dogiel, 1899 in Furness and Costa, 1987) are the sensory neurons of the enteric nervous system. Dogiel Type II neurons have long filamentous processes which terminate in both the mucosa and the myenteric plexus (Kirchgessner *et al.*, 1988; Kirchgessner *et al.*, 1992) and are also immunoreactive for substance P and choline acetyltransferase (Bornstein *et al.*, 1989; Furness *et al.*, 1984). These neurons also appear to have few or no fast excitatory inputs and can respond to chemical stimulation of the mucosa even in the presence of hexamethonium, a nicotinic channel antagonist (Kunze *et al.*, 1995). They thus possess anatomical and neurochemical features typical of sensory neurons in other parts of the nervous system, and can participate in fast cholinergic excitatory neurotransmission when activated. However, Wood (1981, 1984) cautions that the evidence for these cells as enteric sensory neurons is, as yet, purely circumstantial and that these Dogiel Type II neurons may well be interneurons in the sensory/motor reflex pathway and not first-order sensory neurons. Regardless of their position in the pathway, these neurons do respond during mechanical mucosal stimulation and can evoke postsynaptic potentials in motor neurons. Thus, they are important in the transmission of the sensory signals within the gut and can potentially modify motor neuron excitability. Similar afferent neurons and interneurons have been proposed to exist within the intracardiac nervous system (Armour, 1994). However, as in the gut, a specific sensory neuron type has not yet been morphologically or physiologically identified within the heart.

A second example of a reflex pathway in the enteric nervous system which is independent of the central nervous system involves reflexes which influence enteric motility over greater distances. For example, distension of the distal colon will produce relaxation in the proximal small intestine. This reflex begins with intramural neurons which project to the prevertebral ganglia to excite noradrenergic efferent neurons. These efferent neurons contact the interneurons or excitatory neurons of the intramural ganglia to inhibit their activity and thus relax the circular muscle. Anatomical neurotracing studies as well as immunohistochemical and physiological studies have demonstrated the existence of adrenergic intestinofugal fibres which terminate in the prevertebral ganglia and result in inhibitory postsynaptic potentials in the efferent neurons (Furness and Bornstein, 1995). Evidence from the enteric system shows that a large degree of autonomic control of these organs can be accomplished by neurons embedded in neuronal networks within the organ. Evidence for the existence of a similar system associated with the heart is growing.

The classical model for neural control of the heart indicates that all intracardiac neurons should be parasympathetic in function, acting as simple relays for inhibitory drive to the myocardium (Fig. 1). However, there is *in vivo* and *in vitro* evidence that not all intracardiac neurons sampled during extracellular recording experiments receive direct vagal innervation. For instance, only 20% of intracardiac neurons responded to vagal nerve stimulation in the *in situ* canine heart (Armour and Hopkins, 1990). In the guinea-pig heart *in vitro*, some neurons have been shown to receive strong inputs from the vagus nerve whereas others appear to receive only inputs from local intracardiac sources; some neurons do not appear to receive any synaptic inputs (Edwards *et al.*,

1995). Furthermore, anatomical and physiological evidence shows that some cardiac neurons can receive inputs from axons carried in extracardiac sympathetic nerves (Steele *et al.*, 1995; Smith, 1999).

Older studies of the innervation of the heart asserted that all neurons in the intracardiac plexus were uniform in morphology, behaviour and function. However, more recent evidence for neurochemical and morphological differences among intracardiac neurons would suggest these differences reflect different neuronal functions. Schemann *et al.* (1995) have proposed that in the enteric nervous system, subpopulations of neurons may be differentiated based on their neurochemical content. However, there is disagreement among workers in this field concerning the expression of the classical autonomic neurotransmitters NE and ACh within intracardiac neurons. A number of researchers have proposed that the majority, if not all, intracardiac neurons are cholinergic within the guinea-pig heart (Roskoski *et al.*, 1974; Steele *et al.*, 1994; Mawe *et al.*, 1996). Other studies have reported the presence of catecholaminergic neurons (Moravec *et al.*, 1984; Slavikova *et al.*, 1993) in the rat heart *in situ* and in dissociated long term co-cultures of guinea-pig intracardiac neurons with myocytes (Horackova *et al.*, 1993). It has also been suggested that these catecholaminergic neurons may be inhibitory interneurons, forming part of a negative feedback loop within the heart (Moravec *et al.*, 1986). Intracardiac neurons, whether cholinergic or catecholaminergic, also express a number of neuropeptides in multiple combinations. Steele *et al.* (1995) have demonstrated the presence of somatostatin-immunoreactivity (-IR) in the somata of 90% of the cholinergic neurons of the intracardiac nervous system. Of those, half are also immunoreactive for substance P and more than 10% of these neurons contain a third

peptide, neuropeptide Y. Substance P has been localized within sensory neurons of the dorsal root ganglia (Cuello *et al.*, 1982; Dalsgaard *et al.*, 1982) and within putative sensory neurons of the enteric nervous system (Bornstein *et al.*, 1989; Furness *et al.*, 1995), so perhaps the population of substance P-containing intracardiac neurons may be intrinsic sensory neurons.

Convincing anatomical evidence for the existence of interneurons within the intracardiac nervous system was presented in a study whereby hearts, removed from animals, were maintained in organotypic culture for 6 days. This method allowed for the degeneration of the nerves of extrinsic origin (i.e.: from central vagal motor nuclei, and sympathetic and sensory ganglia) (Steele *et al.*, 1994). Intrinsic cardiac axons containing VIP and NPY but not somatostatin remained after 6 days of culture. Furthermore, these terminals were present in intracardiac ganglia but not in association with the myocardium, suggesting that terminals with this peptide profile may be from a population of interneurons which synapsed with other neurons within the intracardiac nervous system.

Evidence for physiologically identified subpopulations of intracardiac neurons has been described in recent years. Edwards *et al.* (1995) proposed three different classes of neurons, based on evidence for different combinations of morphology, membrane properties and synaptic contacts. These three types of neuron were turned S, SAH and P. The majority of S cells did not receive synaptic inputs from the vagus. In the few S cells with vagal inputs, only fast EPSPs which were below threshold for generating action potentials (AP) were elicited by vagal nerve stimulation. However, when local intracardiac nerves were stimulated electrically, an AP could be elicited in these cells. S

cells fired a single AP at the start of a long-duration depolarization of the membrane. The afterhyperpolarization (AHP) following the AP in these cells was of short duration (~30 ms). The mean resting membrane potential of S cells was similar to those of the other types of neuron in the guinea-pig heart. Morphologically, S cells had small somata and an axon which either innervated the myocardium or entered the vagosympathetic trunk. The physiological properties of these S cells resembled S neurons in the canine heart (Xi *et al.*, 1991a, 1994) and of "Type I" cells in the rat heart (Selyanko, 1992).

Edwards *et al.* (1995) termed neurons receiving vagal inputs that could elicit postsynaptic APs, as SAH neurons. This type of cell responded to long depolarizations with repetitive AP discharge and had a longer-duration AHP than S cells (mean AHP duration 144 ms). Morphologically, SAH neurons were monopolar, dipolar or multipolar and their axons projected to either the myocardium or cranially within the vagosympathetic trunk. Physiologically, guinea-pig SAH cells resembled "Type II" neurons of the rat (Selyanko, 1992) but maximal frequency of AP generation was well below that of canine "R" cells (Xi *et al.*, 1994).

In the study of Edwards *et al.* (1995), a third type of guinea-pig intracardiac neuron, designated P cells, did not respond to synaptic inputs, fired repetitively when depolarized intracellularly, and also had long duration AHPs. Morphologically, these cells were either bipolar or pseudobipolar and their processes terminated within the cardiac plexus or entered the vagosympathetic trunk to project cranially. No axons of this cell type were observed to associate with the myocardium. Edwards *et al.* (1995) suggested that these neurons may be afferent in function, perhaps comprising intrinsic sensory neurons within the heart. This suggestion is supported by the results of Cheng *et*

al. (1997) who reported retrogradely labelled neurons within the guinea-pig intracardiac plexus after injection of the neuro-tracer DiI into the nodose ganglion (Cheng *et al.*, 1997). Both groups of workers suggested that these neurons were sensory neurons intrinsic to the heart. It is not known whether the proposed afferent neurons described in these two studies were in fact the same population.

In contrast to the findings of Edwards *et al.* (1995), Hardwick *et al.* (1995) described only two types of intracardiac neuron based on their firing properties: phasic (corresponding to S type neurons of Edwards *et al.*, 1995) and tonic (corresponding to SAH and P cells of Edwards *et al.*, 1995). Unlike the study of Edwards *et al.* (1995), Hardwick *et al.* (1995) reported no morphological differences between phasic and tonic neurons. Thus, while it is clear that there are several physiologically distinct types of neuron in the guinea-pig heart, there remains some uncertainty as to how or if these neuron types are correlated with morphological differences, as has been reported for canine intracardiac neurons (Xi *et al.*, 1991b) and guinea-pig enteric neurons (Furness and Bornstein, 1995).

Function-specific pathways

The existence of function-specific pathways and the presence of neurons of different physiological types in these pathways within the autonomic nervous system is a concept receiving increasing support. For example, in the coeliac ganglion, Janig and McLachlan (1992) determined that tonic neurons received weak inputs from the periphery, whereas phasic neurons and AH-type neurons (which are phasic neurons with long-duration AHPs of 1s) received strong inputs from the CNS and weak inputs from the

periphery. With injection of dyes and double labelling with immunocytochemistry, the authors also determined the functional pathways to which these physiologically identified neurons belonged. Tonic and some phasic neurons were primarily involved in motility and secretion of the enteric tube while the majority of phasic neurons innervated the vasculature. The authors therefore suggested that neurons of particular physiological types received inputs from different sources depending on the function of the pathways in which they were located. On the other hand, it has been proposed that collateral branches of axons of single neurons with their somata in the intramural plexuses of the enteric nervous system may innervate both the mucosa and the vasculature (Furness and Bornstein, 1995). This finding complicates the interpretation of experimental results, and could be a confounding factor for the proposal of Janig and McLachlan (1992).

The apparently hierarchical organization of the intrinsic and extrinsic innervation of the gut is necessary for the orderly and precise control of movement of lumenal contents. Precise localization of sensory input would provide necessary information for highly localized responses such as segmental contraction of circular muscle, increased secretion of the mucosa or increase vascular flow, all designed to aid in digestion and absorption in the affected segment. A non-segmental but nevertheless highly localized separation of neuronal control pathways in the heart, based on different neuron types and differences in the connectivity of subpopulations of intracardiac neurons, may provide the means for rapid and precise regional control of contraction strength, rate and coronary flow on a beat-by-beat basis.

Although the best evidence presented thus far for the existence of function-specific pathways within the autonomic nervous system has been in the enteric nervous

system, there is growing evidence that such pathway segregation may be present in the heart. These pathways may include efferent projections to specific target tissues such as the pacemaker cells, myocytes or vasculature. Evidence from whole-animal studies in the dog has shown that surgical removal of selected groups of atrial neurons results in a loss of vagal influence on either heart rate or contraction strength (Randall, 1985 reviewed by Randall and Brown, 1994). In addition, Gatti *et al.* (1995) described ganglia with segregated functions within discrete fat pads on the feline heart. Using microlitre injections of the ganglionic blocker, trimethaphan, these authors concluded that ganglia, situated near the inferior vena cava and the inferior left atrium, were responsible for controlling atrio-ventricular conduction and that other ganglia, near the right pulmonary veins, influenced sinoatrial nodal rate. These conclusions remain controversial as the full extent of the regionalization of neural control of the heart is not yet understood. Furthermore, there is evidence from studies in the *in vivo* canine heart which indicate that neurons which control particular regional cardiac functions may not all be located within or near the controlled region (Butler *et al.*, 1990a,b).

Adrenergic modulation of neuronal activity in the heart

Pharmacological evidence for sympathomimetic modulation of cardiac neurons supports the anatomical data described in the previous section. NE can modify firing properties of individual porcine intracardiac neurons *in vitro* (Smith *et al.*, 1992), and local application of microlitre quantities of adrenergic agonists to intracardiac ganglia of the *in vivo* canine heart increased the frequency of neuronal discharge as well as modified cardiodynamics (Huang *et al.*, 1993). Pharmacological evidence for the presence of

several adrenergic receptor subtypes on intracardiac postganglionic neurons also supports the suggestion that adrenergic innervation can modulate neuronal activity (Flavahan and McGrath, 1982; Armour, 1997). In the study by Flanahan and McGrath (1982), activation of the intracardiac nervous system with an α_1-adrenergic agent induced bradycardia. In another study, application of α_1- and α_2-adrenoceptor agonists could provoke either an increase or decrease in neuronal activity when applied in the region of spontaneously active neurons (Armour, 1997). In this study, the spontaneous activity of intracardiac neurons along with heart rate, left ventricular chamber pressure, aortic pressure, and other indicators of ventricular inotropic changes were simultaneously recorded during the application of these pharmacological agents. When neuronal activity was increased, there was a concurrent increase in heart rate and right and left ventricular intramyocardial pressure in response to local adrenergic stimulation of neurons. When neuronal activity was depressed by adrenergic agents, no change in any cardiac variable was observed. These responses to α-adrenergic stimulation suggests that there may be at least two functionally different adrenergic mechanisms associated with neurons in the intrinsic cardiac nervous system. The possibility that these agents mediated cardiodynamic effects by acting directly on the myocardium was ruled out in these experiments.

Stimulation of β_1- and β_2-adrenergic receptors on intracardiac neurons *in vivo* resulted in an increase in neuronal activity, heart rate and other cardiac variables (Armour, 1997). These results suggest that ß-adrenoceptors, as well as α-adrenergic receptors, associated with intracardiac neurons, may play a role in neural control of the heart. However, unlike the responses to α-adrenergic agonists, no suppression of

neuronal activity was recorded during the application of ß-adrenergic agonists to neurons in the heart (Armour, 1997). In the rat, intrinsic cardiac neurons have been shown to possess $ß_2$-adrenoceptors (Saito *et al.*, 1988; Baluk and Gabella, 1990). The ß-adrenergic antagonists timolol and ICI-118,551 suppressed spontaneous neuronal activity without changing cardiac variables, suggesting that endogenous release of catecholamines within the intracardiac nervous system can influence ongoing neuronal activity (Armour, 1997). In this study, one third of the neurons sampled by extracellular recording responded to the application of either an α- or ß-adrenergic agonist. This evidence suggests that with respect to the presence of adrenoreceptors, there are functionally different populations of neurons within the intracardiac nervous system and that these populations may be distinguished by the presence of α- and ß-adrenergic receptors.

Studies in which sympathetic inputs to the heart were electrically stimulated also provide evidence for adrenergic modulation of cardiac neurons. In a section of right atrium of the pig heart studied *in vitro*, electrical stimulation of attached cardiopulmonary and vagus nerve stumps evoked adrenergically and cholinergically mediated postsynaptic responses, respectively, from intracardiac neurons. This work showed that a group of intracardiac neurons received dual innervation from extrinsic parasympathetic and sympathetic nerves (Smith, 1999). In this study, it was shown that activation of ß-adrenoceptors facilitated the generation of synaptically-evoked fast excitatory postsynaptic potentials which could sum with vagal inputs to elicit AP discharge in intracardiac neurons.

Adrenergic modulation of neuronal activity in other viscera

In viscera other than the heart, there are several lines of physiological evidence to support the theory that some autonomic ganglion neurons are dually innervated by sympathetic and parasympathetic axons. For example, some pelvic neurons receive input from both the hypogastric (primarily sympathetic) and pelvic (primarily parasympathetic) nerves (Blackman *et al.*, 1969; Crowcroft and Szurszewski, 1971; McLachlan, 1977; de Groat, Booth, and Krier, 1979; Janig and McLachlan, 1987). In the bladder, parasympathetic inputs to ganglion neurons constitute the principal drive that activates and maintains micturition by augmenting contraction of the bladder walls. Stimulation of the pelvic parasympathetic nerves increases the activity of efferent bladder neurons. When the hypogastric and pelvic nerves are concurrently stimulated, efferent neuronal activity is first inhibited, then facilitated (de Groat and Saum, 1972; Keast and de Groat, 1990). In this system, activation of α_2-adrenoreceptors resulted in hyperpolarization of the resting membrane potential of bladder neurons, suggesting that NE can modulate neurotransmission by an α-adrenergic postsynaptic mechanism. This may be one mechanism by which activity of bladder neurons is inhibited by sympathetic input (Keast and de Groat, 1990). Conversely, α_1-adrenoceptors were responsible for sympathetically-mediated presynaptic facilitation of parasympathetic neurotransmission to bladder neurons (Keast and de Groat, 1990).

In other systems demonstrating sympathetic and parasympathetic convergence, sympathetic influences on parasympathetic neurotransmission appear to be primarily inhibitory. Exogenously applied NE has been shown to presynaptically inhibit nicotinic transmission within the gallbladder (Mawe, 1993) and in ganglia of the sphincter of Oddi.

Moreover, in this tissue, β_2-adrenergic agonists decreased the amplitude of the nicotinic fast excitatory postsynaptic potential evoked by stimulation of interganglionic fibre tracts (Wells and Mawe, 1994).

The background information presented above establishes that sympathetic input can play a role in controlling viscera by modulating intravisceral ganglionic neurotransmission. In addition, I have reviewed the evidence suggesting that sympathetic terminals may be present in intracardiac ganglia, that sympathetic nerve stimulation can affect intracardiac neuronal activity, and that adrenergic agents have the potential to affect the operation of individual neurons in the heart. However, the details of this sympathetic influence on ganglionic neurons and neurotransmission remain to be established.

The work presented in this thesis is focussed on the four objectives stated at the beginning of this chapter. Anatomical and functional relationships of amine-containing and amine-synthesizing cells and terminals to intracardiac neurons are investigated, and the distributions of cholinergic and adrenergic cells and nerve fibres within the atria of the guinea-pig have been determined using histochemical and immunohistochemical techniques; these studies constitute Chapter 2. Before functional studies of sympathetic effects on ganglionic neurotransmission in the guinea-pig heart could be carried out, an *in vitro* preparation for this purpose had to be developed and verified; this constitutes Chapter 3. In Chapter 4, this preparation was used to determine the pattern of synaptic input to intracardiac neurons, and modulation of this input by adrenergic compounds was determined for specific types of intracardiac neuron. Intracardiac neurons were classified according to their functional properties, and correlations between basic neuronal

properties, neuronal morphology and firing properties were established. In this manner, potential mechanisms of direct modulation of neurotransmission within the intracardiac nervous system by sympthetic inputs was investigated. Chapter 5 is a general discussion of the implications of the results of these studies for our understanding of neural control of the heart.

Chapter 2: Organization of the intracardiac nervous system and neurochemical content of intracardiac neurons.*

Introduction

Neurons in the mammalian intrinsic cardiac nervous system are capable of modifying dromotropic and inotropic functions of the heart as well as cardiac pacemaker activity. Anatomical studies of the intracardiac nervous system in a variety of mammals have shown that the somata of intracardiac neurons are located within ganglia associated with the left and right atria and ventricles (King and Coakley, 1958; Calaresu and St. Louis, 1967; Anderson, 1972; Ellison and Hibbs, 1976; Tay *et al.*, 1984; Janes *et al.*, 1986; Pardini *et al.*, 1987; Yuan *et al.*, 1994). In *in vivo* studies of the canine heart, activation of intrinsic cardiac neurons by focal electrical stimulation or local application of microlitre quantities of pharmacological agents results in modulation of cardiodynamic variables (Butler *et al.*, 1990b; Huang *et al.*, 1993a, b, c), and functional evidence has been reported for the existence of afferent and interneurons or local-circuit neurons, as well as postganglionic efferent cardiomotor neurons within the heart (see Ardell, 1994 for review). Evidence from these functional studies suggests that neurons of different types are connected in a distributed network within the heart, and that this network is capable of modulating regional and global myocardial function to help match cardiac output to the impedance of the arterial tree. However, at present our knowledge of the anatomical organization of this intracardiac network and the phenotypes of the neurons involved is incomplete.

* Some material presented in this chapter has been published (Leger *et al.*, 1999).

Many of the studies of intracardiac neuron function have been done in larger mammals such as the dog. However, in the hearts of larger mammals ganglionated plexi associated with the intrinsic cardiac nervous system are embedded in a relatively large volume of tissue, posing a problem for studies of the anatomical organization of this system. Serially reconstructed sections have been widely used to study the anatomy of the intracardiac nervous system but the results of these studies have been unsatisfactory because the large-scale relationships between different parts of the system cannot easily be determined from such reconstructions. Recently, the organization of the intracardiac nervous system has begun to be explored by adapting standard histochemical and immunohistochemical techniques for use in whole-mounts of selected portions of hearts taken from smaller mammals such as the guinea pig. The chief advantage of this type of preparation is that all elements of the intracardiac nervous system can be visualized at once. However, the general distribution of neurons within guinea pig atria, their total number and location by region have not been established. The first aim of this study is therefore to determine these characteristics of the intracardiac nervous system in the atria of the guinea pig.

In the intrinsic cardiac nervous system, histochemical surveys have shown that many nerve fibres, terminals and neuronal somata exhibit staining for acetylcholinesterase (AChE; James and Spence, 1966; Jacobowitz, 1967; Ehinger *et al.*, 1968; Bojsen-Moller and Tranum-Jensen, 1971; Anderson, 1972; ; Ellison and Hibbs, 1976; Hancock *et al.*, 1987; Roberts *et al.*, 1989). This evidence has been taken to indicate that these neural elements are potentially cholinergic, since AChE is required for the breakdown of ACh, the classical pre- to postganglionic neurotransmitter in the

peripheral autonomic nervous system. However there is evidence that AChE may also be present in non-neuronal cells (Fibiger, 1982; Satoh *et al.*, 1983). More convincing evidence for the cholinergic nature of intrinsic cardiac neurons would be expression of choline acetyltransferase (ChAT), an enzyme in the synthetic pathway for ACh. ChAT expression, detected immunohistochemically, is accepted as the primary indicator of cholinergic phenotype in neurons of the central nervous system (Satoh *et al.*, 1983) and, more recently, in the peripheral autonomic nervous system (Keast *et al.*, 1995; Wang *et al.*, 1995). In the guinea pig heart, Mawe *et al.* (1996) have demonstrated that neurons in the atrial intercaval region, the basal portion of the interatrial septum and the cardiac sinus region all appear to be immunoreactive (IR) for ChAT. However, neither this study nor earlier histochemical studies of the intracardiac occurrence of AChE covered the entire extent of the atria, so the relative proportion of atrial neurons exhibiting cholinergic attributes is not known. The second aim of the present study is therefore to provide an estimate of the total number and overall distribution of ChAT-IR neurons in the guinea pig atria. Immunoreactivity for protein gene product 9.5 (PGP 9.5), a general vertebrate neuronal marker (Gulbenkian *et al.*, 1987), was used in this study to determine the location of neurons in atrial whole-mounts, and to provide an estimate of the total number of neurons present, for comparison with the number of ChAT-IR neurons.

Direct activation of some intracardiac neurons can evoke cardioinhibitory responses but recent studies have shown that neurons within the heart are also capable of producing cardioaugmentation (Butler *et al.*, 1990a, b; Armour *et al.*, 1993; Huang *et al.*, 1993a, b, c). Some of these augmentatory responses survive acute decentralization (Butler *et al.*, 1990a; Huang *et al.*, 1993a) or cardiac autotransplantation (Murphy *et al.*,

1994), indicating that the neurons in these pathways must be intrinsic to the heart. These augmenting responses are mediated through activation of ß-adrenergic receptors (Butler *et al.*, 1990b; Armour *et al.*, 1993; Huang *et al.*, 1993a, b, c; Armour, 1994) so it follows that the neurally-mediated release of catecholamines from an intracardiac store is a necessary component of this pathway. Intracardiac neurons involved in this type of catecholamine-mediated cardioaugmentation would thus be expected to display some aspects of an adrenergic phenotype, including expression of TH, the rate-limiting enzyme in norepinephrine synthesis. The third aim of this study was to undertake a survey of TH-IR neural elements over the entire extent of the atria in the guinea pig heart, and to establish the relationship of these elements to cholinergic neurons.

An alternate explanation for catecholamine-dependent cardiac augmentation resulting from stimulation of intracardiac neurons is that these neurons may take up and store amines from the surrounding milieu. When activated, these neurons may then release amines to modulate cardiac output. In cell culture experiments, a subpopulation of intracardiac neurons has been shown to take up amines from the culture medium (see Allen *et al.*, 1994 for review). It might therefore be reasonable to expect that, if intracardiac neurons *in situ* were capable of accumulating physiologically significant stores of amines, these stores should be detectable by currently available histochemical assays. However catecholamines have not been reported in the somata of guinea pig intracardiac neurons in the limited regions of the atria which have been examined so far (Baluk and Gabella, 1990). A fourth aim of the present study was to determine whether detectable catecholamine stores were present in any atrial neurons, to attempt to resolve this issue.

The origins and course of extrinsic nerves supplying the heart have been well established in humans and non-human primates as well as in a variety of large domestic mammals (McKibbin and Getty, 1969a, b, c; Randall *et al.*, 1971; Randall *et al.*, 1972; Janes *et al.*, 1986; Furukawa *et al.*, 1990; reviewed by Armour and Hopkins, 1984 and Randall and Ardell, 1988). These studies have provided a firm anatomical foundation for analysis of the regional and function-specific control of the heart by discrete sympathetic and parasympathetic pathways in large mammals (see Randall, 1994 for review). However, despite the extensive use of *in vivo*, *in vitro* and Langendorff-type isolated preparations of the hearts of small mammals such as the guinea pig for investigating the neural control of cardiac function, there are no complete descriptions of the anatomy of the extrinsic cardiac nerves nor of their branches into the intracardiac neural plexus in the hearts of these mammals. The present study thus includes such a description in the guinea pig.

Methods

Experiments were conducted on adult Hartley guinea-pigs (Charles River, Quebec City, Que., Can.) of both sexes, weighing 150-300 g and ranging in age from 3-7 wk. Animals were kept on a 12h light - 12 h dark photoperiod and had free access to food and water. The protocol used in this study was approved by the Dalhousie University Animal Use Committee and conformed with the animal use guidelines established by the Canadian Council on Animal Care.

Gross anatomy of cardiac innervation

To establish the courses of the cardiac branches of the vagus and cardiopulmonary nerves into the cardiac ganglionated plexus, gross dissection of the heart and associated tissues was undertaken in 15 animals. Animals were killed by a blow to the head. A block of tissue consisting of the thorax and root of the neck was separated from the rest of the body, rinsed in saline solution (0.9% NaCl, pH adjusted to 7.4) and submerged for dissection in a dish. Most of the ribcage was removed to expose the thoracic viscera and the dorsal thoracic wall, vagal and cardiopulmonary nerves, and stellate and middle cervical ganglia were dissected free of surrounding tissue. Pathways of the extrinsic nerves into the heart were traced with the aid of a dissecting microscope. The composite description of these pathways given in the Results section was developed from observations and drawings made during these dissections.

Immunohistochemistry

For immunohistochemical studies of the intracardiac nervous system animals were killed as described above, their hearts were immediately removed through a midline sternotomy and washed in 0.1 M phosphate-buffered (pH 7.4) saline (0.9 % NaCl). Both atria were dissected *en bloc* from the ventricles, the interatrial septum was separated from the external atrial walls and atrial tissue was stretched to lie flat when pinned to a layer of silicone rubber on the bottom of the dissecting dish. The tissue was fixed for 18 hours at 4°C in 4 % paraformaldehyde dissolved in 0.1 M phosphate buffered saline, rinsed, dehydrated in a graded series of ethanol solutions, cleared in xylene, then rehydrated and

permeabilized by incubation in a 4% solution of Triton-X 100 in phosphate-buffered saline for 2 days to enhance penetration of the antibodies into the tissue. Atrial and septal tissues were then incubated as free-floating wholemounts in blocking solutions of 2.5% normal goat, donkey or rabbit serum as appropriate for the antibody used (for details and sources of primary and secondary antibodies and dilutions used in this study, see Table 1) to reduce non-specific staining. Double-label immunocytochemistry was performed with an initial incubation (48 hr) in a primary antiserum directed against either TH or ChAT, followed by a second incubation (48 hr) in primary antiserum directed against PGP 9.5 (Table 1). After treatment with primary antisera, tissue was incubated with secondary antibodies conjugated with rhodamine or fluorescein-isothiocyanate (FITC), as shown in Table 1. For viewing and photography, whole-mount tissue was coverslipped in a solution of glycerol and phosphate-buffered saline (3:1 by volume), or was rapidly dehydrated in alcohol and cleared in xylene to improve the contrast between labelled elements and background before being mounted in Accumount mounting medium (Baxter Scientific Products, McGraw Park, IL, USA). Fluorescent labels were visualized with a standard compound microscope equipped for epifluorescence (Aristoplan, Leica Canada Ltd, Willowdale, Ont., Can.) using appropriate filter cubes (Type N21 for rhodamine and Type L3 for FITC). The number of labelled cells in all regions of both atria and the interatrial septum was counted in each specimen. Atrial tissue was photographed (Kodak T-Max 100 film) through the microscope on a grid pattern of overlapping rectangular fields (1.5 by 2.5 mm field size, using a 6.3 magnification

Table 1. Sources and dilution of primary and secondary antibodies used in this study.

Table 1

Primary Antibodies

antigen	host	supplier	dilution
protein gene product 9.5	rabbit	Ultraclone[1]	1:400-800
choline acetyltransferase	goat	Chemicon[2]	1:250
tyrosine hydroxylase	mouse	Incstar[3]	1:500

Secondary Antibodies

antigen	conjugate	host	supplier	dilution
rabbit IgG	rhodamine	goat	Jackson[4]	1:50
goat IgG	FITC	donkey	Jackson[4]	1:50
mouse IgG	FITC	sheep	Jackson[4]	1:50

[1] Ultraclone Limited, Isle of Wight, England
[2] Chemicon International Inc., Temecula, CA, USA
[3] Incstar Corporation, Stillwater, MN, USA
[4] Jackson Immunoresearch Laboratories Inc., West Grove, PA, USA

objective lens). These photographs were digitized with a desktop scanner (Deskjet, Hewlett-Packard, Palo Alto, CA, USA) and stored on disk; the resulting image files were then assembled into montages using image processing software (Photoshop, Adobe Systems Inc., Mountain View, CA, USA) to produce maps of the distribution of labelled nerve fibres and intracardiac neurons. Selected areas of some hearts were also examined with the aid of a confocal microscope (LSM 410 equipped with an Axiovert 100, Carl Zeiss Inc., Thornwood, NY, USA) to clarify details of labelled neurons, and to provide an estimate of possible errors in counting the number of neurons. The majority of intrinsic cardiac neurons occurred in ganglia of less than 20 neurons, and since these ganglia consisted of a single layer of neurons these were easily counted using the standard microscope. However neurons in some ganglia containing more than 20 cells were observed to overlap one another. In order to assess the degree of overlap, and thus evaluate a potential error in neuron counts, the number of neurons in representative ganglia of different sizes was counted first in the Aristoplan microscope. The same ganglia were then imaged in the confocal microscope, making use of the optical sectioning capability of this instrument to determine the proportion of overlapping neurons.

Both positive and negative controls were employed to establish the specificity of the immunohistochemical protocols used in this study. Motor neurons in the ventral horn of the spinal cord of the guinea-pig display ChAT-IR (Eckstein and Sofroniew, 1983), and neurons in the stellate ganglia display strong TH-IR (Bowden and Gibbins, 1992; Heym *et al.*, 1993). Therefore, in the present study samples of spinal cord and stellate ganglia were taken from the same animals yielding cardiac tissue and were processed

with the same protocols as (and in some cases along with) the cardiac tissue. ChAT-IR neurons were observed in the dorsal horn, in the intermediolateral cell column and in the ventral horn; all of these neurons were also immunoreactive for PGP 9.5. These experiments confirmed the efficacy of PGP 9.5-IR as a neuronal marker and also showed that ChAT- and PGP 9.5-IR are co-localized in central neurons in the guinea pig which have been characterized as cholinergic. For both PGP 9.5 and ChAT, non-specific background labelling of cardiac tissue was low, as was autofluorescence. In experiments designed to establish positive controls for TH-IR, neurons in sections of stellate ganglia taken from the same animals as the cardiac tissue (fresh frozen tissue, sections 40 μm thick) were strongly TH-IR, and these neurons were also double-labelled with antibodies against PGP 9.5. Non-specific background labelling in atrial and stellate tissue processed for TH-IR was low, as was tissue autofluorescence at the wavelength used for visualizing the fluorophores used.

To establish negative controls, atria were removed from a separate group of animals and processed with the same protocol used for tissues in the experimental group, with one of the following changes: primary antibodies were omitted from the incubating solution; secondary antibodies were omitted; primary antibodies were preabsorbed with their appropriate antigen (100 times the concentration of the antibodies) for 24-48 hr before being used for tissue incubation. Control cardiac tissue exposed to primary but not to secondary antibodies, and *vice versa*, did not contain any label, nor did tissue in which the primary ChAT antibody had been preabsorbed with ChAT antigen.

Aldehyde histofluorescence

The presence of catecholamines in whole mounts of freshly dissected atrial tissue in 6 animals was detected using a technique modified from that described by Furness *et al.* (1977) and Molist *et al.* (1993). Briefly, cardiac tissue was obtained as described above, pinned flat and fixed in a solution of 4% paraformaldehyde, 0.5% glutaraldehyde and 35% glucose in phosphate-buffered saline at 4°C for 24-48 h. The tissue was then removed from the fixative, placed onto a glass slide, desiccated in a light-proof box for 48 hr, cleared in xylene and mounted in Accumount. Tissue was examined and photographed under ultraviolet epi-illumination (D filter cube: excitation bandwidth 355-425 nm, 460 nm long-pass barrier filter). With this technique cells, nerve fibres and terminals containing catecholamines fluoresced bright blue-green. Tissue which had been fixed only with paraformaldehyde, then desiccated and mounted for viewing served as a negative control for background autofluorescence; this tissue showed no fluorescence under ultraviolet illumination.

Data analysis. Counts of ChAT- and TH-IR cell bodies were made over the entire extent of both atria and the interatrial septum. Statistically significant regional differences in cell counts and other variables among the atrial areas were analyzed by ANOVA (single f-factor); where significant f-values were obtained, pairwise comparisons of means were done using the Tukie's multiple means comparison test (Zar, 1984); $P \leq 0.05$ was taken as the limit of significance. All numerical values are expressed as mean ± 1 standard error.

Results

Extrinsic innervation of the heart

Figure 2 is a composite drawing depicting the gross anatomical organization of sympathetic and parasympathetic innervation of the guinea pig heart. Details of the first-degree ramifications of these nerves into the cardiac nerve plexus, representing observations from dissections in 15 animals, are given below.

A) Parasympathetic innervation. The trunks of the vagus nerves followed the course of the great vessels from the thoracic inlet to the heart. Caudal to the ligamentum arteriosum, the trunk of the left vagus turned medially to pass over the dorsal surface of the left bronchus. Three to five small branches arose from the trunk between the origin of the recurrent laryngeal nerve and the approach of the trunk to the bronchus. These branches coursed to the left pulmonary artery where one or two ran along the artery toward the lungs. The rest of the branches diverged around the pulmonary artery and ran a short distance along the left pulmonary veins to the epicardium of the left atrium as shown diagrammatically in Figure 2. These branches, along with the aortic nerves in some specimens, constituted the vagal innervation of the heart on the left side. The right vagus adhered to the right lateral aspect of the ascending aorta, then as the vagus approached the heart the nerve trunk separated from the aorta to approach and then cross the dorsal surface of the anastomosis of the left and right precaval veins with the superior vena cava. In all animals the right vagal trunk then coursed along the dorsomedial aspect of the venacava to the dorsal atrial wall in the area of the junction of the atrial wall with

Figure 2. Dorsal view of the extrinsic innervation of the guinea pig heart, illustrating the entry paths of branches of the sympathetic and parasympathetic nerves into the intracardiac nervous system. Drawing not to scale. The dots indicate areas where the highest concentrations of neurons were found. Abbreviations: AO, aorta; ASC, ansa subclavia; AZV, azygous vein; CPN, cardiopulmonary nerves; GCV, great cardiac vein; LAA, left atrial appendage; L SIV, left superior intercostal vein; L, R MCG, left and right middle cervical ganglia; OBL V, oblique cardiac vein; PV, pulmonary veins; RAA, right atrial appendage; S, line indicating junction of interatrial septum with external atrial wall; L, R SG, left and right stellate ganglia; SVC, IVC: superior and inferior vena cavae; T2, second thoracic ganglion; L, R VN, left and right vagus nerves. Dashed oval indicates approximate location of sinoatrial node.

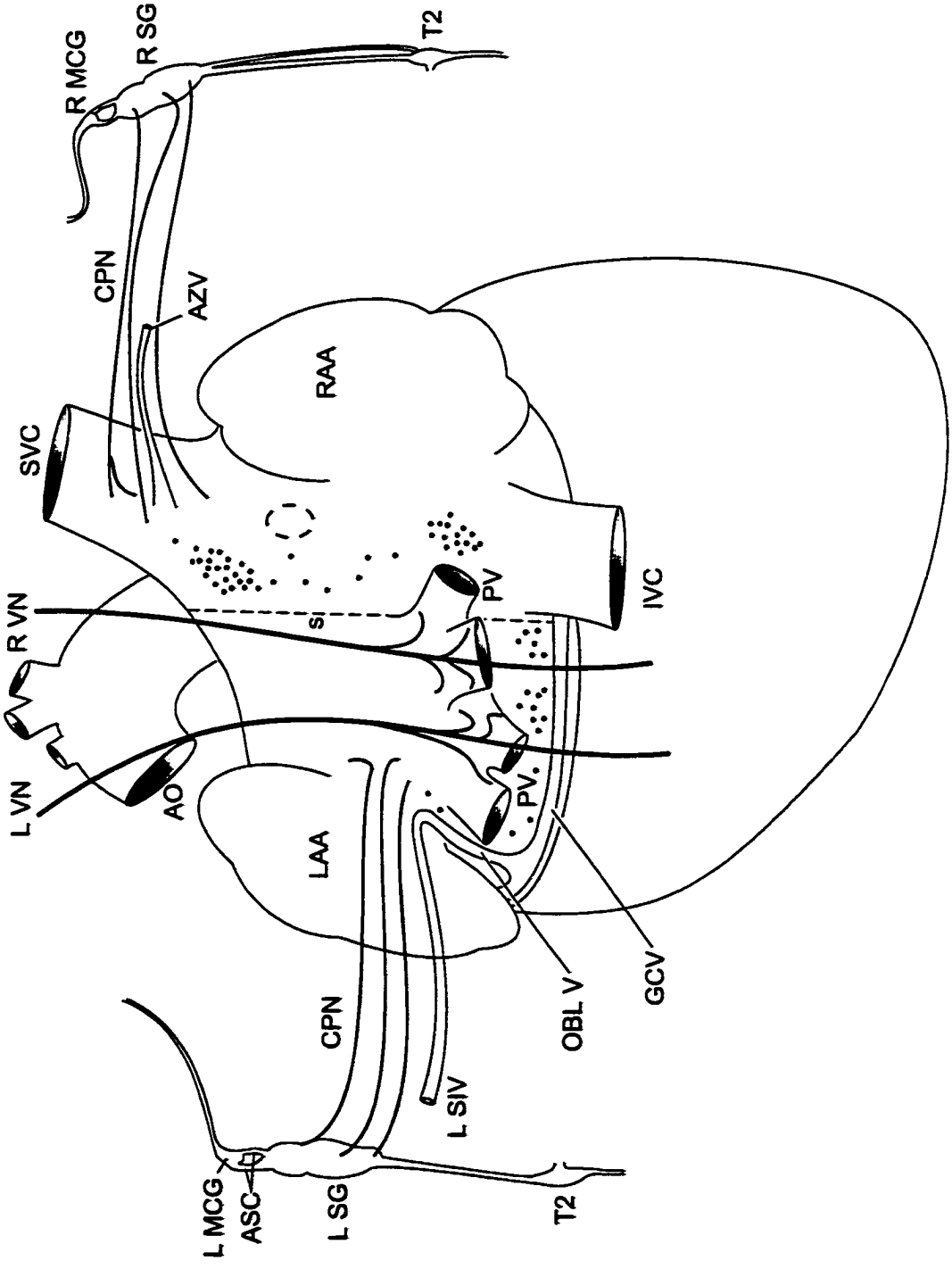
R MCG
R SG
T2
CPN
AZV
SVC
RAA
R VN
si
PV
IVC
L VN
AO
PV
LAA
CPN
OBL V
GCV
L SIV
L MCG
ASC
L SG
T2

Figure 2

the septum. One large and two or three smaller cardiac nerves arose from the right vagal trunk to ramify into the intracardiac plexus in the vicinity of the roots of the right pulmonary veins and to the left of the septum-atrial wall junction (Fig. 2, cf. Fig. 3).

B) Sympathetic innervation. In the guinea pig, cardiopulmonary nerves arising from the left and right stellate ganglia, the ansae subclavii and the middle cervical ganglia convey sympathetic efferent postganglionic fibres to the heart. The pathways of cardiopulmonary nerves on the right and left sides followed fascial planes within the mediastinal pleura to the heart along a course that generally paralleled the venous drainage of the dorsal thoracic wall. On the left side all cardiopulmonary nerves converged on the left superior intercostal vein, accompanying this on its passage through the pericardium to the left atrium (Fig. 2). The nerves then joined the dorsal aspect of the left atrium medial to the appendage where they could be seen to ramify separately into the myocardium (Fig. 2). On the right side cardiopulmonary nerves accompanied the azygos vein toward the heart, following this vein medially to the dorsomedial aspect of the superior vena cava (Fig. 2). These nerves then ran a short distance along the superior vena cava to ramify in the myocardium of the right atrium in the intercaval region close to the junction of the interatrial septum with the external wall of the atrium and near the sinoatrial node pacemaker region (Fig. 2).

Intracardiac nervous system

A) Distribution of PGP 9.5-IR nerve fibres.

The complement of neurons and extrinsic and intrinsic nerve fibres present in the nervous system of 13 guinea pig hearts was visualized with antibodies to the general vertebrate neuronal marker PGP 9.5. Neuronal elements in all regions of the atria showed positive immunoreactivity to PGP 9.5 antibody, and examples of the distribution of these elements in the atrial walls and in the interatrial septum are shown in the composite photomicrographs of Figures 3 and 4 respectively. These composite images were constructed from photomicrographs of tissues taken from a representative heart; the overall pattern of innervation was broadly similar in all hearts examined but there was considerable individual variation in the details of fine fibre distribution and location of intracardiac ganglia. Large nerve bundles with cut ends are visible in the left (LVN, LCPN) and right (RVN, RCPN) atria, representing intracardiac continuations of the branches of the extrinsic parasympathetic and sympathetic nerves illustrated in Figure 2 (see legend for abbreviations).

i) Vagal branches to atrial walls. Branches of the left and right vagi entered the left atrium superior to the roots of the left and right pulmonary veins respectively, as shown in Figure 2. From both of these sites extensive ramifications contributed to the nerve plexus supplying the atrial myocardium. From the left vagal branches numerous small bundles could be traced: 1) laterally toward and along the border between the left atrium and the left ventricle; 2) to more anterior parts of the atrium in the direction of the left atrial appendage and the junction of the cardiopulmonary nerves with the atrium; and 3) toward the midline of the heart where some bundles mixed with those originating from the right vagus. From the right vagal branches nerve bundles were distributed to: 1) the

medial right atrium; 2) along the border of the right atrium with the right ventricle (seen in the lower right portion of Fig. 3); and 3) toward the area of the sinoatrial node, located as indicated by the dashed circle in Figure 3.

ii) Cardiopulmonary nerve branches to atrial walls. Cardiopulmonary nerves arise from the stellate ganglion, middle cervical ganglion and ansa subclavia (Figure 2). Nerves innervating the left side of the heart joined the left atrium in a highly localized region medial to the appendage, and then ramified in several directions (Fig. 3). Major branches travelled dorso- and ventrolaterally around the opening of the left atrial appendage, innervating the atrial myocardium dorsal, lateral and ventral to this opening. In some hearts a few of these branches were traced across the atrioventricular border and into the left ventricle (not shown in Fig. 3). Smaller nerves arising from the sympathetic branches around the dorsal aspect of the opening to the left atrial appendage continued dorsally into the area lateral to the left pulmonary veins; this area was also innervated by lateral branches of the left vagus nerve. The cardiac plexus in this area thus consists of a relatively high density of mixed vagal and sympathetic fibres. Several major branches of the left cardiopulmonary nerves ramified in a dorsomedial direction toward the interatrial septum (see Fig. 4 and description of septum below) and the area just superior to the roots of the pulmonary veins where there was also a dense vagal innervation; here also the nerve intracardiac plexus was mixed. The right cardiopulmonary nerves entered the myocardium of the right atrium more ventrally and medially than did their counterparts on the left. In addition the pattern of distribution of right cardiopulmonary nerve branches within the myocardium appeared to be more diffuse (that is, with smaller and more numerous branches) relative to the pattern on the left. The primary site of entry of

Figure 3: Composite photomicrograph of whole-mount preparation of the external walls of the left and right atria after processing for PGP 9.5-IR. A line running between the tips of the large arrows (top and bottom of the image) delineates the junction of the interatrial septum with the external atrial wall. With the exception of the areas labelled PV, IVC and SVC, the edges of the tissue represent the atrioventricular borders. The approximate location of the sinoatrial node is outlined by the dashed circle near the centre of the figure. Neuronal somata, mostly occurring in ganglia, were found throughout both atria; examples of five large ganglia are indicated by the small arrows. The apexes of the white triangles indicate cut ends of branches of right (RCPN) and left (LCPN) cardiopulmonary nerves and the cardiac branches of the right (RVN) and left (LVN) vagal nerves. AV: atrioventricular border; other abbreviations as for Figure 2. Scale bar represents 2.5 mm.

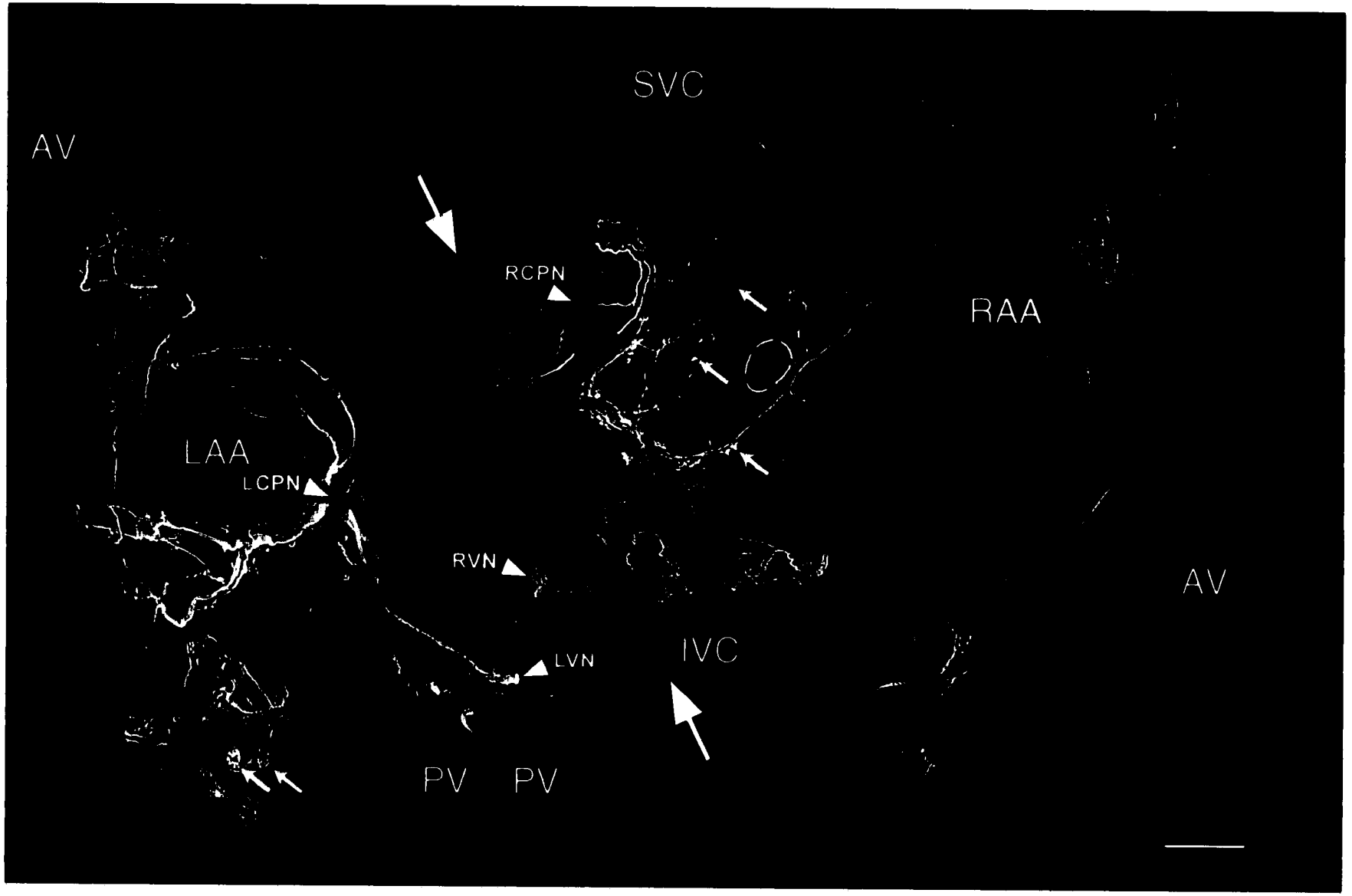

Figure 3

Figure 4: Composite photomicrograph of a whole-mount of the interatrial septum taken from the same heart as the atria shown in Figure 3. The tissue is oriented with the dorsal edge of the septum to the right of the frame and the most cranial portion is uppermost. This figure is shown at a higher magnification than Figure 3 to illustrate more clearly the ganglia and nerves. Scale bar represents 1 mm.

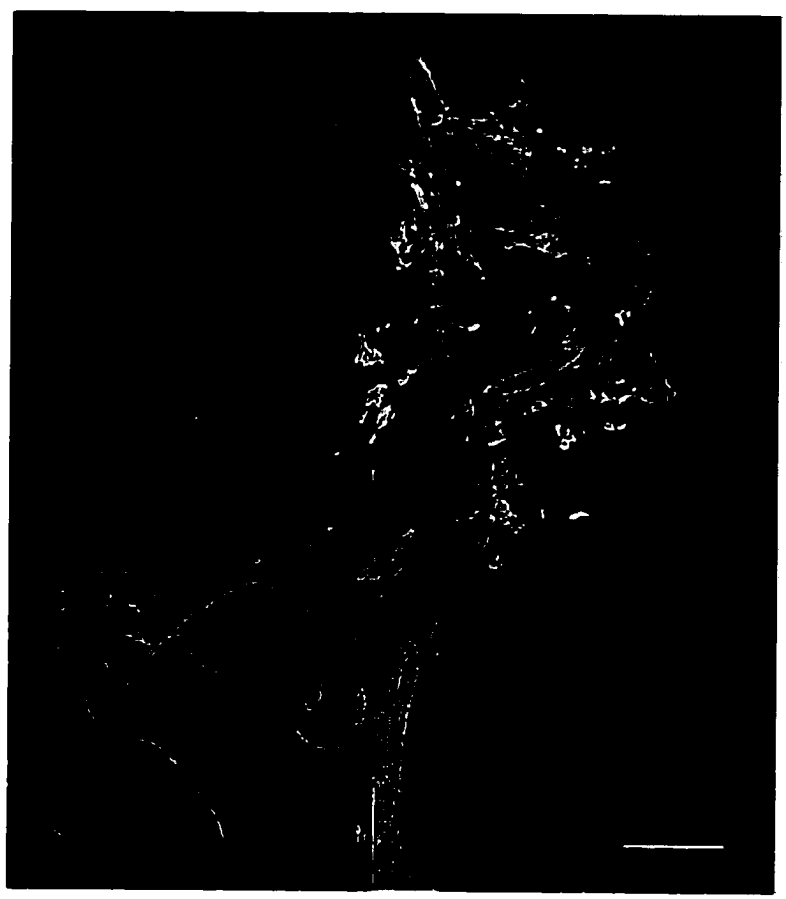

Figure 4

right cardiopulmonary nerve branches into the cardiac plexus of the right atrium was between the openings of the superior and inferior venae cavae in an area just medial to the sinoatrial node, yet only a minority of nerve branches were observed to course directly to the nodal region (Fig. 3). The majority of nerve branches ran: 1) into and along the dorsal and lateral walls of the superior vena cava in a cardiofugal direction; 2) medially and ventrally toward and across the junction of the septum with the external atrial wall, continuing into the left atrium; and 3) toward the inferior vena cava and into an adjacent region of the myocardium which is also heavily innervated by branches of the right vagus. Some small nerve bundles could also be traced from the region of the inferior vena cava laterally into the crista terminalis and on into the wall of the right atrial appendage.

iii) Interatrial septum. The septum was separated from the atrial walls to facilitate penetration of antibodies into the tissue. This procedure consequently precluded tracing specific vagal and sympathetic nerve branches into the septum, so the branches of origin of septal innervation could not be determined in this study. Nerve fibre bundles in the septum were concentrated primarily in the cranial portion (Fig. 4). Both large and small bundles of nerve fibres were visible, with typically one large and several smaller bundles running from the cranial portion toward the atrioventricular valves (off the bottom edge of Fig. 4). The concentration of nerve fibres in the cranial part of the septum corresponded with a pattern of relatively dense innervation of the external atrial myocardium in the area of the septum-atrial wall junction, as described in sections (i) and (ii) above. It therefore appears that the plexus of the external atrial wall is contiguous

with the septal innervation, and septal nerves running in the direction of the ventricles may therefore represent a major pathway for the innervation of these chambers.

B) Distribution of ChAT-IR cells and fibres

i) ChAT-immunoreactive elements. In all 8 hearts processed for ChAT-IR there was complete overlap with PGP 9.5-IR in somata of intracardiac neurons, as shown in the example of Figure 5. The somata of individual neurons in the guinea pig atria were predominantly prolate spheroid in shape (Fig. 5, 6). An estimate of mean neuronal size was obtained by measuring with an ocular micrometer the long and short axes of 60 ChAT-IR neurons randomly sampled from 5 hearts. Mean length of the long axis was 27 ± 1 μm (range 20-45), while the mean length of the short axis was 21 ± 0.5 μm (range 15-30); these dimensions were significantly different (t test, $P \leq 0.05$). Many neurons appeared to have only one large process, likely the axon, which emerged from one end of the soma (e. g. Fig. 6). Other small processes could be observed emerging from the somata of a few neurons, but these were not apparent in most cells.

Neurons were found singly or clustered into ganglia throughout the atria (Fig. 5, 6). Ganglia ranged in size from 2 neurons to more than 100 neurons and were flattened in the plane of the atrial wall so that they were seldom thicker than one layer of neurons. In some ganglia of more than 20 neurons these cells occurred in two layers with the superficial layer overlying the deep layer; the implications of this

Figure 5: Confocal photomicrographs of right atrial ganglion neurons double-labelled with antibodies against ChAT (red; secondary antibody conjugated with rhodamine) and PGP 9.5 (green; secondary antibody conjugated with FITC). A: Rhodamine-filter exposure showing ChAT-positive neuronal somata and nerve fibres. B: FITC-filter exposure of same ganglion as (A), showing PGP 9.5-positive elements. C: Double-filter exposure showing same ganglion as in (A) and (B), together with surrounding tissue. In this example and throughout the atria, all PGP 9.5-IR neurons were ChAT-positive. Scale bar represents 50 μm.

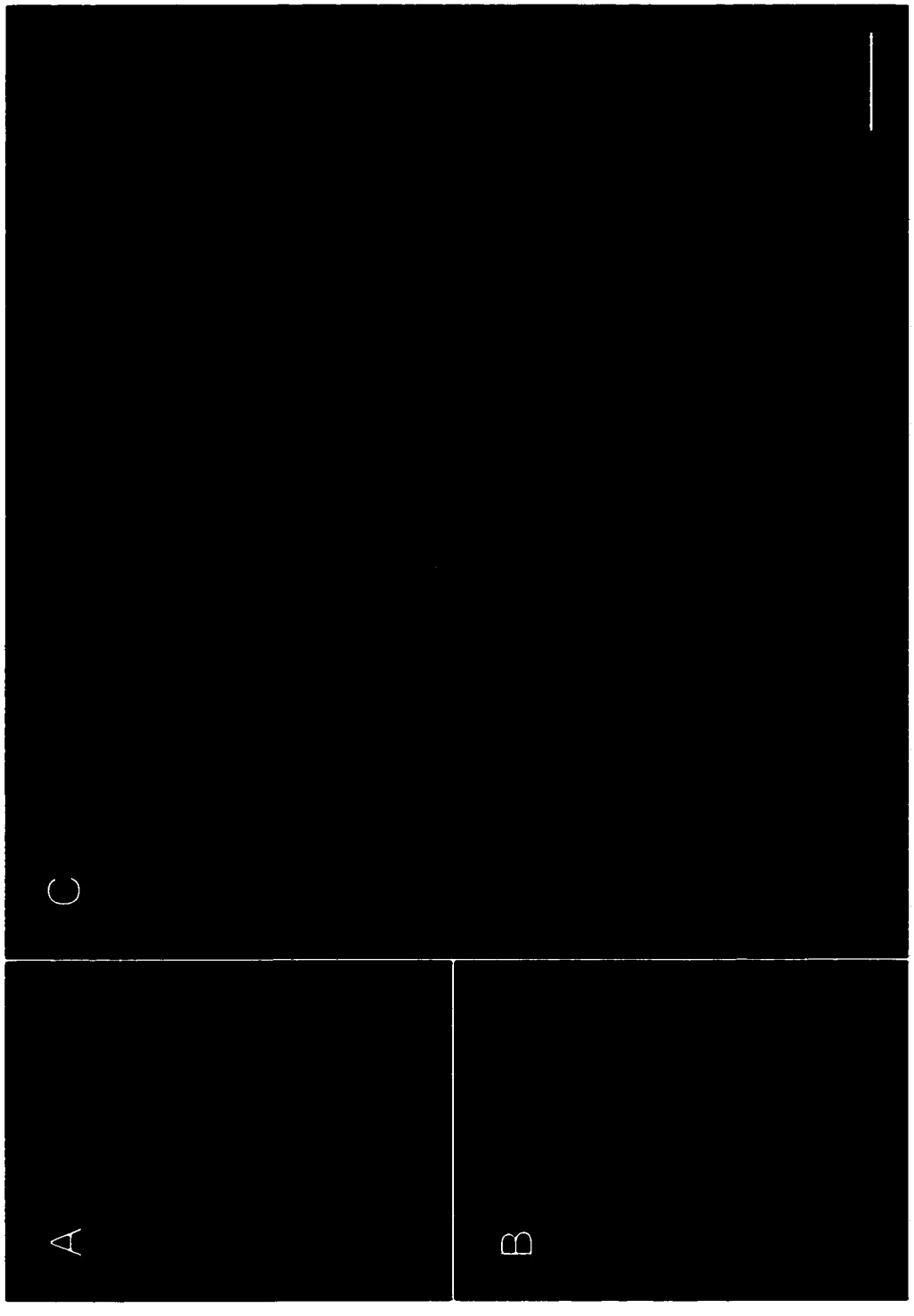

Figure 5

Figure 6: Confocal photomicrograph of atrial tissue double-labelled with antibodies against PGP 9.5 (green; FITC) and TH (red; rhodamine). No colocalization of the two labels was observed in cells intrinsic to the heart. Note the short proces extending from one of the TH-IR cells (triangle with asterisk). Some TH-IR varicosities are visible within the ganglion (triangles). Scale bar represents 50 μm.

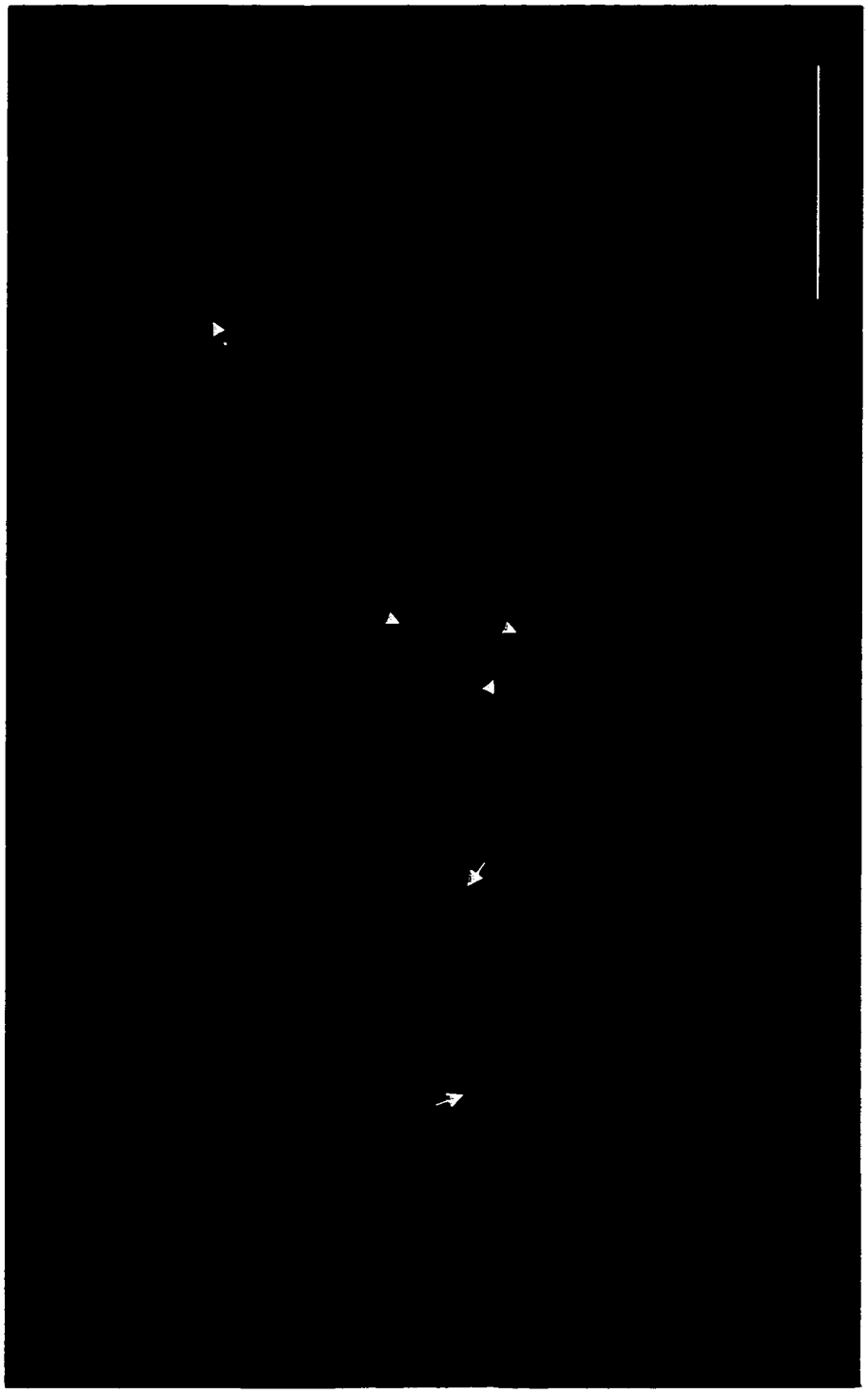

Figure 6

finding for the accuracy of neuron counts are further addressed below. Ganglia were always connected to the intracardiac plexus by more than one fibre bundle; in some cases more than 10 nerves of varying sizes were counted in association with individual small to medium sized ganglia (20 to 50 neurons). Ganglia were frequently located at the junctions of large nerves, or were situated to one side of a large nerve with a number of smaller nerves connecting to other ganglia (e. g., Fig. 5, 6) or to the myocardium. Ganglia throughout the external atrial walls were associated with the epicardium, being bounded superficially by the mesothelium with its subendocardial layer of connective tissue and more deeply by myocytes. Even in areas where the myocardium consisted of multiple layers of myocytes, no ganglia were seen embedded among the myocytes. However, within the interatrial septum, which had the thickest myocardium of all atrial regions, numerous ganglia were embedded among layers of myocytes.

Table 2 gives the mean total number of ChAT-positive neurons counted in the atria (1510 ± 251) and the distribution of these neurons by region. The standard error of the mean total neuron count was relatively large (17 % of the mean value), indicating a substantial variability of total atrial neuron populations among the hearts in this study. This variability was further reflected in the range of total counts, from 717 to 2542 atrial neurons per individual in the 8 hearts sampled. These counts may have underestimated the total number of neurons present because of potential overlap of neuronal somata in a deep layer by neurons in a superficial layer within some larger ganglia. This degree of overlap was estimated to be 10 % in ganglia having two layers; that is, confocal microscopy of ganglia in which neuron counts had been previously made using the standard microscope showed that 10 % of the neurons were missed in such ganglia

because those in the superficial layer obscured some neurons in the deep layer. An estimated 15 % of the total number of neurons in the atria were located in ganglia larger than 20 cells. However an error of 10 % in this portion of the total number of neurons is relatively small (1.5 % of the total). Since this error factor could not be determined precisely without examining all large ganglia in the confocal microscope, and since it was likely of small magnitude in any case, no corrections were made in the neuron counts.

In Table 2 the results of quantitative regional analysis of atrial neuron distribution are presented. The atria were divided into 3 territories: right atrium (RA), left atrium (LA), and the interatrial septum (S). The region designated as RA consisted of the external wall of the right atrium extending from the septum-atrial wall junction (along a line running between the large arrows in Fig. 3) to the right ventricular border. The LA region consisted of the external wall of the left atrium extending from the septum-atrial wall junction to the border of the left ventricle. The left atrial appendage, because it projected further from the atrial wall than did the right appendage, caused tissue folding when the preparation was flattened during the preparation of whole-mounts and was therefore removed from all specimens. The right appendage did not hinder preparation of whole-mounts and was left attached. Neither the right nor the left atrial appendage contained neurons in any of the specimens. The region designated S (Fig. 4) consisted of the septal tissue dividing the right and left atrial chambers.

The mean area of the RA region, representing 59 % of the total atrial area, was significantly larger than that of the LA (36 % of total area), the difference between these areas being due at least partly to the exclusion of the left atrial appendage from the area measurements. However, despite the difference in areas between the two regions, the

Table 2. Mean number and proportional distribution of ChAT-IR neurons (n=8) and TH-IR cells (n=5) in guinea-pig atria, and regional density of neuron occurrence (neurons/mm^2). LA: left atrium; RA: right atrium; S: interatrial septum. Values expressed as mean ± 1 SE.

Table 2

	LA	RA	S	mean total
ChAT-IR neurons	714 ± 127	485 ± 124	# 312 ± 56	1510 ± 251
% of total neurons	47%	32%	21%	
area (mm^2)	+ 129 ± 6	210 ± 9	• 19 ± 1	359 ± 14
% of total area	36%	59%	5%	
density	6.4 ± 1.2	2.4 ± 0.7	* 16.3 ± 4.0	5.2 ± 0.7
TH-IR cells	46 ± 11	60 ± 27	18 ± 6	124 ± 33
% of total cells	37%	48%	14%	
area (mm^2)	+ 120 ± 12	193 ± 13	• 22 ± 1	372 ± 24
% of total area	32%	52%	6%	
density	0.4 ± 0.1	0.3 ± 0.1	0.8 ± 0.3	0.3 ± 0.1

mean number of ChAT-IR neurons in S region significantly less than in LA.

+ LA area significantly smaller than RA.

• S area significantly smaller than areas of LA and RA.

* density of neurons in S significantly greater than in RA and LA.

number of neurons in the RA was not significantly different from the number in the LA. To develop a general numerical index of the regional distribution of atrial neurons, a value for the density of neuron occurrence in each region was obtained from the quotient of mean regional number of neurons and mean regional area ("density" in Table 2). A comparison of density values for RA and LA showed that there was no significant difference between these areas, indicating that, overall, numbers of neurons were relatively even between the atria. The distribution of neurons within these regions was different, however. The majority of neurons in the RA was concentrated near the SA node and near the ostium of the IVC (Fig. 2, indicated by dots). Neurons in the LA tended to concentrate in a broad band between the roots of the pulmonary veins and the atrioventricular border (Fig. 2, dots) but were in general more widely scattered in the LA than in the RA.

The mean area of the septum was significantly smaller than RA and LA areas (Table 2), representing only 5 % of the total area of the atria. The mean number of neurons contained in the septum (21 % of mean total number) was also significantly less than the numbers in the RA and LA, yet the value of neuron density in the septum was significantly greater than the density of neurons in either the LA (2.5 times as dense) or the RA (more than 6 times as dense). These results show that atrial neurons were located in greatest concentration in the septum.

If neurons in different atrial regions subserve different functions as has been proposed on the basis of functional evidence (Ardell, 1994), this functional differentiation might be reflected by differences in the relative number of cells per ganglion in the different regions. To analyze this, the number of neurons in each

ganglion found in the atria of the 8 hearts studied was determined. To examine the frequency of occurrence of ganglia of different sizes, the ganglia were categorized into 11 size ranges. The smallest size category included single neurons together with ganglia containing 2 to 4 cells; size categories increased in increments of 4 cells each until the largest size category which included ganglia with 41 or more neurons. The increment of 4 neurons per category was chosen to cover the full range of ganglion sizes observed while providing a large enough number of categories to ensure accurate representation of changes in frequency of occurrence with ganglion size. An analysis of the overall frequency-ganglion size relationship is shown for all ganglia regardless of location in the top left panel of Figure 7. It is apparent from this panel that the majority of atrial neurons were organized into small ganglia; 85 % of all neurons were found in ganglia of fewer than 20 neurons. This general trend is reflected in the graphs for each of the specific atrial regions, as illustrated in the panels of Figure 7 representing distribution by the three regions. In summary, even though a few large (> 100 neurons) ganglia were found in all atrial regions there was no trend toward a preponderance of larger ganglia in any particular region.

C) Distribution of TH-IR elements

Both fibres and cell bodies within the atria of 5 hearts were immunoreactive for TH (Fig. 6, in red). Some nerve fibres were double-labelled for TH- and PGP 9.5-immunoreactivity and these fibres could be observed to run in bundles in nerve trunks and singly in association with myocardial cells throughout the atria. In addition, TH-immunoreactive fibres were present within intracardiac ganglia; some of these nerve

Figure 7: Bar graph of proportional distribution of atrial neurons, expressed as percent of mean total number of neurons, in ganglia of different size categories (number of cells in each category indicated under each bar) for both atria combined ("all regions", top left panel) and by region. Ganglion size increases by 4 neurons per size category until the largest category, which represents the proportion of neurons present in ganglia of 41 neurons or greater. The majority (85 %) of neurons were contained in ganglia of fewer than 20 neurons. Error bars represent ± 1 SE.

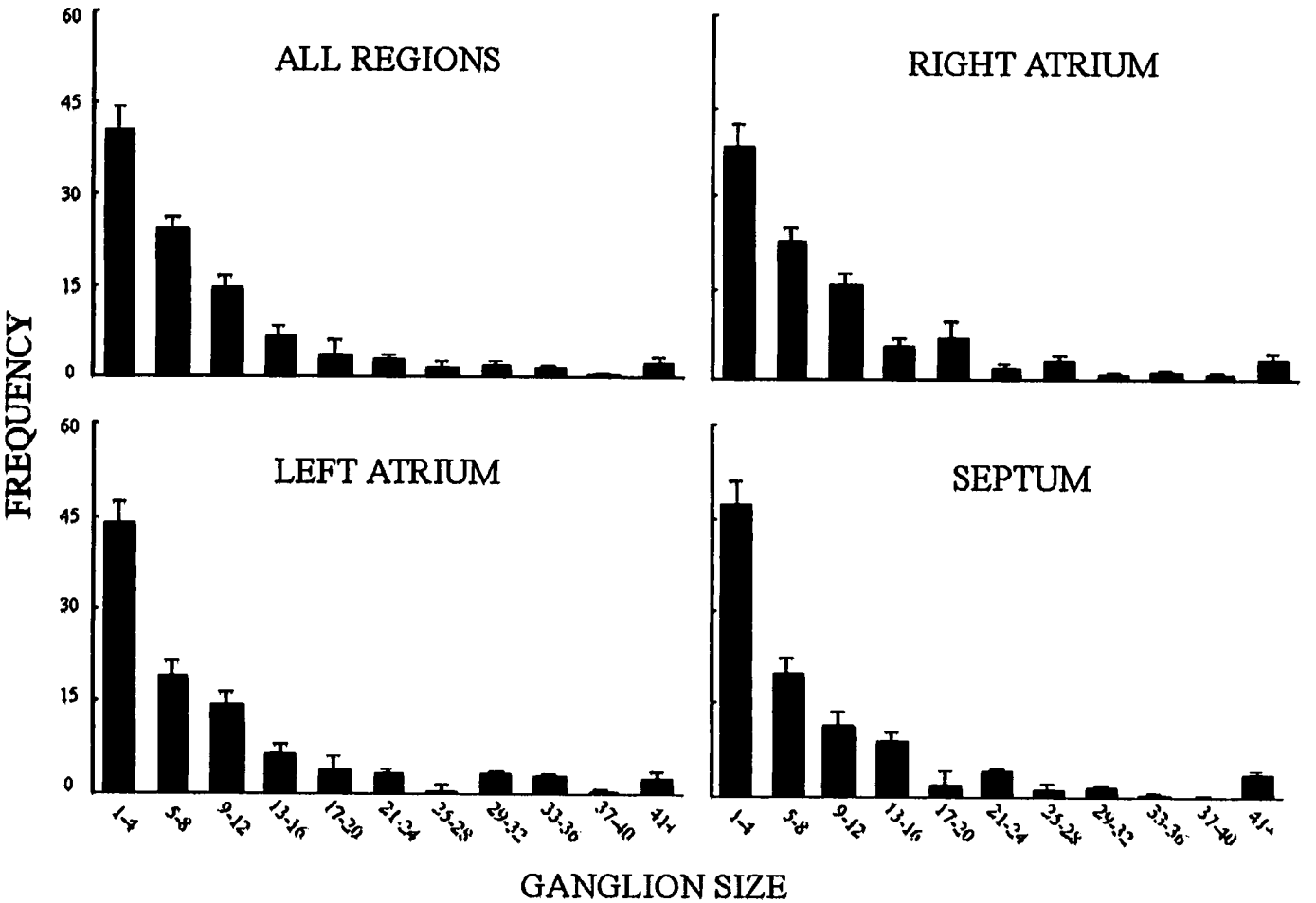
ALL REGIONS
RIGHT ATRIUM
LEFT ATRIUM
SEPTUM
FREQUENCY
GANGLION SIZE
60
45
30
15
0
1-4
5-8
9-12
13-16
17-20
21-24
25-28
29-32
33-36
37-40
41+

Figure 7

fibres had varicosities near ganglion neurons (Fig. 6, triangles). However, no TH-IR cell bodies were double-labelled for the neuronal marker PGP 9.5; instead, TH-IR was found in small, spheroid cells in the atria. These cells had a mean long axis length of 10 ± 0.4 μm (range 9-12) and a mean short axis length of 7.4 ± 0.3 μm (range 5-10 μm; data from 21 cells randomly sampled from 3 hearts). The largest of these cells was smaller than the smallest ChAT-immunopositive neurons. Confocal microscopy showed that TH-IR cells usually had one or two short (length 5-30 μm) processes; an example of such a process can be seen in Figure 6 (small triangle with asterisk).

The mean total number of TH-IR cells was approximately 12 % of the mean total number of neurons found in the atria. 85 % of TH-IR cells were found in the right and left atrial regions (Table 2). There was no significant difference in the number or the density of TH-IR cells between the right and left atria. The mean number of TH-IR cells in the septum (15 % of mean total) was significantly less than the numbers of cells in the right or left atrium, but cell density in the septum was not significantly different than in the external atrial walls. The results of this analysis indicate that TH-IR cells are generally not concentrated preferentially in any region of the atria.

TH-positive cells occurred singly or were grouped together in clusters with the majority (more than 90 %) of TH-IR cells located in, or closely associated with, intracardiac ganglia; Figure 6 shows a typical example of the anatomical relationship of TH-IR cells to principal ganglion neurons. Only a few TH-IR cells were associated with the myocardium in areas remote from nerve trunks or ganglia; these cells were found singly or in small clusters of fewer than 10 cells. An analysis of the frequency of

occurrence of TH-IR cells in clusters of different sizes over the whole extent of the atria showed a qualitatively similar pattern (top left panel, Fig. 8) to that for ChAT-positive neurons (cf. Fig. 7). Overall 85 % of TH-positive cells occurred singly or were contained in clusters of up to 8 cell bodies. The other 15 % were distributed in a few clusters ranging in size from 9 to 40 cell bodies, and this overall pattern is reflected in the analyses of distribution by individual region shown in Figure 8. Th-IR cells thus appear, like ChAT-IR neurons, to be preferentially distributed in clusters containing relatively few cells.

A number of small TH-IR varicosities associated with individual nerve fibres was observed within ganglia when viewed with the confocal microscope, and an example of this is shown in Figure 6 (triangles). However it was not clear whether these varicosities were associated with extrinsic sympathetic postganglionic axons or with processes of intracardiac TH-IR cells. Using the optical sectioning capability of the confocal microscope, the paths of some of the processes emerging from a number of TH-IR cells, like that shown in Figure 6 (triangle with asterisk), were followed to determine whether these processes had varicosities, but none was observed in the specimens examined. However, the processes of some TH-IR cells closely approached the somata of other nearby TH-IR cells (not shown), raising the possibility of direct cell-to-cell communication within this population.

Histochemical location of biogenic amines

In order to determine if there was any similarity in the morphology of TH-IR and catecholamine-containing elements within the atria, aldehyde-induced fluorescence was

Figure 8: Bar graph of proportional distribution of TH-IR cells in the atria, expressed as percent of mean total number of cells, in clusters of different size categories (number of cells in each category indicated under each bar) for both atria combined and by region, presented in a format similar to that used for neurons in Figure 7. 85 % of TH-IR cells were found in clusters of 8 cells or less. Error bars represent ± 1 SE.

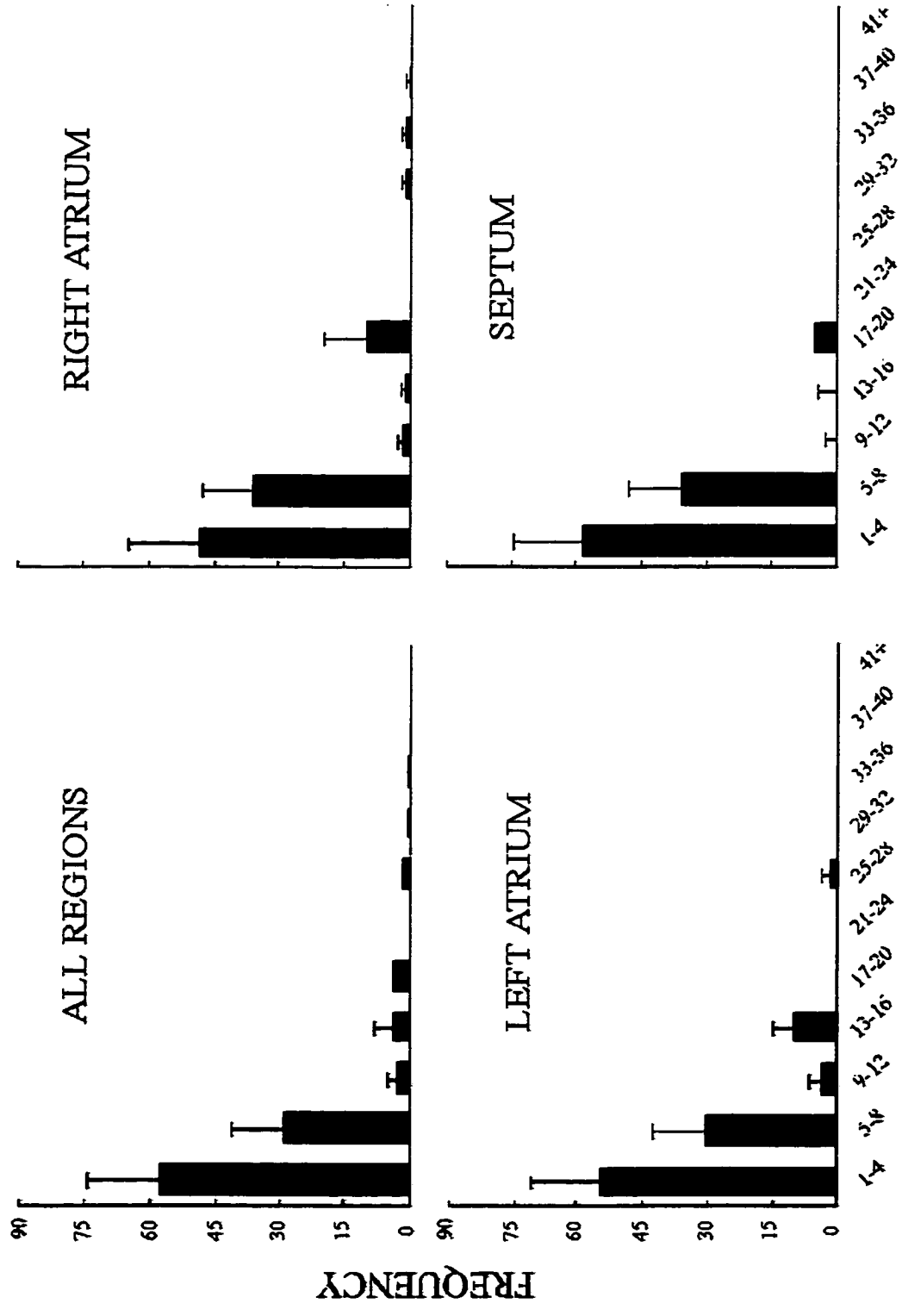
ALL REGIONS
RIGHT ATRIUM
LEFT ATRIUM
SEPTUM
FREQUENCY
CLUSTER SIZE
0
15
30
45
60
75
90
1-4
5-8
9-12
13-16
17-20
21-24
25-28
29-32
33-36
37-40
41+

Figure 8

used to identify catecholamines histochemically. In this technique, intracardiac elements containing catecholamines fluoresce a bright blue-green which is easily distinguishable from the faint background autofluorescence (Fig. 9). This method was not compatible with the immunochemical visualization of TH, so the two procedures were not combined. Catecholamine-containing cells, nerve fibres and their associated varicosities had an appearance similar to the atrial cells and fibres, which were visualized by TH immunohistochemistry. In addition, the relationship of the catecholamine-containing cells and terminals to surrounding tissue was similar to that of TH-IR elements. The similarities in morphology and distribution of catecholamine-containing and TH-IR intracardiac elements suggests that the atrial elements containing catecholamines may also be capable of synthesizing these compounds. One of the most striking findings was that amine-containing varicosities were observed not only in association with cardiac muscle cells but also within atrial ganglia (Fig. 9A, B) where they formed networks closely apposed to some principal ganglion neurons. Intraganglionic varicosities appeared to be more intensely labelled after processing for catecholamine histochemistry than those visualized using TH-IR (cf. Fig. 7 and Fig. 9B). Aldehyde histochemistry thus appears to afford a better view of the intraganglionic distribution of these terminals than does TH immunohistochemistry in guinea pig atria.

Material stained for catecholamines with the aldehyde-induced fluorescence technique could not be viewed in the available confocal microscope due to the lack of an ultraviolet light source, so the superior spatial resolution inherent in this type of microscopy could not be used to determine whether the small catecholamine-containing

Figure 9: Composite photomicrographs of whole-mount preparations of two different left atrial ganglia after histochemical processing for aldehyde-induced fluorescence, showing catecholamine-containing cells (arrows), terminals (arrow heads) and nerve fibres. A: Low magnification view of a ganglion showing a cluster of SIF cells (arrowhead) and fine networks of catecholamine-containing varicosities (triangles). One of these networks is shown enlarged (area indicated by corner brackets) in (B) below. Scale bar represents 50 μm. B: Enlarged portion of (A) to illustrate network of catecholamine-containing intraganglionic varicosities in close apposition to ganglion neurons. The cluster of brightly fluorescing cells in the upper left part of the panel (arrow) is the same cluster appearing in (A) but is out of the focal plane. Scale bar represents 25 μm.

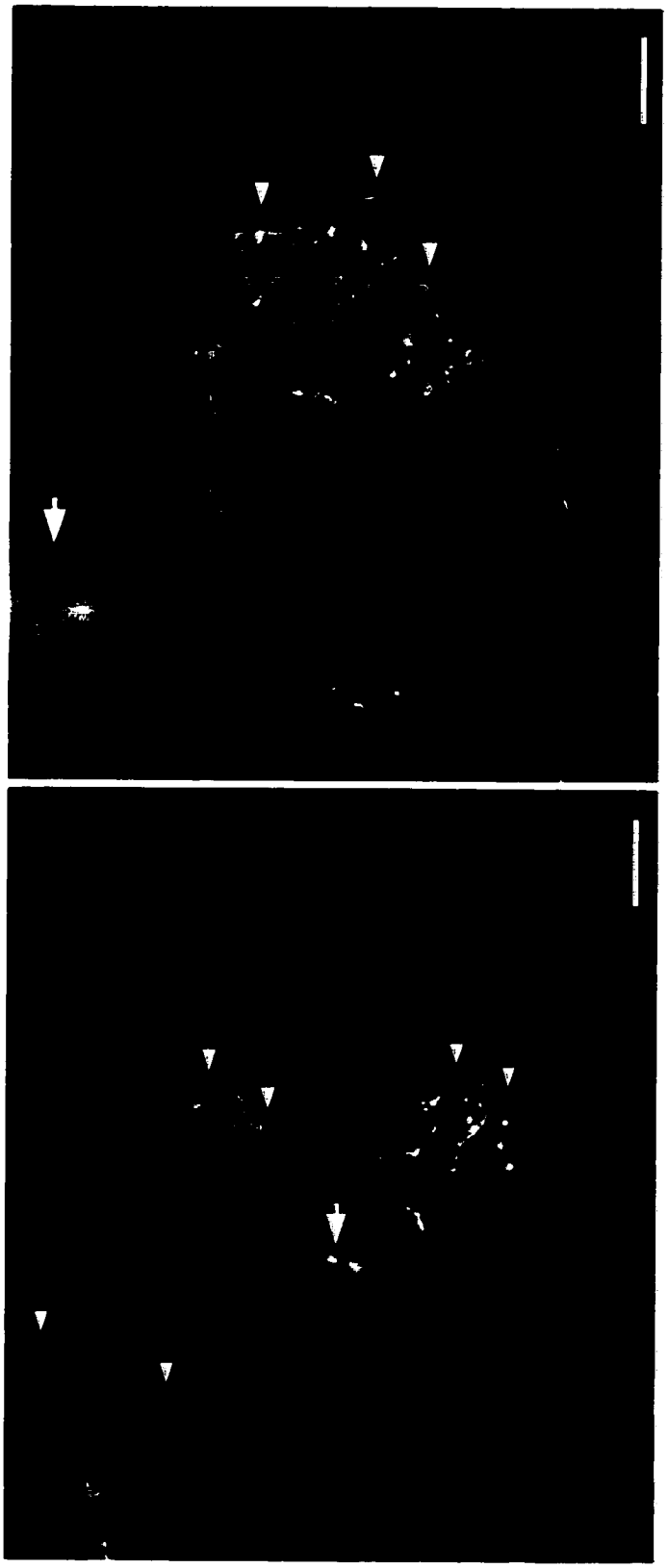

Figure 9

ultraviolet light source, so the superior spatial resolution inherent in this type of microscopy could not be used to determine whether the small catecholamine-containing cells had varicosities associated with their processes. However, observation of whole-mount material in the standard microscope at high magnification showed no evidence of varicosities in processes which originated from intrinsic cardiac catecholamine-containing cells. Fine internal details of ganglia in whole-mount tissue preparations were difficult to discern at high magnification using the standard microscope, so resolution of this issue must await the use of a more sensitive method, such as the reconstruction of serially sectioned material.

Discussion

The results of this study show that all neurons in the guinea pig atria expressing immunoreactivity for the general neuronal marker PGP 9.5 are also immunoreactive for the enzyme ChAT, the rate-limiting enzyme in ACh synthesis. The expression of this enzyme in intracardiac neurons supports the contention that these neurons express aspects of cholinergic phenotype. The occurrence of ChAT expression in groups of neurons in the central nervous system has for many years been accepted as the primary indicator of the cholinergic nature of these neurons (Kuhar, 1976; Fibiger, 1982; Eckenstein and Sofroniew, 1983; Satoh *et al.*, 1983; Rende *et al.*, 1995; Sann *et al.*, 1995). Histochemical reactions for AChE (Koelle, 1963) have also been used to investigate the distribution of cholinergic neurons in the central (Jacobowitz and Palkovits, 1974; Kobayashi *et al.*, 1975) and peripheral nervous systems (reviewed by Kuhar, 1976), and most investigations of phenotype of intracardiac neurons have relied on this technique.

However some non-cholinergic neurons and some non-neuronal elements associated with the nervous system also express AChE (Fibiger, 1982; Satoh *et al.*, 1983), leading to concern about the usefulness of AChE as a reliable indicator of cholinergic neurons in the heart. Specific antibodies against ChAT have been commercially available for some time and been widely used to map cholinergic neurons in the central nervous system, as described above. However, ChAT immunohistochemistry has only recently been applied to the problem of determining the phenotype of neurons in the peripheral nervous system. ChAT-IR neurons have been found in pelvic ganglia (Keast *et al.*, 1995), enteric ganglia (Furness *et al.*, 1983; Schemann *et al.*, 1995), gall bladder ganglia (Talmage *et al.*, 1996), tracheal plexus neurons (Dey *et al.*, 1996) and neurons of the sympathetic chain (Wang *et al.*, 1995). In the guinea pig heart, a recent survey found that all neurons in the atrial intercaval region, basal portion of the interatrial septal region, and the cardiac sinus region which expressed immunoreactivity for MAP-2, a microtubule-associated protein which has been proposed as a general neuronal marker, were also ChAT-IR (Mawe *et al.*, 1996). These authors' results have confirmed the findings of previous studies which suggested, on the basis of positive responses to histochemical reactions for AChE, that most if not all neurons in the heart were cholinergic. However, the study of Mawe *et al.* (1996) excluded major areas of both atria. The present study has confirmed the presence of large numbers of ChAT-IR neurons in the regions analyzed by Mawe *et al.* (1996) and in addition demonstrated the presence of cholinergic neurons along the atrioventricular border, throughout the full extent of the interatrial septum, and in the region around the pulmonary veins, areas which were not included in the study of Mawe *et al.* (1996). The results of the present study also confirm and extend the findings of previous studies

which showed that the majority of neurons in the hearts of a number of mammalian species are cholinergic, based on AChE histochemistry (Jacobowitz, 1967; Ehinger *et al.*, 1968; Bojsen-Moller and Tranum-Jensen, 1971; Hancock *et al.*, 1987; Roberts *et al.*, 1989; Seabrook *et al.*, 1990; Steele and Choate, 1994; Steele *et al.*, 1994; Edwards *et al.*, 1995).

The mean total number of neurons found in the adult guinea pig atria in the present study (1510, Table 2) was 1.5 times the approximately 1000 neurons reported by Mawe *et al.* (1996) in the atria of adults of the same species. This difference reflects the larger atrial area included in whole-mounts in the present study. The value for number of atrial neurons in the present study was established using antibodies against the general vertebrate neuronal marker PGP 9.5, which has been widely used in the central (Thompson *et al.*, 1983; Suburo *et al.*, 1992; Buller and Rossi, 1993; Rueff and Dray, 1993; Trowern *et al.*, 1996) and peripheral nervous systems for quantitative assessments of neuronal number and to determine the anatomy of organ innervation. In the heart in particular, the use of PGP 9.5-IR has been a reliable technique for determining the location and extent of the innervation of the myocardium and the locations of intracardiac neurons in several species including humans (Gulbenkian *et al.*, 1987; Chow *et al.*, 1993; Gordon *et al.*, 1993; Gulbenkian *et al.*, 1993; Crick *et al.*, 1994; Fu *et al.*, 1994; Gulbenkian *et al.*, 1994; Marron *et al.*, 1994).

The quantitative data for regional distribution of neurons within the atria (Table 2, Fig. 7) shows that these neurons were associated with all atrial regions. However, there were large variations in total number of neurons per heart, and in number of neurons per region, among the specimens sampled. Furthermore, these variations were emphasized

when comparing photomontages of the atria of each specimen (example shown in Fig. 3) to attempt to discern common patterns of neuronal distribution. One consistent distribution pattern occurring in the right atrium of all specimens was a clustering of ganglia in the intercaval area close to the SA node and near the IVC ostium. This pattern was also noted in the guinea pig heart by Mawe *et al.* (1996) and is similar to the pattern observed in other species. Another area of high concentration of neurons in the present study was around the base of the pulmonary veins in the left atrium, similar to the situation in rat (Burkholder *et al.*, 1992), dog (Yuan *et al.*, 1994) and human (Janes *et al.*, 1986) hearts. The interatrial septum of the hearts of both large and small mammals also contains a high concentration of neurons; in the present study one fifth of the total number of atrial neurons was located in the septum, and this area had the highest density of neurons per mm^2 (Table 2). This area also was richly innervated by nerves and single fibres, primarily in the cranial portion (Fig. 4). These nerves were probably contiguous with those in the heavily innervated areas of the external atrial walls at the septum-wall junction. Neurons and nerves in the interatrial septum are in close proximity the cardiac valves, pacemaker and conductive tissues, and are thus well positioned to modify valvular, chronotropic and dromotropic functions as proposed by Moravec and Moravec (1987).

There was a difference in the pattern of distribution of neurons in the left and right atria in the present study, but the reason underlying this difference is not clear. The area of the right atrium was significantly larger than that of the left atrium, yet the right atrium contained, statistically, the same number of neurons as did the left atrium. With the exception of a high concentration of neurons near the pulmonary veins, ganglia in the

left atrium were more widely scattered than those in the right atrium, where neurons were clustered largely near the SA node. This difference may reflect the functions of the neurons in the two chambers. Presumably a major function of right atrial neurons is control of the pacemaker and conducting tissues, which would account for the aggregation of these neurons near pacemaker tissue, but the total number of neurons which might be engaged in control of these functions is not known. In addition, neurons in the right atrium were not preferentially clustered into large ganglia, as the analysis in Figure 6 shows. In the left atrium most of the neurons would be expected to be involved in the control of myocyte contractile function, presumably dictating a more distributed pattern of location. Neurons would thus be closer to the myocardial cells they control in order to participate more effectively in local-reflex feedback loops. In summary, a more distributed neural network in the left atrium may be necessary for efficient local control of myocyte properties, while neurons in the right atrium may act more effectively in a condensed network to control pacemaker and conduction functions.

The differences in regional intracardiac neuronal distribution which were observed in this study have important implications for functional investigations of the roles of these neurons. As described above, variations in regional patterns of neuron distribution will likely be correlated with the regional control functions of these neurons. The anatomical data on the organization of the intracardiac nervous system in the present study will facilitate *in vitro* studies to physiologically define the roles of single neurons involved in control of nearby myocardial tissue, such as the rate of discharge of pacemaker cells in the SA node or control of myocyte contractile properties in the left atrium.

No TH-IR or catecholamine-containing neuronal somata were observed in the present study. Yet, *in vivo* functional studies in the hearts of other species such as the dog have shown that some intrinsic cardiac neurons are capable of evoking cardioaugmentation when activated (Butler *et al.*, 1990b; Armour *et al.*, 1993; Huang *et al.*, 1993a, b, c). This response is at least partly dependent on ß-adrenergic mechanisms. It was proposed on the basis of such functional evidence that there are neurons in the canine heart which are adrenergic in phenotype, capable of synthesizing and storing monoamines, for release when these neurons are activated. The presence of TH-IR in neurons is generally accepted as a primary indicator of adrenergic phenotype, but no evidence has so far been presented for TH-IR neuronal somata in the dog heart. In an *in vitro* preparation of the guinea pig left atrium I have evoked positive chronotropic responses by activation of intracardiac neurons near the SA node using local application of nicotine (Chapter 3). These responses were eliminated by the nicotinic cholinergic antagonist hexamethonium and by ß-adrenergic antagonists, suggesting that a neuronal mechanism for cardiac augmentation similar to that in the canine heart is also present in the guinea pig. However, in the present study no intracardiac neuronal somata were found to be TH-immunoreactive in guinea pig atria (Fig. 6), leading to the conclusion that these neurons therefore will not be capable of synthesizing the adrenergic neurotransmitter norepinephrine.

The results of recent studies using antibodies against TH in the heart have been controversial. The findings in the present study concur with those of Baluk and Gabella (1990), Steele *et al.* (1994, 1996), and Mawe *et al.* (1996), who reported an absence of TH-IR in intracardiac neurons in the guinea pig heart; in addition a review by Allen *et al.*

(1994) summarized reports that guinea pig atrial neurons in primary culture lack TH-IR. In contrast to these reports Dalsgaard *et al.* (1986) found TH-IR in a small group of neurons in the guinea pig heart and Horackova *et al.* (1996) reported that guinea pig intracardiac neurons in short- and long-term culture can express TH-IR; some of the neurons in the latter study even co-expressed TH and ChAT-IR. In the rat heart there is also evidence for TH-IR in atrial and ventricular neurons (Moravec and Moravec, 1989; Moravec *et al.*, 1990; Slavikova *et al.*, 1993). The reasons for these disparate findings are not obvious but may lie in differences in the immunohistochemical procedures used. In the present study, as a positive control for the presence of TH-IR in neurons known to express this enzyme, I processed sections of stellate ganglia taken from the same animals used to source cardiac tissue. TH was detected in high concentrations in stellate ganglion neurons, and these neurons also displayed co-localization of PGP 9.5-IR, so it appears that the immunohistochemical protocol used in this study should have detected TH-IR in intrinsic cardiac neurons if this enzyme was present at levels greater than the detection threshold. It is possible that in guinea pig intracardiac neurons the somatic level of TH may have been below the threshold for detection by our primary anti-TH antibody. In an attempt to address this possibility, the concentrations of the primary antibody against TH was increased to 10 times the concentration necessary to label stellate ganglion neurons. The incubation time was also lengthened in some experiments, but with negative results. If neurons within the atria of the guinea pig heart do express TH, this enzyme may be transported somatofugally as soon as it is made and so might not be present at high enough levels in the somata to bind a sufficient amount of the antibody used in our study.

Given that no intracardiac neurons in this study contained detectable levels of TH, the cellular basis for the cardioaugmentatory effects of activating intracardiac neurons is not clear. If our results and those of the other studies which did not demonstrate TH-IR in intracardiac neurons can be taken at face value, the cardioaugmentatory responses evoked by activation of neurons in the intracardiac nervous system may not have been generated by adrenergic neurons. In the present study TH-IR was found in a class of cells with somata which were smaller than, and morphologically distinct from, the somata of intracardiac neurons (Fig. 6); there was in fact no overlap in somatic dimensions between the smallest neurons and the largest TH-IR cells. Furthermore the morphology of atrial TH-IR cells in the present study was similar to that of small, intensely fluorescent cells (SIF cells) observed throughout the viscera and in the peripheral autonomic nervous system after staining for catecholamines using an aldehyde fluorescence reaction (Jacobowitz, 1967; Biscoe, 1971; Burnstock and Costa, 1975; Dail *et al.*, 1975; Dail, 1976; Howe *et al.*, 1978; de Groat and Booth, 1980; Wurster *et al.*, 1990; Kriebel *et al.*, 1991). SIF cells have also been found in other studies to contain TH in high concentrations (Heym *et al.*, 1994; Mawe *et al.*, 1996). To determine if there were any morphological similarities between small atrial TH-IR cells and cells in the atria which might contain catecholamines, aldehyde histofluorescence was employed in the present study to determine cellular catecholamine content. Brightly fluorescent catecholamine-containing cells with a morphology very similar to that of small TH-IR cells were found in or near ganglia (Fig. 9) and scattered in the myocardium. For reasons given in the Methods section, the protocols for determining catecholamine content and TH-IR were not compatible so the same tissue samples could

not be analyzed for both TH and catecholamine content, but based on the morphological similarities of cells visualized by these techniques, the catecholamine-containing cells and the TH-IR cells comprised the same population.

The functional role of SIF cells in the heart is not yet clear, but these cells have the potential to play a role in cardioaugmentation. De Groat and Booth (1980) have proposed that SIF cells in autonomic ganglia controlling bladder function may act to mediate ganglionic neurotransmission, and it has been shown that some SIF cells, including those in the heart, receive cholinergic inputs (Dail, 1976) although the source of these inputs has not been determined. Furthermore, release of catecholamines stored in SIF cells can be induced by activation of cholinergic receptors on the membranes of these cells (de Groat and Booth, 1980). If a subpopulation of intrinsic cholinergic neurons projects to SIF cells in the heart, then activation of neurons in this pathway may evoke catecholamine release from SIF cells to augment cardiac function. This mechanism, if present, would be blocked by both hexamethonium and ß-adrenergic antagonists, and would thus provide an explanation for the effectiveness of these agents in blocking neurally mediated cardioaugmentation in the *in situ* canine heart (Butler *et al.*, 1990b).

An alternative explanation for ß-adrenergic cardioaugmentation produced by intrinsic cardiac neuron activation may be that some neurons in the heart can take up monoamines from the surrounding milieu, storing and then releasing these neurochemicals when stimulated. That is, neurons may not necessarily need to express catecholamine-synthesizing enzymes to employ catecholamines as neurotransmitters. In support of this idea, some intracardiac neurons in culture have the ability to accumulate

biogenic amines from the culture medium (reviewed by Allen *et al.*, 1994). However, in the present study no atrial neuronal somata were observed to contain catecholamines in tissue processed for aldehyde histofluorescence (Fig. 9), confirming the results of Baluk and Gabella (1990) in the guinea pig. If intracardiac neurons do take up amines for use in control of cardiac function *in vivo*, it may be that these compounds are stored in somata or terminals at a concentration below threshold for detection by aldehyde histochemistry, and thus would not have been observed in the present study. In this scenario a relatively large number of intracardiac neurons in a particular atrial region, each storing a small amount of amine, could conceivably release enough amines from their terminals to produce cardioaugmentation when activated. A large number of catecholamine-containing varicose terminals were observed both in the myocardium and in ganglia in the present study (Fig. 9), but it was not possible to determine whether these terminals were associated with the axons of intrinsic cardiac neurons, with axons of extracardiac origin (i. e. axons of sympathetic postganglionic neurons with their somata in thoracic ganglia) or with the processes of SIF cells. Regarding the latter possibility, no SIF cell processes in tissue which had been prepared for amine histofluorescence could be traced far enough from the cell bodies to determine whether they included amine-containing varicosities; tissue samples were too thick to visualize these cell processes well at high magnification in the standard fluorescence microscope. However, an attempt was made using the confocal microscope to determine whether processes of intracardiac TH-IR cells contained varicosities. No varicosities were found along the processes of TH-IR cells as far as these could be traced (up to 30 μm distal to the cell bodies). It is therefore

possible that catecholamine-containing varicosities and TH-IR varicosities were associated with neuronal axons.

The results of the immunohistochemical experiments in this study suggest that neurons in the guinea pig atria are cholinergic. In the classical model of neural control of the heart these neurons would all be postganglionic, acting as simple relays conveying parasympathetic cardiomotor drive to the myocardium. However, cholinergic neurons not necessarily limited to one functional role. Physiological studies in several mammalian species have demonstrated the existence of multiple functional types of neurons including afferent neurons, interneurons and local circuit neurons as well as efferent cardioaugmentatory and cardioinhibitory neurons (Armour, 1994). Intrinsic cardiac neurons are neurochemically very complex, expressing a number of peptides as well as ACh (Steele *et al.*, 1994; 1996) in a manner similar to cholinergic neurons elsewhere in the peripheral autonomic nervous system. Janig and McLachlan (1992) have proposed that a variety of peptides co-localized with classical neurotransmitters in specific subpopulations of autonomic neurons chemically code these neuronal populations to subserve specific functions. In atrial neurons of the guinea pig, multiple peptides are co-expressed in distinct subpopulations (Steele *et al.*, 1994; 1996), and it is likely that, even though most or all of these neurons synthesize ACh, the co-localization of specific peptides dictates different functional roles for neurons in these subpopulations. Furthermore, Steele *et al.* (1996) reported that a group of intrinsic cardiac neurons which co-localized the peptide somatostatin in the guinea pig appeared to project selectively to the pacemaker nodes and cardiac valves, but the primary targets of other neurons which co-localized vasoactive intestinal polypeptide and neuropeptide Y but not somatostatin

appeared to be other neurons in intracardiac ganglia. The latter population of neurons may thus represent a type of local circuit neuron in the heart.

In the canine heart physiological and anatomical studies have shown that different regions are innervated by discrete vagal and sympathetic nerve branches (see Randall, 1994 for summary). *In vitro* and isolated preparations of rodent hearts have also been used extensively for investigating functional aspects of neural control of the heart, yet anatomical details of sympathetic and parasympathetic cardiac innervation have not been established in these species. A general description of the main branches of the vagus nerve to the rat heart has been provided by Burkholder *et al.* (1992) but this study did not provide any details of these pathways. Seabrook *et al.* (1990) developed a detailed picture of the vagal innervation of rat intracardiac ganglia associated with a small area of the dorsal atrial wall near the attachment of the interatrial septum, but these authors did not explore the innervation of other cardiac regions. On the sympathetic side, Yasunaga and Nosaka (1979) described the overall arrangement of the cardiopulmonary nerves innervating the rat heart but provided no details of the anatomy of these nerves as they approach the myocardium. Such a detailed analysis is necessary before determining which subpopulations of intrinsic cardiac neurons are innervated by axons in specific branches of the extrinsic cardiac nerves. In the present study I have shown that both vagal and cardiopulmonary nerves ramify extensively on the heart, following the general pattern shown in Figure 3. Sympathetic and parasympathetic nerves appeared to enter the cardiac plexus in specific regional patterns which were consistent among the specimens. In addition, a major feature of all the hearts studied was that particular atrial regions such as the left atrium around the base of the pulmonary veins, the area of the attachment of

the septum to the external atrial wall, and the SA node, appeared to be dually innervated by branches of the sympathetic and parasympathetic nerves. These results have elucidated the anatomical basis for regional cardiac innervation by extrinsic autonomic nerves, thus providing an organizational substrate on which further functional studies of the autonomic control of regional cardiodynamics can be based. This study thus provides an anatomical foundation for the physiological studies of Chapters 3 and 4.

Conclusions

In summary, all neurons found in the guinea pig atria were co-reactive for PGP 9.5 and ChAT, implying that these neurons are cholinergic. No neurons contained either TH-IR or detectable levels of catecholamines. However both TH-IR and catecholamines were detected in small atrial cells which resembled SIF cells reported by others to be present in the heart and elsewhere in the peripheral autonomic nervous system. Catecholamine-containing varicosities were observed within intracardiac ganglia and associated with the atrial myocardium, as were TH-IR varicosities. The distribution patterns of neurons varied in different regions of the atria, likely reflecting the different roles of these neurons in controlling inotropic, chronotropic and dromotropic functions of the heart.

Chapter 3: Development of an *in vitro* model to investigate the function of the intracardiac nervous system:

Introduction

The objective of this project was to develop an *in vitro* preparation of the guinea-pig heart which would facilitate physiological evaluations of the properties of intracardiac neurons without the confounding influences of circulating hormones and spontaneous extrinsic autonomic activity. In the past, a number of investigators have used *in vitro* preparations to conduct pharmacological analysis of autonomic innervation of the heart in rats and guinea-pigs (Amory and West, 1962; Trendelenburg, 1965; Blinks 1966; Saito *et al.*, 1986). Transmural electrical stimulation was used in many of these studies as a means of effecting the release of autonomic neurotransmitters and assessing their effects on spontaneous heart rate or contraction strength. This type of field stimulation produced simultaneous activation of all types of neuronal elements present in the heart, including sympathetic, parasympathetic and sensory terminals and cell bodies. Obviously, this type of experiment can yield only limited information concerning the integration of specific inputs to subsets of neurons, or the function of those neurons in cardiac control.

At the other extreme, some researchers have examined the characteristics of individual guinea-pig and rat intracardiac neurons isolated from their effector site, the myocardium (Edwards *et al.*, 1995; Hardwick *et al.*, 1995). These authors could only speculate as to the function of any proposed sub-classification of the intracardiac neurons. After filling neurons with an intracellular marker dye, Edwards *et al.* (1995)

described labelled axons entering nerves which presumably innervated the myocardium, but in their preparation, the myocardium had been removed and all nerves innervating the muscle were cut. In addition, small interganglionic nerves would likely have been damaged during the removal of the myocardium in this preparation. Thus, it may not be prudent to make the assumption that all cut nerves in this study projected toward the myocardium. Furthermore, as pointed out in Chapter 2, controversy persists concerning the existence of morphologically and physiologically distinct neuronal populations within the guinea-pig heart. To address the shortcomings of earlier experimental models, I have developed an *in vitro* preparation of the guinea-pig heart which can include both atria or portions of the atria, along with attached extrinsic cardiac nerves. This preparation was designed to facilitate examination of the physiological, morphological and functional properties of single intracardiac neurons with respect to their role in regulating heart rate and the ability of adrenergic terminals, within ganglia, to modulate their activity. Since this preparation can contract spontaneously *in vitro* if the SA node is included, the rate of pacemaker discharge was chosen as an important cardiac variable which could be easily measured. Furthermore, factors influencing changes in rate in the *in vitro* preparation presumably will directly reflect control of this variable in the *in situ* heart. To verify that the responses of the *in vitro* preparation approximate the *in situ* response to extrinsic vagus nerve stimulation, the right vagus nerve was electrically stimulated over a range of frequencies while changes in heart rate were recorded *in situ*. Then the heart and attached vagus nerve were removed, placed in the *in vitro* recording chamber and the effectiveness of vagal stimulation was tested.

Methods

Animals were killed by a blow to the head, the heart was removed rapidly through a midline sternotomy and placed in a modified Krebs solution containing (in mM): 117 NaCl, 4.7 KCl, 2.5 $CaCl_2$, 1.2 $MgCl_2$, 25 $NaHCO_3$, 1.2 NaH_2PO_4, 11.5 glucose; at room temperature (pH = 7.4). The solution was bubbled with 95% O_2 and 5% CO_2. The ventricles were removed and the atria, with the stumps of the vagus, stellate ganglia and all cardiopulmonary nerves still attached, were pinned to a layer of silicone rubber on the bottom of a chamber. This preparation was constantly perfused at 37°C with oxygenated Krebs solution (5-10 ml/min). The intracardiac nervous system of this preparation was intact and extrinsic nerves were available for stimulation.

Extrinsic vagal nerve stumps were stimulated by ring electrodes placed over the cut ends of the stumps. Trains of square wave electrical pulses (5 mA, 0.5 ms duration) were delivered to the nerves over a range of frequencies for 30 sec - 1 min. The stellate ganglion or cardiopulmonary nerves were stimulated with either bipolar pipette suction electrodes or ring electrodes. A stimulation frequency which produced a 20-30% change in heart rate from the baseline rate was considered sufficient for further experimental study. The ß-adrenergic receptor antagonist timolol and the cholinergic receptor antagonists hexamethonium, a nicotinic channel blocker, and atropine, a muscarinic receptor antagonist were used to assess the relative contributions of the sympathetic and parasympathetic nerves the observed changes in heart rate. Heart rate was derived from an atrial electrocardiogram, recorded via a bipolar silver wire electrode placed lightly on the surface of the myocardium in the region of the SA node.

The pharmacological effects of neurochemicals with well-established sympathomimetic and parasympathomimetic influences on heart rate were determined in this preparation to confirm its viability. Nicotine (100 μM delivered in the perfusate) was used to activate nicotinic cholinergic receptors on intracardiac neurons, methacholine (100 μM) was used to activate muscarinic receptors on the myocardium (and potentially on neurons) and ACh (100 μM) was used to activate both muscarinic and nicotinic receptors non-specifically. Norepinephrine (NE, 10μM) was used to activate both α- and ß-adrenergic receptors simultaneously and isoproterenol (ISO, 100μM) was used to activate ß-receptors. The receptor-specific antagonists used in the nerve stimulation trials were used here as well. The drug concentrations used in this study were chosen on the basis of effectiveness in preliminary trials.

For confirmation that the *in vitro* responses to vagus nerve stimulation were similar to those obtained with the heart *in situ*, some animals were first anaesthetized with ketamine (25-44 mg/kg, i.m.) and a incision was made in the neck to expose the carotid sheath. A stimulating electrode was placed on the peripheral cut end of the right vagus nerve and EKG leads were placed into the thoracic wall. The vagus nerve was stimulated with trains of pulses (0.5 ms duration, 5 mA, various frequencies) for 30 seconds and the responses of heart rate were recorded. Immediately following these stimulations, the atria and attached extrinsic nerves were removed from the thorax, placed in the recording chamber and the vagus nerve stimulations were repeated.

As a final test of the viability of the *in vitro* preparation, cardiac ganglia were identified and extracellular recordings using bipolar pipette suction electrodes were made

from these during electrical stimulation of interganglionic nerves. Intramural ganglia and intracardiac nerves were located with minimal dissection of the atrial wall when the preparation was pinned flat in the recording chamber. Transillumination of the tissue with a small fibre optic light guide angled at 45° to the optical axis aids visualization of nerves and ganglia. Intracardiac nerves were stimulated with a bipolar silver electrode.

Results

Base Line heart rate in vivo and in vitro

Heart rate *in situ* ranged from 150-175 beats per minute (bpm; mean 160 ± 2) in two animals over a 40 minute recording period. The same hearts, placed *in vitro*, had heart rates of 141-190 bpm (mean 154 ± 8) over an equivalent period. Although the variability of heart rate with time was greater in the *in vitro* preparation, mean rates were similar under both *in vivo* and *in vitro* conditions. For *in vitro* hearts from a larger group of animals (n=13) the heart rate ranged from 100-250 bpm. Mean heart rate for this group of hearts was 158 ± 17, and heart rate was well maintained over a 6 hr period (see Fig. 10).

Stimulation of the right vagus nerve *in situ* produced decreases in heart rate which were dependent upon stimulus frequency; this relationship is shown by the solid line in the example of Figure 11. For atria from the same heart placed *in vitro*, the relationship between the vagal stimulation and rate is represented by the dashed line in Figure 11. The response to *in vitro* vagal stimulation was very similar to that obtained *in vivo*.

Some *in vitro* preparations did not respond to vagus nerve stimulation (n = 8), while 30 atrial preparations either showed an initial, transient bradycardia which could not be reproduced in later trials (n = 18), a consistently monophasic response (bradycardia only, n = 12) or a biphasic response (bradycardia followed by tachycardia over the duration of vagus nerve stimulation, n = 9). As shown in Table 3, stimulation of the right vagus nerve, in two-thirds of the hearts which responded, produced a monophasic response: heart rate decreased by a mean of -24 ± 6 % from the pre-stimulation value. This effect was blocked by both atropine and hexamethonium in the perfusate. In one third of the preparations, a biphasic response, consisting of a mean decrease of 12 ± 4% followed by an increase of 9 ± 2% in heart rate, was observed during stimulation of the vagus nerve. In these preparations, atropine potentiated the increase while blocking the decrease in rate. Timolol, on the other hand, did not suppress the increase. However, in the presence of hexamethomium, stimulation of the vagus nerve did not produce bradycardia but enhance the tachycardic response.

Stimulation of the right stellate ganglion, innervating the heart via cardiopulmonary nerves, consistently resulted in an increase in rate in all preparations tested, mean change in heart rate was +30 ± 5 % (n=25; Table 3). Atropine potentiated the response of the heart to cardiopulmonary nerve stimulation. Stimulation-induced cardioacceleration was consistently blocked by application of timolol.

Figure 10. Mean heart rate for 13 isolated guinea-pig hearts during a 6 hour period. Error bars indicate ± 1 standard error of the mean.

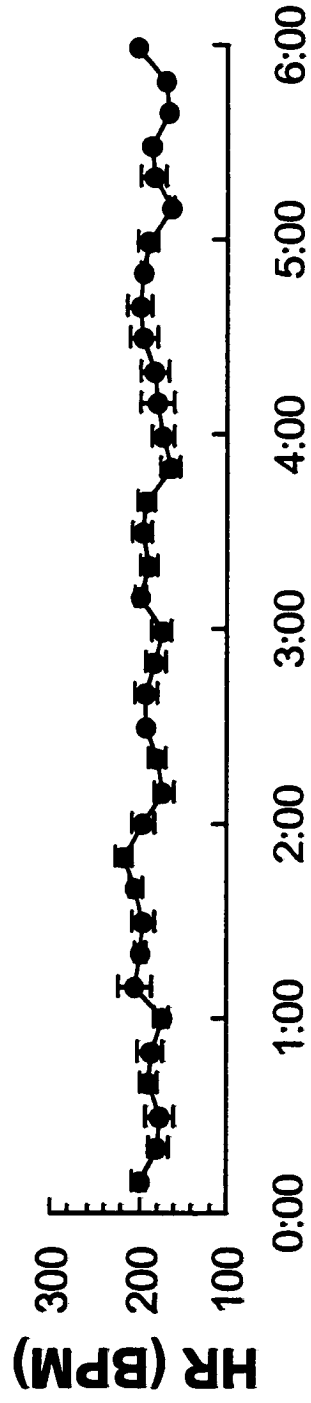

Figure 10

Figure 11. Percent change in heart rate of an individual heart to electrical stimulation of the right vagas nerve *in situ* and *in vitro*. The nerves were stimulated with a train of variable frequency, 0.5 ms duration pulses with a current of 5 mA for 30 s

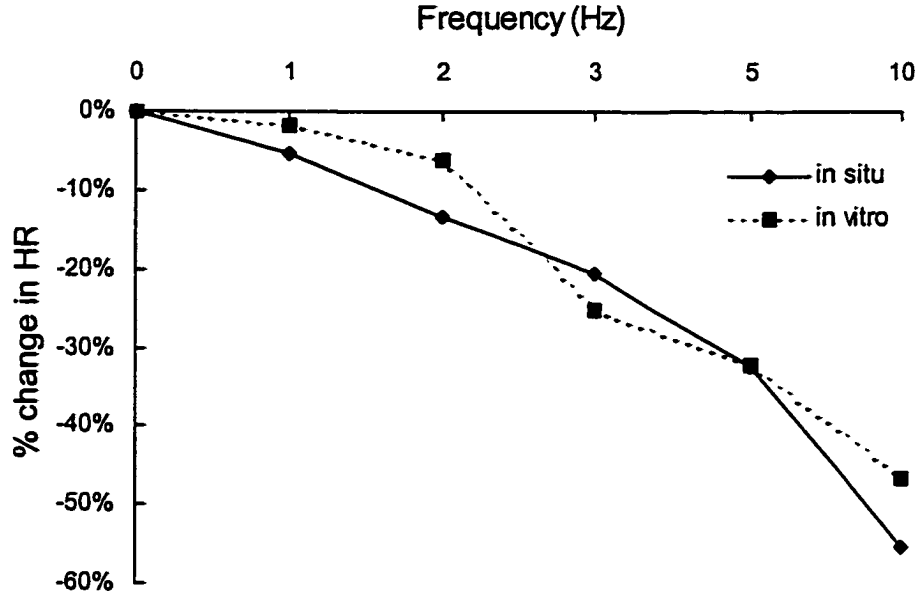
Frequency (Hz)
0
1
2
3
5
10
0%
-10%
-20%
-30%
-40%
-50%
-60%
% change in HR
in situ
in vitro

Figure 11

Table 3. Effects of stimulation of the right vagus nerve and right stellate ganglion/cardiopulmonary nerves on atrial rate *in vitro*. Values represent mean percent change (± 1 SE) from prestimulation rate, before (control) and during application of adrenergic and cholinergic antagonists (refer to text for details). Number of animals tested is indicated by the columns labelled (n) to the right of each mean. Absence of a sign preceding a value indicates an increase, and a (-) indicates a decrease in rate. An asterisk (*) denotes an increase in rate following vagal nerve stimulation.

Table 3

	Control	n	Atropine	n	Timolol	n	Hex	n
*R.Vagus	8.9 ± 1.8	9	37.7	1	9.0	1	11.0	1
R.Vagus	-23.9 ± 5.9	30	-1.9 ± 2.6	6	-4.7 ± 2.7	3	0.8 ± 1.5	6
R.CPN	29.8 ± 5.2	25	36.5 ± 11.5	2	5.7 ± 3.3	8	18.4 ± 3.7	4

Effects of cholinergic and adrenergic agonists

The effects of cholinergic and adrenergic agonists on atrial rate before and during application of receptor-specific antagonists are shown in Table 4.

ACh: In experiments in which ACh was applied via the perfusate, a 30% decrease in heart rate resulted. Presumably this was due to the activation of both nicotinic and muscarinic receptors. Atropine acting to block muscarinic receptors, eliminated the response to ACh, while hexamethonium did not block the negative chronotropic effect of ACh on heart rate.

Methacholine: Methacholine, an agonist which acts primarily at muscarinic receptors, also decreased heart rate in this preparation. Atropine blocked the effect of methacholine on heart rate while hexamethonium did not.

Nicotine: There were two types of response to bath-applied nicotine. In one, atrial rate showed a monophasic response, decreasing in 11 of 21 cases. This response was reduced but not blocked by hexamethonium. In the other type of response, nicotine had a biphasic effect on rate, causing first a decrease from the control rate, then an increase in rate to a value greater than the control rate. In these hearts, the negative phase was eliminated but the positive phase was potentiated enhanced during exposure to atropine, with rate during this phase rising to a value 60% above the control rate. Both phases were eliminated by exposure to hexamethonium. This type of effect was observed in 10 of 21 hearts tested with nicotine.

Table 4. Chronotropic responses *in vitro* to cholinergic and adrenergic agonists before (control) and during application of receptor antagonists. Values represent mean percent changes (± 1 SE) in of atrial contraction. The numbers of animals contributing to the values are listed in the (n) columns to the right of each column of values, absence of a sign preceding a value indicates an increase, and a (-) indicates a decrease in rate.

Table 4

	Control	n	Atropine	n	Timolol	n	Hex	n
ACh	-30.6 ± 23.1	4	-2.6	1	-10.7	1	-55.3	1
*NIC	27.7 ± 8.4	10	62.0	1	6.7 ± 3.0	5		
NIC	-25.0 ± 6.6	20	-8.0 ± 2.6	3	-19.8 ± 15.8	3	-6.2 ± 3.9	7
MCh	-40.0 ± 13.7	6	3.1	1			-48.5	1
NE	84.4 ± 6.8	6			0.3 ± 1.4	2		
ISO	36.1 ± 8.6	11			-2.8 ± 2.0	4		

NE and ISO: Norepinephrine and isoproterenol both consistently increased atrial rate (Table 4). These effects were blocked by timolol, suggesting that ß-adrenergic receptors mediated responses to both agonists.

Ganglionic Potentials

Nerve stimulation, nicotine, ACh, NE and ISO could all be acting at multiple sites in this preparation; these include intraganglionic sites, at the neuroeffector terminals, and at myocardial sites. Actions at these sites cannot be distinguished in this type of experiment. Therefore, to confirm that intraganglionic synaptic responses to nerve stimulation were evoked, extracellular potentials were recorded from intracardiac ganglia during stimulation of interganglionic nerves. Stimulation of nerves produced responses within associated ganglia, as shown in Figure 12. In the example shown here, a single-pulse stimulus delivered to a nerve evoked both positive and negative deflections indicating mass electrical activity within the ganglion. Such activity was presumably the result of pre- and postsynaptic responses elicited by activation of axons in the nerve which made synaptic contacts with ganglion neurons. Ganglionic potentials were eliminated by hexamethonium and by a perfusate solution modified to contain 0.5 mM Ca^{++} and 10 mM Mg^{++}.

Discussion

Viability of the preparation and parasympathetic responses

This *in vitro* preparation of the guinea-pig atria has two major advantages for the present study: 1) intrinsic neural control mechanisms can operate independent of from

Figure 12. Ganglionic responses to interganglionic nerve stimulation. Top trace: control response elicited by simple-pulse stimulation (parameters; delivered at black square). Middle trace: hexamethonium (100 μM in perfusate) eliminated response to nerve stimulation. Bottom trace: low calcium (0.5 mM), high magnesium (10 mM) perfusate also eliminated response to nerve stimulation. Vertical bar represents 100 μV; horizontal bar represents 5 ms.

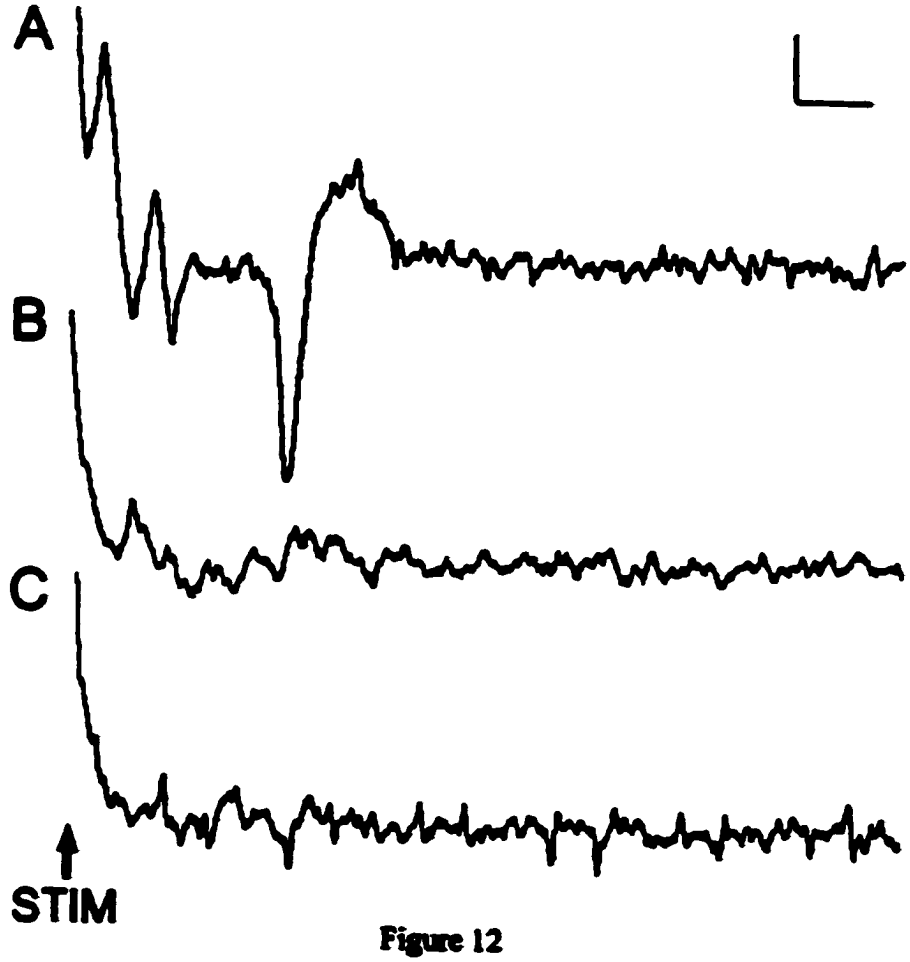

Figure 12

higher centres of the autonomic nervous system and will also be free of circulating hormonal influences; and 2) both atria together are small enough to fit in a 35 mm chamber so that the entire atrial intrinsic nervous system can be visualized and accessed for physiological and pharmacological manipulations.

Several methods were used to verify the viability of this preparation *in vitro*. Baseline pacemaker discharge rate was in the range of 100-250 beats per minute (bpm) at 36-37 °C, similar to rates reported in other studies using isolated guinea-pig atria (e.g. Opthof *et al.*, 1985) and *in vivo* studies of the guinea-pig with rates ranging from 214 to 360 bpm (for review see Sisk, 1976). Specifically, isolated atria had mean base rates of 120 (Campbell *et al.*,1989), 177 ± 4 (Gurnett *et al.*, 1993) and 223 ± 5 (Olmez *et al.*, 1995) have been reported for this preparation *in vitro*, consistent with the range of rates in the present study. Furthermore, this is the first study that has shown by direct comparison between baseline heart rates in both *in situ* and *in vitro* preparations from the same heart that rate is similar under both conditions. Moreover, I have established that similar changes in rate can be evoked by activating the vagus nerve in the same preparation under *in vivo* and *in vitro* conditions. These observations are important as they validate the viability of vagal control of atrial rate *in vitro*.

Since preganglionic axons from the vagus nerve regulate cardiac functions through synapses with intracardiac neurons, the response of the heart to vagal stimulation and the suppression of this response by antagonism of nicotinic receptors, on ganglionic neurons confirms that these neurons are involved in this control pathway and are functional *in vitro*. In addition, this preparation responds to pharmacological agents in a manner similar to such preparations in previous studies, indicating the suitability of this

type of preparation for investigating the details of the cardiac response to neurochemicals. The advantage of this *in vitro* preparation is that the intracardiac nervous system is isolated from circulating hormones and control autonomic drive which has complicated studies of cardiac control *in vivo.*

Furthermore, both nicotinic activation of intrinsic cardiac neurons and vagal nerve stimulation produced biphasic rate responses in some preparations. Similar observations have been reported during local application of nicotine and electrical stimulation of intracardiac ganglia in the dog (Butler *et al.*, 1990a, Huang *et al.*, 1993a, 1993b, 1993c). In some of these cases, nicotine could augment cardiac function in the presence of atropine in the canine heart *in situ* (Huang *et al.*, 1993a, 1993b, 1993c). In addition, cardioaugmentatory responses to the activation of the intrinsic cardiac nervous system persisted in acutely and chronically decentralised hearts (Butler *et al.*, 1990b; Ardell *et al.*, 1991; Huang *et al.*, 1993a) suggesting that these responses were the result of cardiac plexus activation. However, studies using isolated guinea-pig atria have not previously reported a biphasic response to right vagal nerve stimulation (Campbell *et al.*,1989) or to the application of carbachol, a cholinergic agent which activates nicotinic receptors (Olmez *et al.*, 1995). In these studies, monophasic changes in heart rate ranging from 10 to 100% resulted from either electrical or pharmacological stimulation.

A confounding factor in the present study was that a proportion of *in vitro* hearts exhibited either a complete lack of, or an attenuated and transient response to, stimulation of the right vagus nerve. The reason for this effect is not clear. However, given the complexity of responses that the preparation displayed to various cholinergic agonists and antagonists as illustrated in Table 3 and 4, it is possible that there may be multiple synapses within the heart in the parasympathetic pathway from preganglionic axons of the vagus nerve to the postganglionic efferent neurons innervating the SA node. Stimulation of the vagus nerve may therefore set in train a cascade of events within the

intracardiac ganglia which are not yet understood. The ultimate effect of this cascade, whether a clear inhibition of SA nodal rate or an attenuated response, may depend upon the milieu of neurotransmitters and neuromodulators in the circuitry of the intracardiac neurons involved in the rate-control pathway.

Sympathetic responses

Cardiopulmonary nerve stimulation produced consistent cardioacceleration in the *in vitro* preparation. This effect was blocked by antagonizing ß-adrenergic receptors, presumably located on myocardial muscle, suggesting that sympathetic terminals on the myocardium may be primarily responsible for the overall sympathetic chronotropic effect on heart rate. Thus, sympathetic cardioaugmentatory mechanisms are functional in this preparation. Similar observations have been reported in studies using electrical field stimulation performed on atria *in vitro* (Trendelenburg, 1965; Blinks 1966; Saito *et al.*, 1986). In addition, a study using a Langendorff preparation of whole guinea-pig heart reported increases of 38% in rate after stimulating the attached right stellate ganglion for 1 min at 4 Hz (Gurnett *et al.*, 1993).

Intracardiac nerve stimulation

The response of intracardiac neurons to local intracardiac nerve stimulation has been demonstrated extracellularly in the canine heart *in situ* (Armour and Hopkins, 1990) and intracellularly in the dog (Xi *et al.*, 1991b; 1994), porcine (Smith *et al.*, 1992, 1997) and guinea-pig (Edwards *et al.*, 1995; Hardwick *et al.*, 1995) hearts *in vitro*. The present study has shown that activation of guinea-pig intracardiac neurons can be evoked by interganglionic nerve stimulation. The loss of the ganglionic response in low Ca^{++}

perfusate indicates that this response was a postsynaptic response, due to synaptically-mediated excitation of intrinsic cardiac neurons, and not to activity of axons of passage. Furthermore, hexamethonium blockade of the ganglionic response indicates that the synaptic mechanisms involved were primarily cholinergic.

Conclusions

I have verified the suitability of this *in vitro* preparation for physiological experiments in 3 ways: 1) pacemaker rate can be altered by extrinsic nerve stimulation (Table 3); 2) appropriate bath-applied agonists mimic the chronotropic effects of nerve stimulation (Table 4); and 3) intracardiac neurons respond postsynaptically to nerve stimulation (Fig. 12). Experiments in Chapter 4 establish the intracellular electrical properties of neurons in the intracardiac ganglia, and investigate the nature of adrenergic modulation of neuronal activity. For the first time, using this preparation, the effect of a particular experimental intervention can be correlated with changes in activity of intracardiac neurons and the electrophysiological and morphological properties of these neurons. This is the focus of the remainder of my thesis.

Chapter 4: Modulation of intraganglionic neurotransmission by adrenergic agents:

Introduction

The overall objective of this study was to determine the degree to which adrenergic receptor activation of intracardiac neurons could modulate their physiological properties and responses to activation. Anatomical evidence for catecholamine-containing terminals within guinea-pig intracardiac ganglia was presented in Chapter 2. This evidence corroborates that of other studies in the guinea-pig and rat showing the presence of intraganglionic adrenergic terminals (Ellison and Hibbs, 1976; Dalsgaard *et al.*, 1986; Moravec and Moravec, 1987; Moravec *et al.*, 1990; Slavikova *et al.*, 1993; Steele *et al.*, 1994). In addition to this anatomical evidence, strong functional evidence for adrenergic modulation of neuronal behaviour in the heart has been reported. Local application of adrenergic agents to intracardiac ganglia of the *in vivo* canine heart enhanced the frequency of neuronal discharge (Huang *et al.*, 1993; Armour, 1997), while in the pig heart *in vitro*, it was demonstrated that norepinephrine (NE) altered the transmembrane properties of intracardiac neurons and facilitated synaptically induced firing (Smith *et al.*, 1992). A group of pig intracardiac neurons responded to cardiopulmonary nerve stimulation with fast EPSPs which, in some cases, could sum with vagal inputs to elicit AP firing (Smith, 1999).

Convincing evidence for dual innervation of visceral ganglion neurons by sympathetic and parasympathetic nerves has been reported in the pelvic ganglia, bladder and gall bladder, as summarized in Chapter 1. In the pelvic plexus, a group of neurons

received inputs from both the hypogastric (sympathetic) and pelvic (parasympathetic) nerves (Blackman *et al.*, 1969; Crowcroft and Szurszewski, 1971; McLachlan, 1977; de Groat, Booth, and Krier, 1979). More specifically, activation of α_2-adrenergic receptors induced hyperpolarization of the membrane potential in cat vesical neurons (Keast *et al.*, 1990) suggesting that catecholaminergic neurotransmitters can affect neurotransmission in vesical ganglia by a postsynaptic mechanism. In intrinsic cardiac neurons, the α_1-adrenoceptor appears to mediate some catecholaminergic effects. Exogenous application of NE, in an *in vitro* preparation, inhibited acetylcholine release from neurons in the atria of the rat (Wetzel *et al.*, 1985). The α_1-adrenergic antagonist prazosin attenuated these effects of NE, suggesting a role for this receptor subtype in regulation of neurotransmitter release. Application of NE also inhibited the release of this neurotransmitter from sympathetic terminals but this effect was antagonized by yohimbine, an α_2-receptor antagonist (Wetzel *et al.*, 1985). Radioligand binding studies have shown that rat intracardiac neurons predominately expressed $ß_1$-adrenergic receptors whereas, cardiac myocytes expressed $ß_2$-adrenergic receptors (Saito *et al.*, 1988). Evidence from studies in *in situ* canine heart suggest that α_1-, α_2-, $ß_1$- and $ß_2$-adrenoceptors can modulate the activity of intracardiac neurons and that a subpopulation of neurons possessing ß-adrenergic receptors can exert a tonic influence on cardiodynamics (Armour, 1997).

Pharmacological, physiological and morphological characteristics have been used to segregate intracardiac neurons following the logic that basic neuronal membrane and AP firing properties of intracardiac neurons will determine how these neurons respond to synaptically released neurotransmitters and neuromodulators and therefore determine the integrative capabilities of these neurons. Thus, these basic neuronal properties must first

be established so that the effects of endogenously released and externally applied neurochemicals can be assessed. Several classification schemes have been used to categorize peripheral autonomic neurons in the past, including classification by neurotransmitter phenotype, neuronal morphology and schemes based on various functional properties of neurons. For the purpose of this study, neurons will be classified functionally, by the time course of their AHP responses following the replarization phase of the AP. The membrane properties and patterns of synaptic input to these neuronal types will then be analyzed as part of the basic characterization of intracardiac neurons.

The α-adrenergic receptor agonist, phenylephrine, and the ß-adrenergic receptor agonist, isoproteronol, will be used to assess the involvement of the α- and ß-adrenergic receptors in adrenergically mediated effects on neuronal activity. In addition, the α_1- and ß-adrenergic receptor antagonists, prazosin and timolol, will be used to confirm the specific activation of these receptor subtypes in the present experiment. Adrenergic receptor subtypes and more commonly used receptor-specific agonists and antagonists are presented in Table 5. The biological consequences of G-protein linked adrenergic receptor activation, are also included in Table 5. Modulation of the membrane channel conductances have profound affects on neuronal activity.

Specific Aims

The aims of the studies in this portion of the thesis are:

1) to physiologically identify the types of neurons in the guinea-pig intrinsic cardiac nervous system, and to characterize the electrophysiological properties of these cell types.
2) to analyze the types and characteristics of synaptic inputs to intracardiac neurons.
3) to establish the effects of adrenergic agents on electrophysiological properties and postsynaptic responses of intracardiac neurons.

Table 5. Adrenergic receptor subtypes, receptor specific-agents and most common biological effects.

Table 5

Subtype	Agonist	Antagonist	Cytosolic second messenger cascade*	Biological effect
α_1	Phenylephrine	Prazosin	↑DAG/IP_3	↓I_K, ↓I_A
α_2	Clonidine	Yohimbine	↓adenylate cyclase/protein kinase	↑I_K
β_1	Isoproterenol	Timolol	↑adenylate cyclase/protein kinase	↓I_{AHP}, ↓I_{Ca}
β_2	Isoproterenol	Timolol	↑adenylate cyclase/protein kinase	↓I_{AHP}, ↓I_{Ca}

* some adrenergic receptor effects are G-protein coupled but membrane-delimited

Methods

Adult guinea-pigs aged 3-6 weeks were used for these studies. Animals in this age range have smaller hearts and less fatty tissue surrounding the heart than do older animals, thus facilitating the visualization of the cardiac plexus. Animals were killed, the atria were isolated as described in Chapter 3, and placed in the recording chamber. Intramural nerves were located and followed visually to locate intracardiac ganglia. Connective tissue was removed from the surface of the ganglia in preparation for making intracellular recordings from the neurons. In some experiments, stimulating electrodes were placed on the vagus and cardiopulmonary nerves, and on intraganglionic nerves. Intracellular glass pipette micro-electrodes with 80-120 MΩ resistance (3M KCl filled), were used to impale ganglion neurons under visual guidance. A stable resting membrane potential more negative than -40 mV indicated a successful penetration and only recordings made from these neurons were included in subsequent analyses. Membrane potentials were recorded with reference to an indifferent electrode consisting of an Ag/AgCl wire immersed in 3M KCl, in a capillary tube coupled to the bath through an agar plug. Prior to penetrating neurons, electrode tip potential and other artefact potentials were ruled out by the amplifier's bridge circuitry with the tip of the recording electrode in the bath.

Characterization of intracardiac neurons

To characterize the passive membrane properties of intracardiac neurons, changes in membrane potential were measured in response to stimulus current pulses injected into

the neuron through the intracellular recording electrode. Whole-cell membrane resistance was determined by calculating the slope of the voltage/current relationship during graded intensities of hyperpolarizing stimuli. In current clamp mode, membrane current was controlled while the membrane potential was free to change, so that active cellular properties such as the voltage threshold for generation of an action potential, the amplitude and duration of the action potential, and the time course and amplitude of the after-hyperpolarization could be analyzed. A prolonged depolarizing pulse, with a current intensity sufficient to generate action potentials, was delivered through the recording electrode to establish the firing behaviour of the neurons.

Morphological analysis

To correlate the morphology of intracardiac neurons with their physiological types, a 1% solution of tetramethylrhodamine dextran (3000 MW, dissolved in 3 M KCl; excitation 555nm, emission 580nm) was injected from the intracellular recording electrode into the cell bodies of sampled neurons. A depolarizing current in the form of a square wave (50% duty cycle) was injected through the recording electrode (2 Hz and 3-5 nA) for 15-30 min to inject the negatively-charged marker. Cells were filled with marker at the end of some recording experiments, the tissue was fixed overnight in 4% paraformaldehyde and was viewed under epifluorescence with a compound microscope or in a confocal microscope. Digitized images of labelled neurons were captured with the confocal microscope and analyzed with proprietary software to determine cell volume.

Synaptic neurotransmission

In voltage-follower mode, postsynaptic responses of impaled neurons were recorded as changes in membrane potential during episodes of parasympathetic or intraganglionic nerve stimulation. Current pulses (0.5 ms duration) ranging from 0.1 to 10 mA were used to activate nerves. The extent of activation of axons in these nerves was established in some experiments using an extracellular recording electrode placed on the surface of the nerve, between the site of stimulation and the recording site. The contribution of nicotinic cholinergic receptors, activated by endogenously released neurotransmitter, to the postsynaptic responses of neurons was assessed by application of the cholinergic antagonists, hexamethonium, a nicotinic receptor channel blocker, and mecamylamine, a nicotinic receptor antagonist. These antagonists were applied via the perfusate before and during nerve stimulation.

Adrenergic experiments

Local application of adrenergic agents was achieved by pressure ejection (200 - 500 ms duration pulses) from a multibarrel micropipette placed near ganglia from which neurons were sampled. Once the physiological properties of a neuron had been characterized, either phenylephrine (PHEN) or isoproteronol (ISO) was applied in one of two concentrations: 100 μM or 1 mM. Subsequent to application of the adrenergic agonist, neuronal properties and effects of nerve stimulation were reassessed. The preparation was then perfused with drug-free solution for 5 to 30 min to allow recovery of baseline neuronal properties before further experimentation.

The α_1-adrenergic antagonist, prazosin was used to block the effects of PHEN, and timolol, a β-adrenergic receptor antagonist, was used to antagonize the effects of ISO. Both antagonists were applied at a concentration of 100 μM via the perfusate. This concentration was established in a series of preliminary experiments.

Statistical analysis of differences between mean values of intracellularly recorded neuron properties was performed using appropriate tests. ANOVA procedures were used to test for significant differences among means of variables in the three types of neurons. Where significant F values were found, Tukey's test was used to complete the analysis. In cases where pair-wise comparisons of mean values were performed, these were accomplished by t-tests. For all statistical analyses, $P \leq 0.05$. All data are expressed as the mean ± 1 standard error of the mean.

Results

Membrane properties of intracardiac neurons

A total of 107 neurons was sampled from 45 hearts. Nerves and ganglia were located immediately beneath fibres of loose connective tissue of the epicardial sheath. Upon removal of this connective tissue, individual neurons became accessible for impalement, and Figure 13 shows the appearance of a typical intracardiac ganglion as viewed through the dissecting microscope under oblique illumination. Blood vessels

Figure 13. Photomicrograph of an intracardiac ganglion containing 4 neurons (N), viewed and photographed with oblique illumination under the dissecting microscope. The epicardial sheath and loose connective tissue overlapping the ganglion were removed to expose the neurons. The intracellular electrode can be observed as it approaches a neuron (asterisk) from the right hand side of the image. Blood vessels coursing through the ganglion are also visible (arrows). Calibration bar: 100 μm.

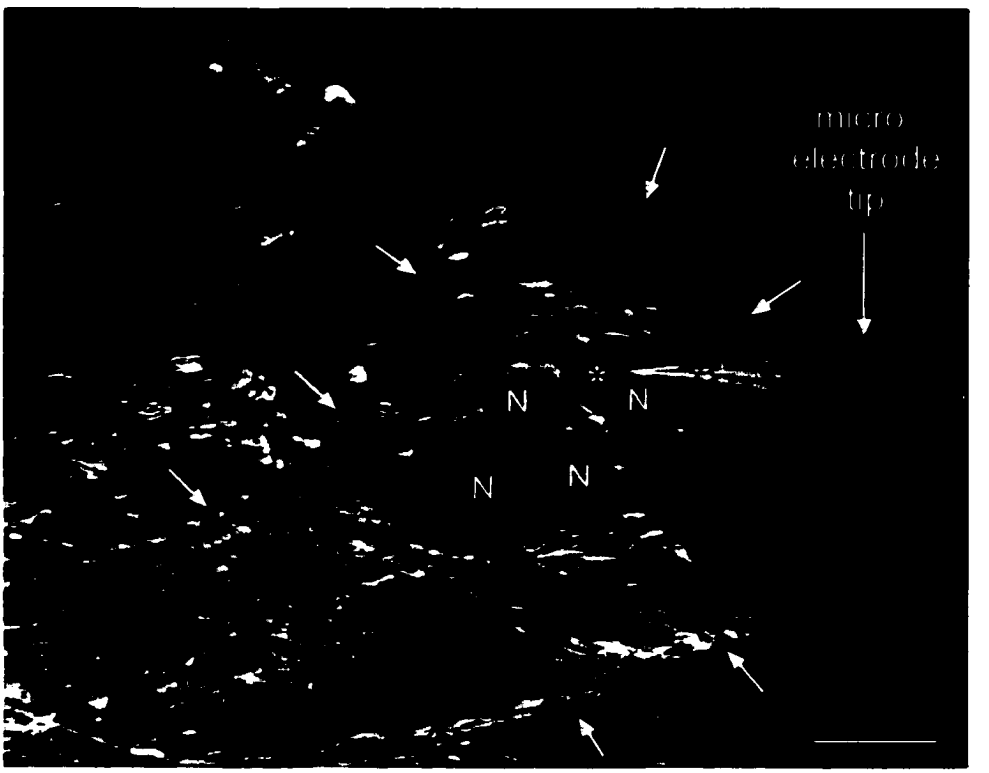

Figure 13

Figure 14. Intracardiac neurons displayed three types of afterhyperpolarization (AHP; upper traces in each panel represent membrane potential) in response to brief (5 ms) intracellular depolarizing current pulses (lower traces in each panel). A: Type I neuron had short-duration, small-amplitude AHP. B: Type II neuron had larger-amplitude, longer-duration AHP; these characteristics were intermediate between those of Type I and III. C: Type III neuron displayed the largest amplitude and longest duration AHP. Vertical bar: 30 mV and 1 nA. Horizontal bar: 50 ms.

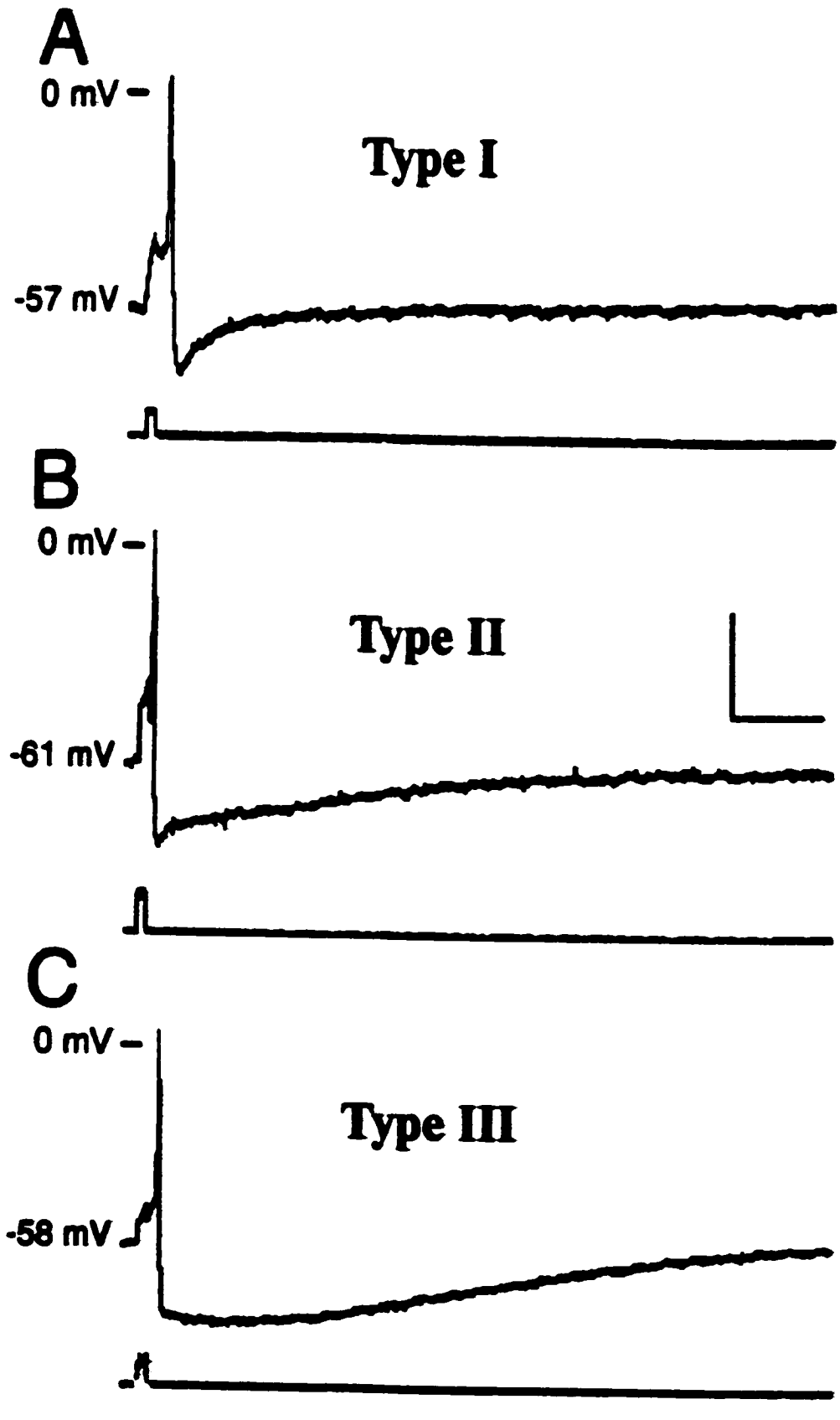

Figure 14

were observed coursing through the collection of neurons and nerve fibres within many ganglia.

Resting membrane potentials recorded from the entire population of intracardiac neurons in this study ranged from -40 to -87 mV, with a mean value of -56 ± 1 mV (Table 6). An impalement was deemed acceptable if the neuron had a resting membrane potential more negative than -40 mV and if action potentials with amplitudes which overshot 0 V, could be evoked by either intracellular or orthodromic stimulation. Further examination of trends in neuronal properties showed that these neurons could consistently be placed into one of three categories based on the time course of their afterhyperpolarization (AHP, see Fig. 14). Once the neurons were partitioned in this manner it became obvious that values of some of the other variables recorded showed consistent patterns of clustering within these categories, forming the basis for Table 6. Such clustering patterns are likely to reflect functional differences among neurons within the intrinsic cardiac plexus.

All neurons displayed one of the three types of AHP shown in Figure 14, immediately following the depolarizing phase of the AP. The time course of the AHP appeared to be relatively unchanged during the course of experimental manipulations. Furthermore, an analysis of variance (ANOVA) in conjunction with Tukey's post-hoc analysis showed that, for neurons assigned to any one of the classes illustrated in Figure 14, mean AHP duration was significantly different from those of neurons in the other classes (see Table 6). Type I neurons (n=15, 14% of the total number of neurons impaled in this study) displayed short-duration AHPs with the smallest amplitude (Table 6) and the repolarization phase of the AHP of these neurons had a relatively steep slope (Fig.

14A). Type II neurons, comprising 50% (n=53) of the total number of neurons, displayed AHPs with a mean duration and amplitude which were intermediate between those of Type I and Type III neurons (Table 6) but had a repolarization rate that was slower than that of Type I neurons (Fig. 14B). Type III neurons, making up 36% of the neurons sampled, had a mean AHP duration of more than four times that of Type I neurons; Type III neurons also displayed the largest AHP amplitude of the three neuron types (Table 6). In Type II neurons, AHPs were characterized by membrane potential remaining at a plateau level of hyperpolarization immediately after the transient hyperpolarization phase for some time before beginning to repolarize (Fig. 14C), a pattern not shown by either Type I or Type II neurons.

Table 6 summarizes the patterns of differences among properties of intracardiac neurons revealed by partitioning these neurons into subpopulations by AHP type. The results of the ANOVA performed on these data showed that, overall, significant differences in basic cellular properties were observed most frequently when comparing Type III neurons to the other two types, while there were relatively fewer differences between Type I and Type II neurons. Differences among the three subpopulations of neurons are described in detail below.

The mean resting membrane potentials for Type I and II neurons were statistically similar (Table 6) while resting membrane potential of Type III neurons was significantly more negative than that of Type II neurons. There was no statistical difference between mean resting membrane potentials of Type I and III neurons, possibly due to the smaller sample size of the Type I pool and the greater degree of variance of the resting membrane potential in this group.

Table 6. Mean values (± S.E.) of electrophysiological variables of three classes of intracardiac neurons. Neurons were classified based on the time course of the afterhyperpolarization (AHP). For each variable, significant differences among the neuron types were estimated by ANOVA in combination with Tukey's multiple means comparison test ($p \leq 0.05$). Asterisks (*) indicate variables of Type II or Type III neurons that were significantly different from those of Type I neurons. Filled circles (•) indicate significant differences between variables of Type II and Type III neurons. Values are expressed as mean ± one standard error.

Table 6

		Type I (n=15, 14%)	Type II (n=53, 50%)	Type III (n=39, 36%)
RMP	mV	-54 ± 2	-53 ± 1	•-59 ± 1
R_{in}	MΩ	79 ± 8	84 ± 7	•118 ± 11
Time const	ms	7 ± 1	10 ± 1	*• 15 ± 2
AP threshold	mV	15 ± 2	13 ± 1	13 ± 1
I_{thr}	nA	0.25 ± 0.04	* 0.16 ± 0.01	* 0.15 ± 0.02
AP amplitude	mV	56 ± 3	57 ± 2	* 64 ± 2
AP duration	ms	2.3 ± 0.2	* 1.9 ± 0.1	1.9 ± 0.1
AHP amplitude	mV	13 ± 2	16 ± 1	* 18 ± 1
AHP duration	ms	34 ± 7	* 101 ± 5	*• 149 ± 7

Statistical significance $p<0.05$. * Type II or III - I, ° Type III - II

The resistance to induced inward current flow, which is a measure of whole-cell resistance, was determined from the membrane potential responses to a series of incremental hyperpolarizing current pulses. Each pulse was 800 ms in duration and was injected via the recording electrode, producing responses like those shown in Figure 15. While some neurons displayed no rectification during hyperpolarization (Figure 15A), others displayed transient rectification (Figure 15B). Use of a long duration pulse ensured that resistance measurements could be taken after membrane potential had stabilized following this early-onset rectification (see further description below). For each neuron, the changes in membrane potential resulting from a range of current pulses of varying amplitudes, were recorded, and a current-voltage relationship was plotted. For the range of hyperpolarizing voltages, this relationship was close to linear. The slope of this relationship was then taken as whole cell resistance for each neuron; samples of these plots are shown beside the data traces for the neurons in Figure 15A and B. Figure 16 presents a graphic summary of the mean values of resistance for each class of neuron. The slopes of the current-voltage relationships for Type I and II neurons were not significantly different at any current, and this is reflected in the lack of significant differences in whole-cell resistance for these three types in Table 6. However, Type III neurons displayed significantly greater voltage displacements than did Type I and Type II neurons for all values of current within the range tested, and consequently had a significantly higher mean whole-cell resistance than did the other types (Table 6).

The time constant, a measure of the time required to reach maximal response, was calculated by the curve fitting program Clampfit (pClamp software) using a Chebyshev transformation, that is, the sum of a finite number of polynomial functions which

Figure 15. Response of membrane potential (upper set of traces in each left hand panel) of two intracardiac neurons to hyperpolarizing current clamp. Current pulses (lower set of traces in each left hand panel) were delivered through the recording electrode. A: Non-rectifying response: clamping currents of increasing amplitude produced graded hyperpolarization of membrane potentials without transient responses. B: Rectifying response: time-dependent rectification of membrane potential occurred in the initial segments of the responses of this neuron. In all cases, measurements of voltage displacement were taken in the last 50 ms of the responses (after arrows) to determine whole-cell resistance. Measurements of voltage displacement were plotted against stimulation current intensities, are shown in the right hand panels for each neuron. The slope of the current-voltagerelationship represents whole-cell resistance. Both neurons were Type II. Vertical bar: 30 mV and 1 nA; Horizontal bar: 100 ms.

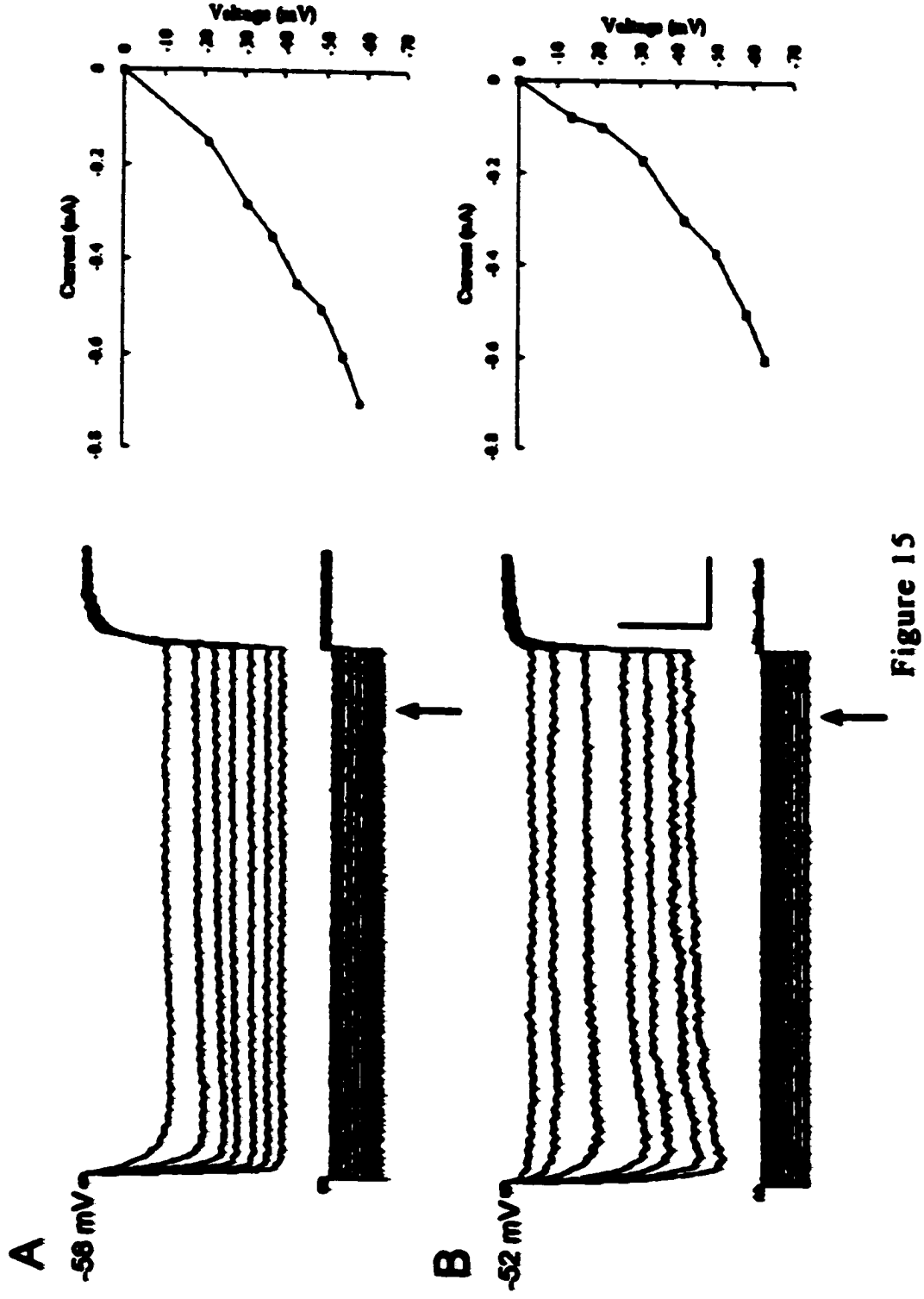

Figure 15

describe the curve. For a typical response, the waveform generated by the hyperpolarizing current (0.01-0.5 nA), fits a single exponential equation, as indicated by the close correspondence between the simulated waveform generated by the equation and the recorded waveform in Figure 17. Type I neurons had a mean time constant half that of Type III neurons, a significant difference (Table 6). The value for the time constant of Type II neurons, while larger than that of Type I neurons, was not significantly different from the mean value for Type III neurons.

The regenerative membrane properties of the three types of intracardiac neurons displayed different trends. Type I neurons had significantly higher current threshold values for generating an AP than did either Type II or Type III neurons. However, mean voltage threshold for generating an AP did not differ significantly among the groups of intracardiac neurons. The mean duration of the AP for Type I neurons was significantly greater than that of Type II neurons but not Type III neurons, even though the mean duration of the AP for Types II and III neurons was identical. The lower confidence statistic for the comparison between Types I and III neurons was likely due to the smaller sample size of Type III neurons. As reported above, the mean duration of the AHP was significantly different among the classes of neurons while the amplitude of the AHP of Type I neurons was significantly smaller than that of Type III neurons. Type II neurons had a mean AHP amplitude which was intermediate between those of Type I and III neurons.

Rectification (see example in Fig. 15B) was displayed by 22% of the Type I neurons. A larger percentage of Type II and III neurons showed rectification (65% and 85%, respectively). In every case, however, the onset of rectification occurred at a

similar potential level, approximately 30 mV in the hyperpolarizing direction from the resting membrane potential.

Morphological study

Six neurons were successfully filled with the fluorescent dye, tetramethylrhodamine dextran (3000 m.w.) from the intracellular recording electrode. The morphology of cell soma and processes of each cell were photographed and analyzed with the confocal microscope (Fig. 18). A single large process, presumably the axon, typically extended from the cell soma, through the ganglion and into a nerve of the intracardiac plexus, extending past the cut edge of the tissue. The axon of one neuron was observed to bifurcate approximately 100 μm from the axon hillock (not shown). Small support cells were seen surrounding the somata of all neurons and were intermingled amongst short neuronal processes and blood vessels which coursed through each ganglion. Reconstruction of whole-cell neuronal volume was accomplished by summing the cross sectional areas of each one of a series of optical sections of a neuron and multiplying that value by the depth of each section (usually less than 1 μm). There was a large degree of variance in the volumes of these neurons, but one apparent relationship between volume and neuron type was revealed. The smallest cell volume was 2,948 μm^3 and this cell exhibited the AHP properties of a Type I neuron (Fig. 18A). Three intracardiac neurons which demonstrated properties of Type II neurons ranged from 4,500 - 5,300 μm^3 in volume (Fig. 18B-D). The two largest cells had volumes of 5,655 and 13,213 μm^3 and the time course of their AHPs corresponded with that of the

Figure 16. Mean current-voltage plots for Type I (filled circles, ●), Type II (squares, ■) and Type III (triangles, ▲) neurons were constructed with data compiled from individual neurons (see Fig. 3 for examples). At each current intensity, the mean displacement from resting potential in Type III neurons was significantly greater (asterisks, *, $p \leq 0.05$) than displacement for Types I and II.

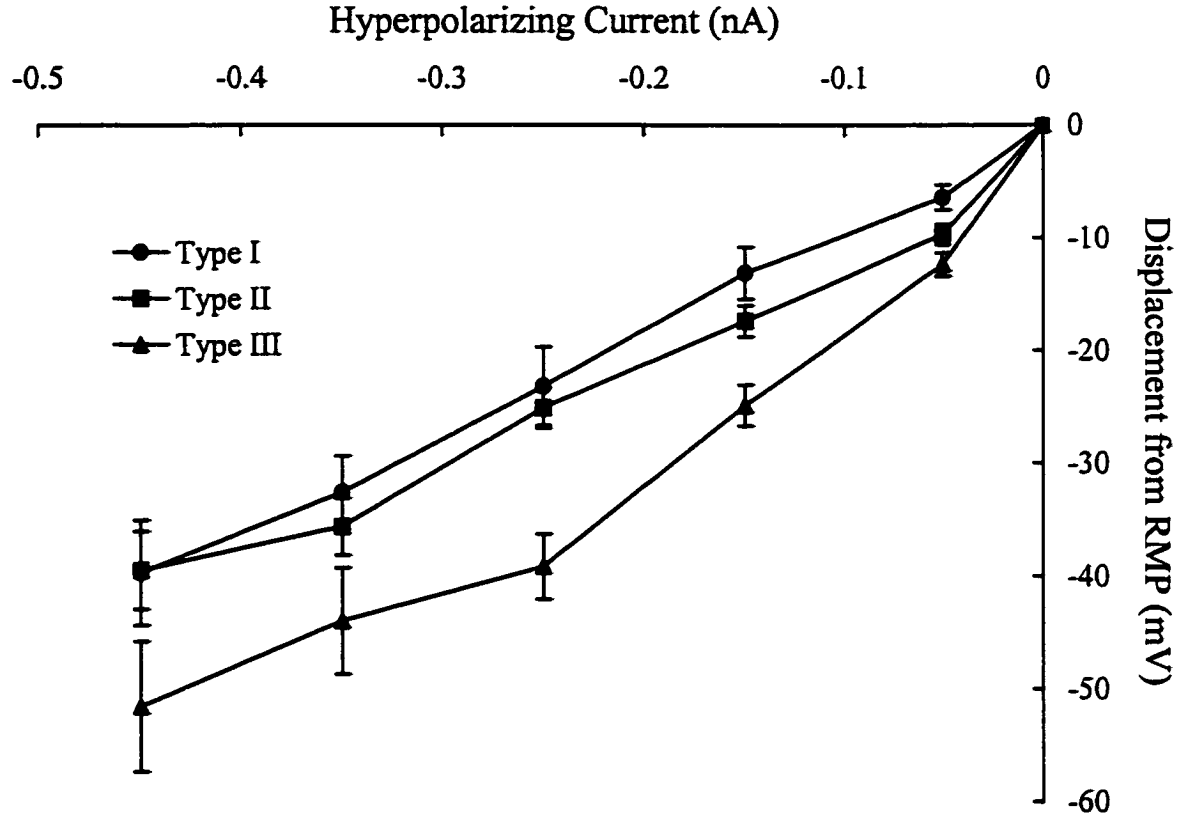
Hyperpolarizing Current (nA)
-0.5
-0.4
-0.3
-0.2
-0.1
0
Type I
Type II
Type III
0
-10
-20
-30
-40
-50
-60
Displacement from RMP (mV)

Figure 16

Figure 17. Example of data used for calculation of the whole-cell time constant, derived from the membrane potential response to a small hyperpolarizing current step (< 0.5 nA). The top trace illustrates the recorded change in membrane potential as the current was applied (bottom trace). The centre trace represents a plot of the first-order exponential equation which best fits the recorded trace and provides the value for the time constant, τ (9 ms). Horizontal bar: 5 ms; Vertical bar: 4 mV and 0.1 nA.

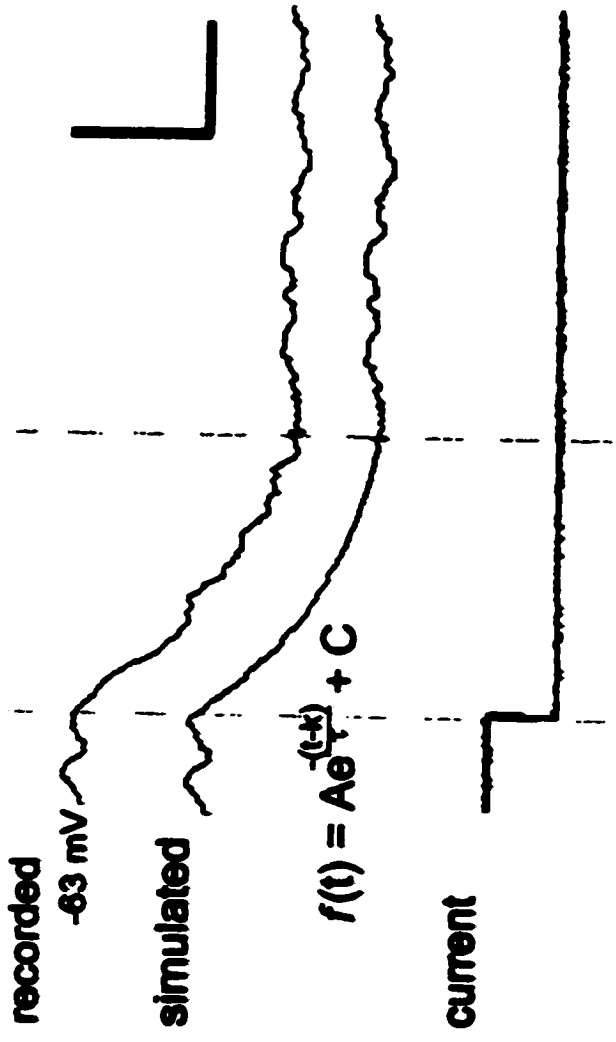

Figure 17

type III classification (Fig. 18E-F). This apparent relationship between cell volume and neuron type was, therefore, supported by the values of the time constants for these neurons. The smallest neuron had the shortest time constant while the larger neurons had longer time constants, conforming to the trend in the relationship between time constant and neuron type shown in Table 6.

Firing properties

A method of classification of autonomic neurons which has been proposed in previous studies is based on firing behaviour of neurons in response to long depolarizing current pulses from the intracellular electrode. Neurons with two distinct types of firing behaviour were found in the present study; there were termed "phasic" and "accommodating". Phasic neurons discharged only one action potential in response to long intracellular depolarization (Fig. 19A). In contrast, accommodating neurons produced repetitive action potentials whose interspike interval increased, or accommodated, during long depolarizations (Fig. 19B). The firing behaviour of neurons is an index of their excitability, with accommodating neurons being relatively more excitable than phasic neurons. Overall, phasic neurons outnumbered accommodating neurons by almost 3:1. Within neuron types, it was found that Type I neurons were equally likely to have phasic or accommodating discharge patterns. However, 92% of Type II neurons demonstrated phasic firing properties. Type III neurons, however, like Type I neurons, were equally likely to be accommodating or phasic.

Figure 18. Morphology and estimated volumes of cells representative of the three classes of guinea-pig intracardiac neurons. Each cell was injected with the fluorescent dye, tetramethylrhodamine dextran (3000 m.w.) from the intracellular recording electrode after electrophysiological characterization was complete. Large neurites, presumably axons, could be observed for distances of more than 2 mm from cell somas. A: Type I neuron had the smallest cell volume; B-D: Type II neurons had intermediate volumes (mean = 4,900 μm^3), E-F: Type III neurons had the largest cell volume (mean = 9,400 μm^3). Calibration bar: 30 μm.

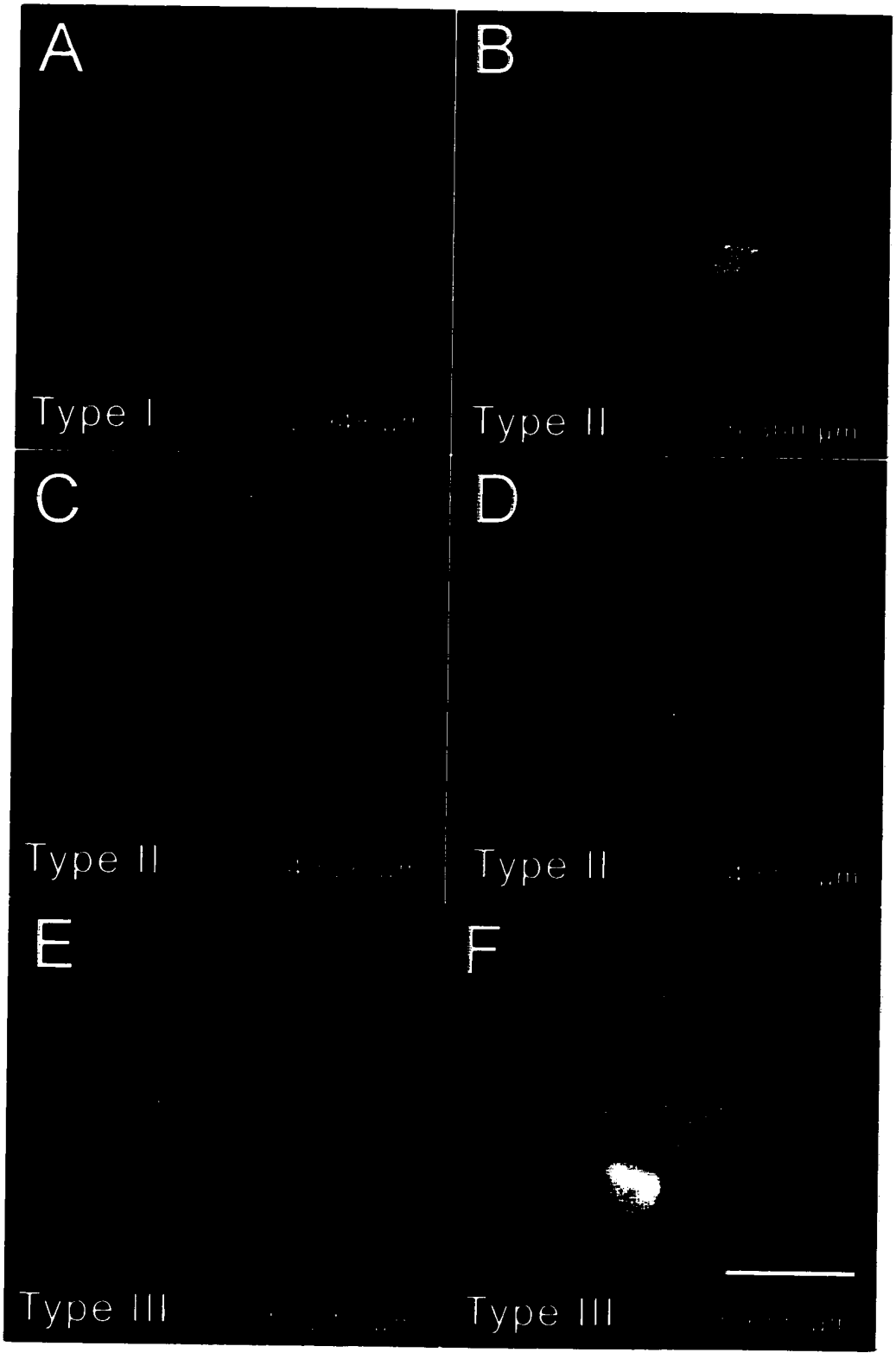

Figure 18

Analyzing this data in another way, it was found that 72% of all accommodating neurons fit into the Type III category. Thus, neurons with relatively long duration AHPs were more likely to fire APs at high frequency when depolarized through the intracellular electrode.

Synaptic transmission

Neuronal responses to synaptic inputs from axons in intracardiac nerves innervating the ganglia were characterized. Fast excitatory postsynaptic potentials (EPSPs) were produced by stimulation of interganglionic nerves, as shown in Fig. 20B-C. As the strength of the stimulus current was increased, EPSP amplitude increased and in some neurons reached threshold for AP generation. Several nerves were connected to intracardiac ganglia, as described in Chapter 2, and some of these nerves were considerably smaller in diameter than the stimulating electrode. It was thus difficult or impossible to stimulate all nerves connecting to a particular ganglion. A response to nerve stimulation was produced in 75 neurons tested, however of these, only 25 neurons appeared to be activated orthodromically. Orthodromic activation was confirmed by lowering the concentration of Ca^{++} (0.5mM) and increasing the concentration of Mg^{++} (10mM) in the bath solution. The observation that this procedure suppressed neuronal responses to nerve stimulation, indicating that the effects of stimulation were orthodromically mediated. Figure 20 demonstrates the effect of perfusate containing low Ca^{++}, high Mg^{++} on synaptic neurotransmission. A robust response evidenced in the control trace (Fig. 20C) was abolished in the modified perfusate (Fig. 20D). Application of hexamethonium (Fig. 21B) or mecamylamine (Fig. 22B,C,D) to the perfusate also

Figure 19. Intracardiac neurons exhibited two types of response (upper trace in each panel) to long depolarizing current pulses delivered through the intracellular recording electrode (lower traces in each panel). A: Phasic neuron discharged one AP at the start of stimilation. B: Accommodating neuron discharged repetitive APs with increasing inter-spike intervals over the duration of the stimulus pulse. Horizontal bar: 50 ms; Vertical bar: 4 mV and 0.1 nA.

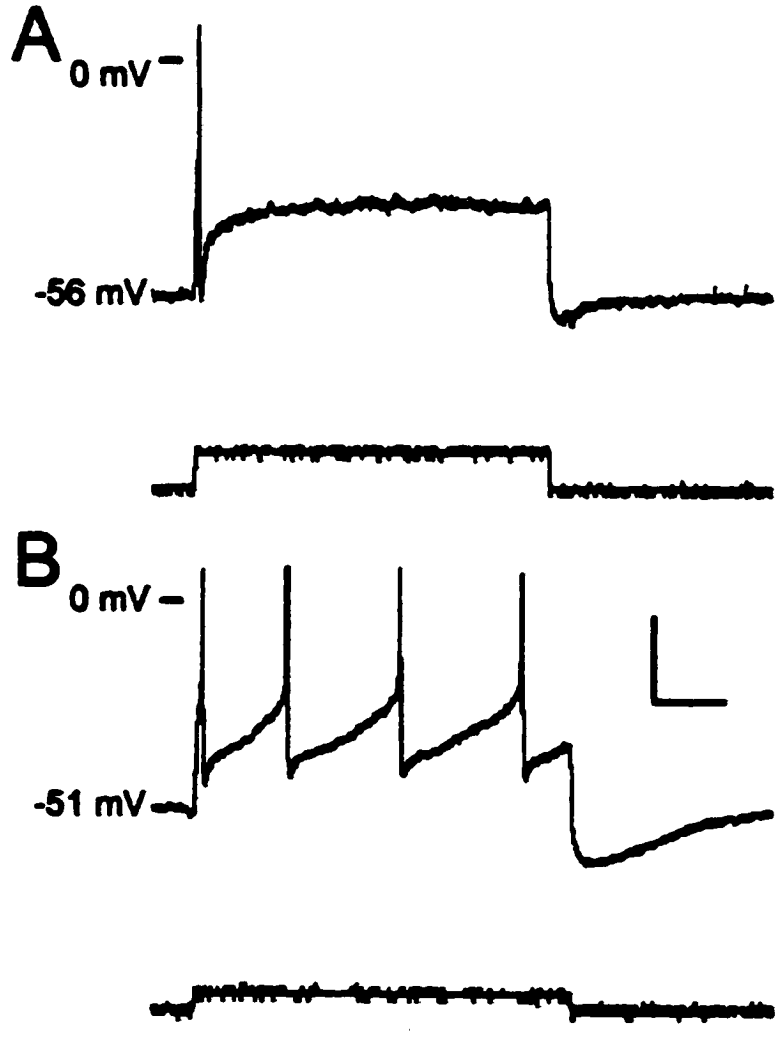

Figure 19

eliminated or inhibited neurotransmission, showing that, at these synapses, fast nicotinic transmission was responsible for the postsynaptic events. In Figure 21, an AP generated by interganglionic nerve stimulation (Fig. 21A) was lost after a 5 min exposure to 10 μM hexamethonium (Fig. 21B). With a 10 min rinse of the tissue, responses to nerve stimulation recovered (Fig. 21C). Similarly, mecamylamine attenuated the response of another neuron to orthodromic nerve stimulation (Fig. 22B-C). No inhibitory potentials were generated from the stimulation of interganglionic nerves in this study.

Effects of adrenergic agents on intracardiac neurons

Agonists acting both at α- and ß-adrenergic receptors influenced basic cellular properties, firing behaviour and orthodromic responses of intracardiac neurons. These effects are described separately below.

α-adrenergic effects

Pressure application of the α_1-agonist, phenylephrine (PHEN), from a pipette with its tip placed close to the impaled neurons, resulted in changes in one or more of membrane conductance, membrane potential, firing behaviour and synaptic transmission, in 91% of all neurons tested.

i) Effects on membrane potential

Figure 23 (A and B) illustrates the range of responses of the membrane potential to the application of PHEN. In those cells in which changes in membrane potential occurred in response to activation of α-adrenergic receptors, either hyperpolarization or

Figure 20. Responses of an intracardiac neuron to single-pulse stimulation (STIM, arrow; 0.5 ms pulse duration) of an interganglionic nerve. Stimulus current for each trace is indicated on the left; stimulus artifacts have been truncated for clarity. A-C: increases in current intensity evoked an EPSP (B) and an AP (C) indicating that this neuron summed multiple inputs to reach firing threshold. D: perfusion of the preparation with a modified perfusate containing 0.5 mM Ca^{++} and 10 mM Mg^{++} eliminated the response to nerve stimulation, confirming that this response was synaptically mediated. Vertical bar: 10 mV; horizontal bars 10ms.

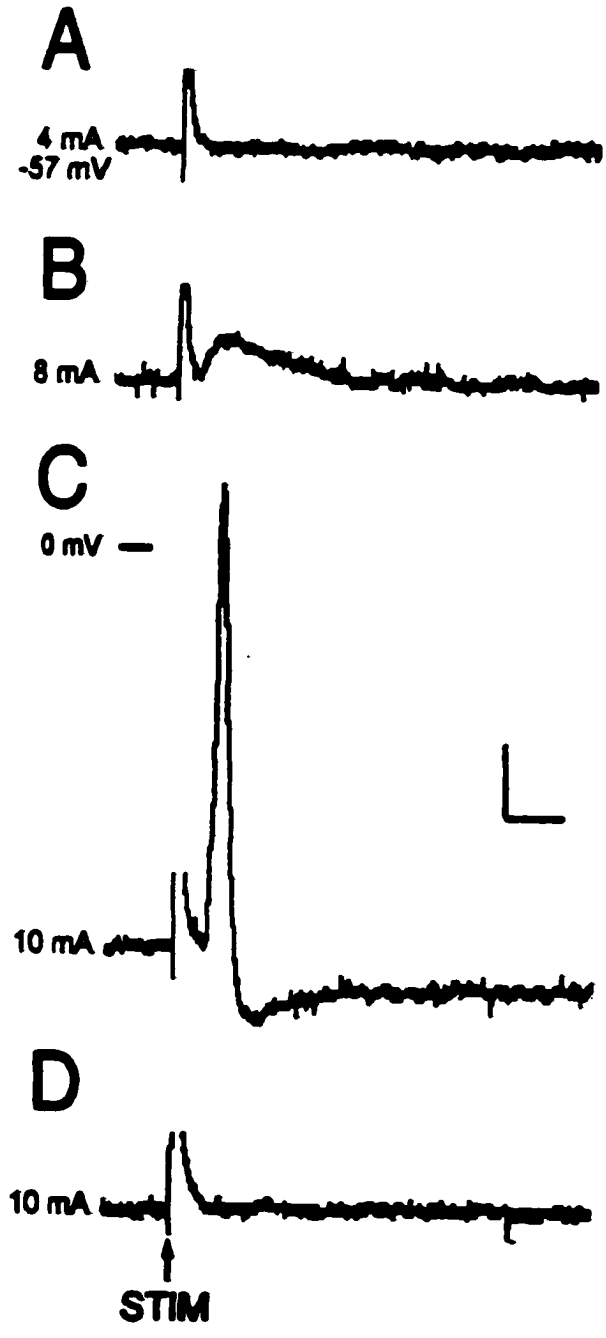

Figure 20

Figure 21. The nicotinic channel blocker hexamethonium eliminated the response of a neuron to suramaximal nerve stimulation (STIM, arrow). A: pre-hexamethonium control response. B: 5 min perfusion with hexamethonium (100 μM in perfusate) eliminated response. C: response recovered after a 10 min washout. Vertical bar: 20 mV; horizontal bar: 20 ms.

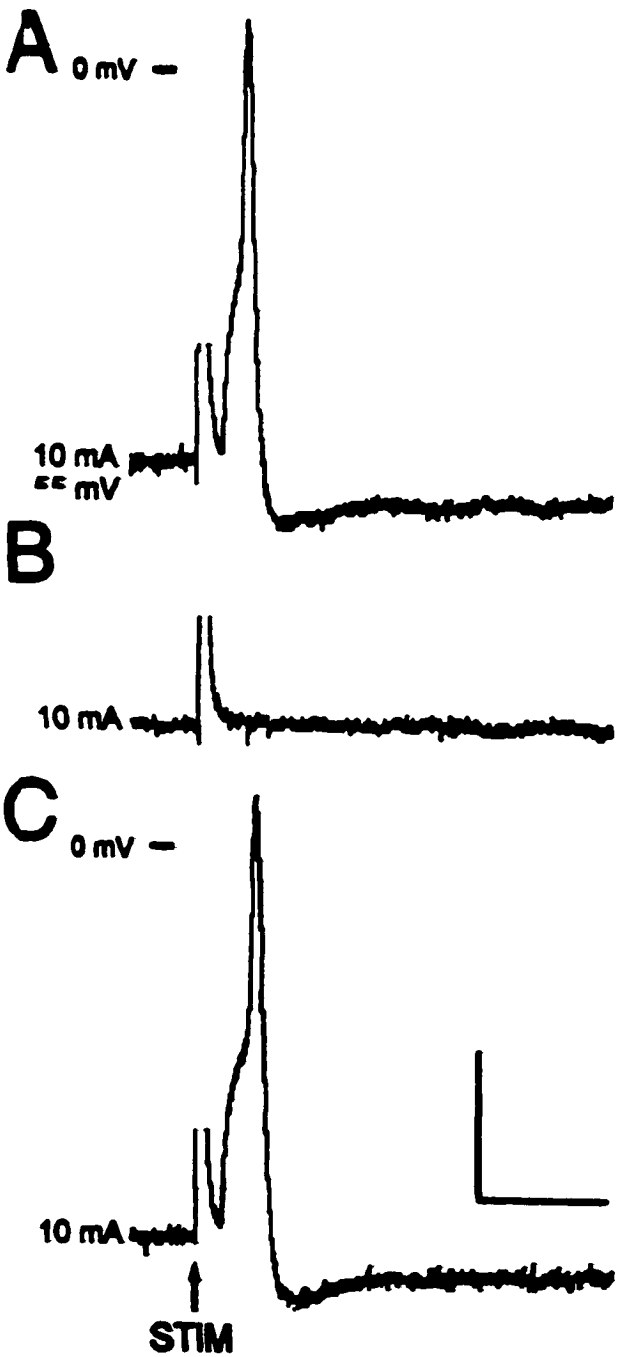

Figure 21

Figure 22. The nicotinic receptor channel antagonist mecamylamine attenuated the response of a neuron to supramaximal nerve stimulation (STIM, arrow). A: pre-mecamylamine control response. B: 2 min perfusion with mecamylamine (100 μM in perfusate) eliminated the AP and reduced the EPSP amplitude. C-D: 3.5 and 5 min perfusion with mecamylamine reduced EPSP amplitude further. Vertical bar: 20 mV; horizontal bar: 20 ms.

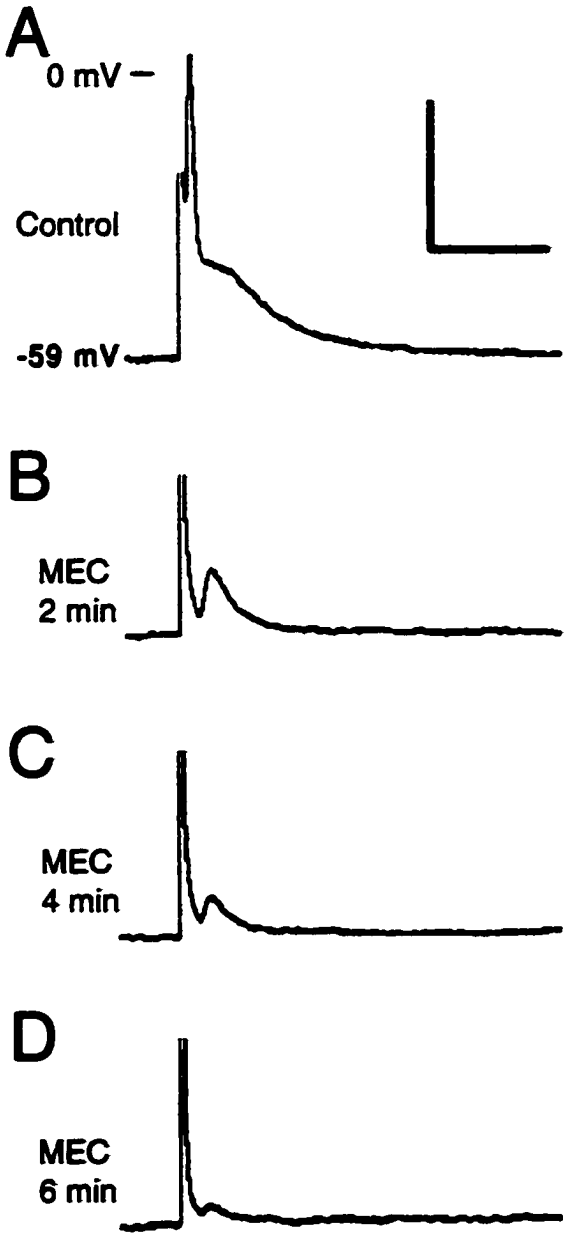

Figure 22

Figure 23. Examples of effects of phenylephrine (PHEN) on membrane potential and whole cell conductance in three intracardiac neurons. Changes in conductance were established by recording the amplitude of displacement of membrane potential (upper traces in each panel) to repetitive hyperpolarizing intracellular current pulses (800 ms duration, lower traces in each panel). In this and subsequent similar figures, arrows indicate points where current-induced voltage displacement before application of pre-PHEN was compared to the post-PHEN response. The membrane potential was returned to the pre-PHEN level by a steady injection of current before conductance was estimated. A: PHEN (100 μm, 200 ms pulse), applied from a nearby pipette tip (at square), hyperpolarized membrane potential and decreased conductance in a Type II neuron. B: PHEN (1 mM, 200 ms pulse) evoked a larger hyperpolarization but no change in conductance in a Type II neuron. C: PHEN (100 μM, 200 ms pulse) depolarized membrane potential with no change in whole cell conductance in a Type III neuron. Vertical bar: 40 mV and 2.5 nA; horizontal bar: 15 s.

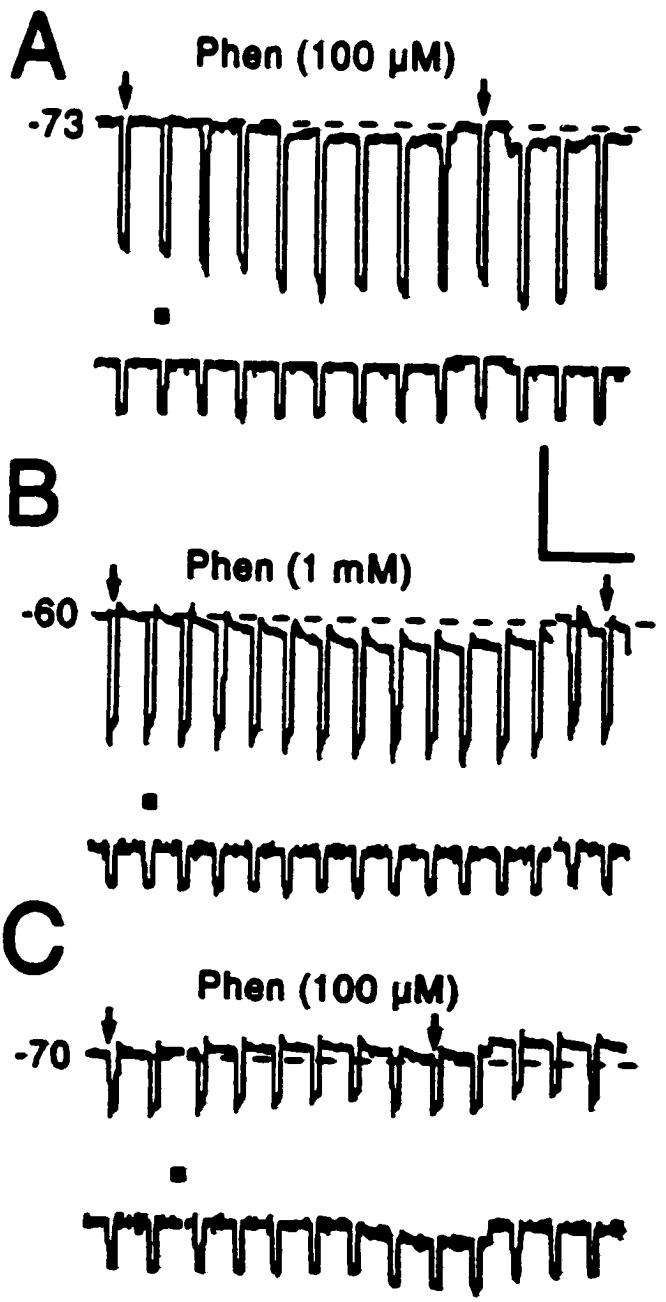

Figure 23

depolarization was observed. For neurons displaying hyperpolarization, the degree of their response was dependent on the concentration of PHEN. In Figure 23A, a Type II neuron was maximally hyperpolarized within 6 seconds of the application of PHEN. In response to the application of a 1 mM concentration of PHEN, another Type II neuron (Fig. 23B) was hyperpolarized to a greater degree, and for longer than the response to the lower concentration. Neither the concentration of PHEN nor the cell type was a reliable predictor of the response of membrane potential. The mean changes in membrane potential in response to the application of the two concentrations of PHEN are summarized in Figure 24; 4 neurons (14% of the 29 neurons tested) showed hyperpolarizing responses which were larger at the higher concentration.

The neuronal response illustrated in Figure 23C was typical of neurons displaying depolarization of membrane potential following the application of PHEN. The mean depolarization of the membrane potential from rest is summarized in Figure 24. The degree to which the membrane was depolarized was not dose dependent, at least for the range of doses used, suggesting that maximal activation of α-adrenergic receptors may have been achieved at the lower dose of 100 μM. The majority of responsive neurons were depolarized to the same degree by either 100 μM or 1 mM PHEN (3 and 12 respectively of 29 neurons tested). The mean values of membrane potential of neurons exposed to 1 mM PHEN were significantly different from mean resting potential values. Any further statistical analyses of these responses were not performed because of the low sample size for each drug dose. However, of the 29 cells tested with PHEN, 10 cells showed no change in the membrane potential. When PHEN was substituted with

perfusate containing no drug in the pipette, no response to pressure application was observed, indicating that responses obtained with PHEN were not the result of pressure artefacts, or due to application of the vehicle for the drug.

ii) Effects on membrane conductance

Adrenergically-mediated changes in conductance were implied from membrane potential responses to 800 ms hyperpolarizing current pulses of constant amplitude delivered through the recording electrode before and after pressure application of the agent. If neurons also exhibited an adrenergically-induced change in membrane potential from the resting level, the potential was first restored to the resting level by injecting a steady current through the recording electrode, before estimating any change in conductance. All but 2 neurons demonstrated monophasic conductance responses to PHEN; the two neurons with biphasic responses (that is, increased and decreased conductance after a single application of PHEN) were excluded from the calculation of means. Examples of the change in conductance following pressure application of PHEN are presented in Figure 23. The response of the neuron shown in Figure 23A indicated an decrease of 15% in whole-cell conductance. The mean changes in conductance in response to the application of both concentrations of PHEN are summarized in Figure 25. Nine neurons of 29 tested (31%) showed an increase in conductance. Conversely, the neuron in Figure 23B had shown a decrease in whole- cell conductance of 12% in response to PHEN.

Figure 24. Mean changes in membrane potential in 29 neurons after local application of PHEN at two concentrations (100 μM and 1 mM). Bars represent mean responses to PHEN for each of three groups of neurons: those neurons that depolarized (designated as a positive displacement from the resting potential), hyperpolarized (designated as a negative displacement from the resting potential) or showed no change (short bar). The number of neurons included in each group is indicated in parentheses.

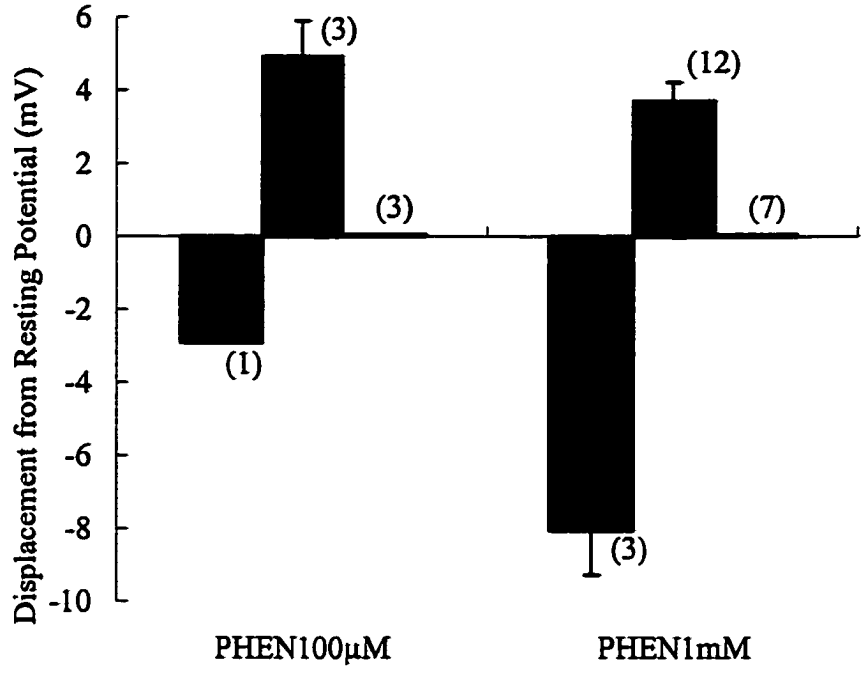
Displacement from Resting Potential (mV)
6
4
2
0
-2
-4
-6
-8
-10
(3)
(3)
(1)
(12)
(7)
(3)
PHEN100µM
PHEN1mM

Figure 24

A decrease in conductance was observed in 15 of 29 neurons tested; the mean conductance decrease for this group is summarized in Figure 25. A 1 mM concentration of PHEN induced a significantly larger depression in conductance than did a 100 μM concentration. In Figure 23C is shown an example of a neuron in which conductance was not altered by PHEN. A total of 5 neurons (of 29 tested) did not respond with a change in conductance to the application of PHEN.

Changes in conductance were not necessarily accompanied by changes in membrane potential in the same neuron; some neurons showed only membrane potential responses, while in others only conductance was affected by PHEN. In neurons which responded with both potential and conducntance changes, no overall correlation was found between the effects of PHEN on these variables. That is, a change in conductance in a particular direction did not necessarily correspond to a change in membrane potential of the same direction, in these neurons. Analysis of the variables describing the AP or the AHP showed that these did not change after PHEN.

iii) Effects on firing behaviour

PHEN had both inhibitory and excitatory effects on the frequency of APs generated by long depolarizing current pulses (500 to 800 ms duration) delivered from the intracellular recording electrode. Figure 26 provides examples of PHEN-induced changes in firing behaviour. The neuron in Figure 26A initially displayed accommodating firing behaviour in response to a long depolarizing current pulse. Following the application of 1 mM PHEN, this neuron displayed phasic firing. Thus, the

excitability of this neuron was inhibited by activation of α-adrenergic receptors. An example of facilitation of neuronal firing is presented in Figure 26B. In this example, a phasic neuron was converted to show an accommodating firing pattern following the application of PHEN (1mM). Either facilitation or inhibition of neuronal firing was observed in 20% of all neurons tested with PHEN.

The effects of PHEN on firing behaviour varied with the type of neuron. None of the Type I neurons sampled displayed any change in firing behaviour under the influence of PHEN, while 24% of Type II and 33% of Type III neurons were induced to alter their firing patterns by PHEN (Table 7). Surprisingly, these changes in firing behaviour did not correspond to changes in membrane conductance in the appropriate direction. In other words, neurons which initially had accommodating firing behaviour and later showed phasic firing after the application of PHEN, did not also exibit increased membrane conductances. Regression analysis of these data demonstrated no correlation between changes in firing behaviour and changes in conductance or membrane potential. The duration of the AHP was the only property which was consistently modified in conjunction with neuronal excitability following exposure to PHEN. Neurons which showed a small increase in excitability consistently displayed an increase in duration of the AHP.

Figure 25. Mean changes in whole cell conductance in the same group of neurons as in Figure 24 after local application of PHEN at two concentrations (100 μM and 1 mM). Bars represent percent changes in whole-cell conductance from the normalized pre-PHEN control value (100%) for each of three groups of neurons: those neurons that displayed an increase, a decrease, or no change (short bar). The number of neurons included in each group is indicated in parentheses; an asterisk (*) denotes a significant difference in conductance after PHEN application ($P \leq 0.05$).

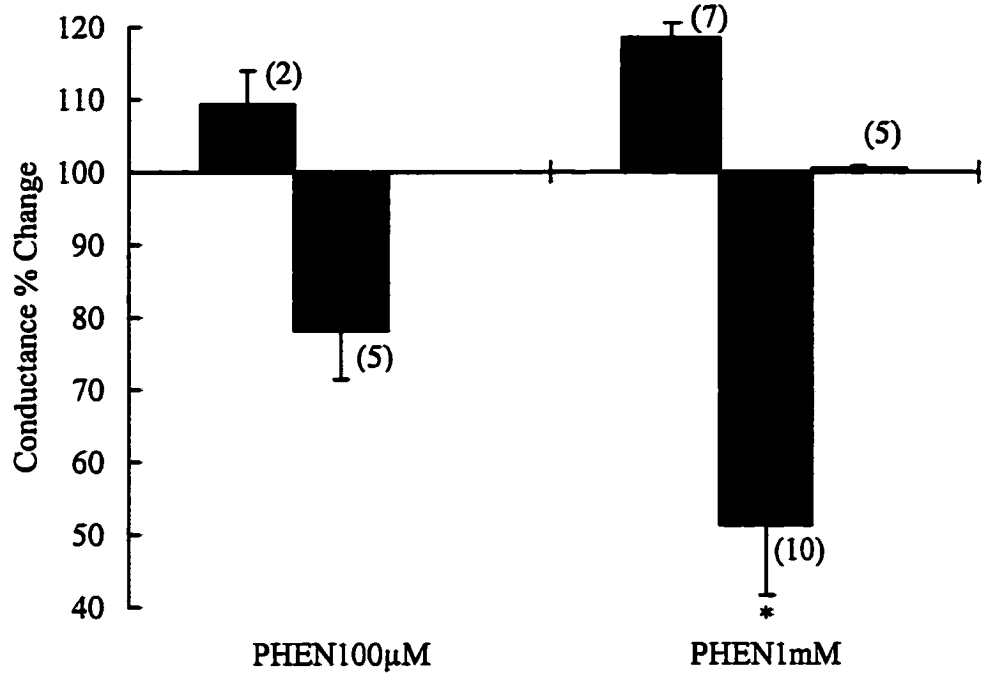
120
110
100
90
80
70
60
50
40
Conductance % Change
(2)
(5)
(7)
(5)
(10)
*
PHEN100μM
PHEN1mM

Figure 25

iv) Effects on neurotransmission

PHEN (1 mM) inhibited AP generation in response to suprathreshold levels of orthodromic activation, in 4 of 5 intracardiac neurons tested. Figure 27 demonstrates abolition of both the AP and the superimposed EPSP in an intracardiac neuron upon nerve stimulation 3 minutes after the application of 1 mM PHEN. An increase in the stimulation current applied to the nerve could occasionally elicit an AP (n=2) after inhibition by PHEN, however, typically those neurons would not fire an AP in this condition.

v) Effects of prazosin

Subsequent to completion of the α-agonist study, neurons in some intracardiac ganglia were exposed to prazosin, an antagonist specific for α-adrenergic receptors, prior to a second application of PHEN. This part of the study proved to be exceedingly

Table 7. Neuron excitability was influenced by both α- and ß-adrenergic agonists. PHEN could convert phasic to accommodating firing behaviour, or vice versa. ISO could convert accommodating to phasic firing behaviour, but not the reverse. For each agonist, the number of neurons which were converted are indicated by the number under the "converted" column.

Table 7

	1mM PHEN		1mM ISO	
	Tested	Converted	Tested	Converted
Accom	8	4 (50%)	10	4 (40%)
Phasic	17	3 (18%)	28	0
Total Neurons	25	7 (28%)	38	5 (13%)

	1mM PHEN		1mM ISO	
	Tested	Converted	Tested	Converted
Type I	5	0	2	1 (50%)
Type II	17	4 (24%)	21	1 (5%)
Type III	6	2 (33%)	11	2 (18%)
Total Neurons	28	6 (21%)	34	4 (11%)

Figure 26. Examples of α-adrenergic modification of firing behaviour in two neurons. A: Control: neuron fired repetitively (upper trace) in an accommodating pattern during membrane depolarization (800ms current pulse, lower trace). Approximately 2 min after applying PHEN (1mM) firing frequency was decreased in response to the same intracellular stimulation. B: Control: a single AP was elicited during membrane depolarization (500 ms current pulse, lower trace). Application of PHEN (1mM) increased the firing frequency in response to repeated stimulation. Vertical bar: 30 mV and 2 nA; horizontal bar: 100 ms.

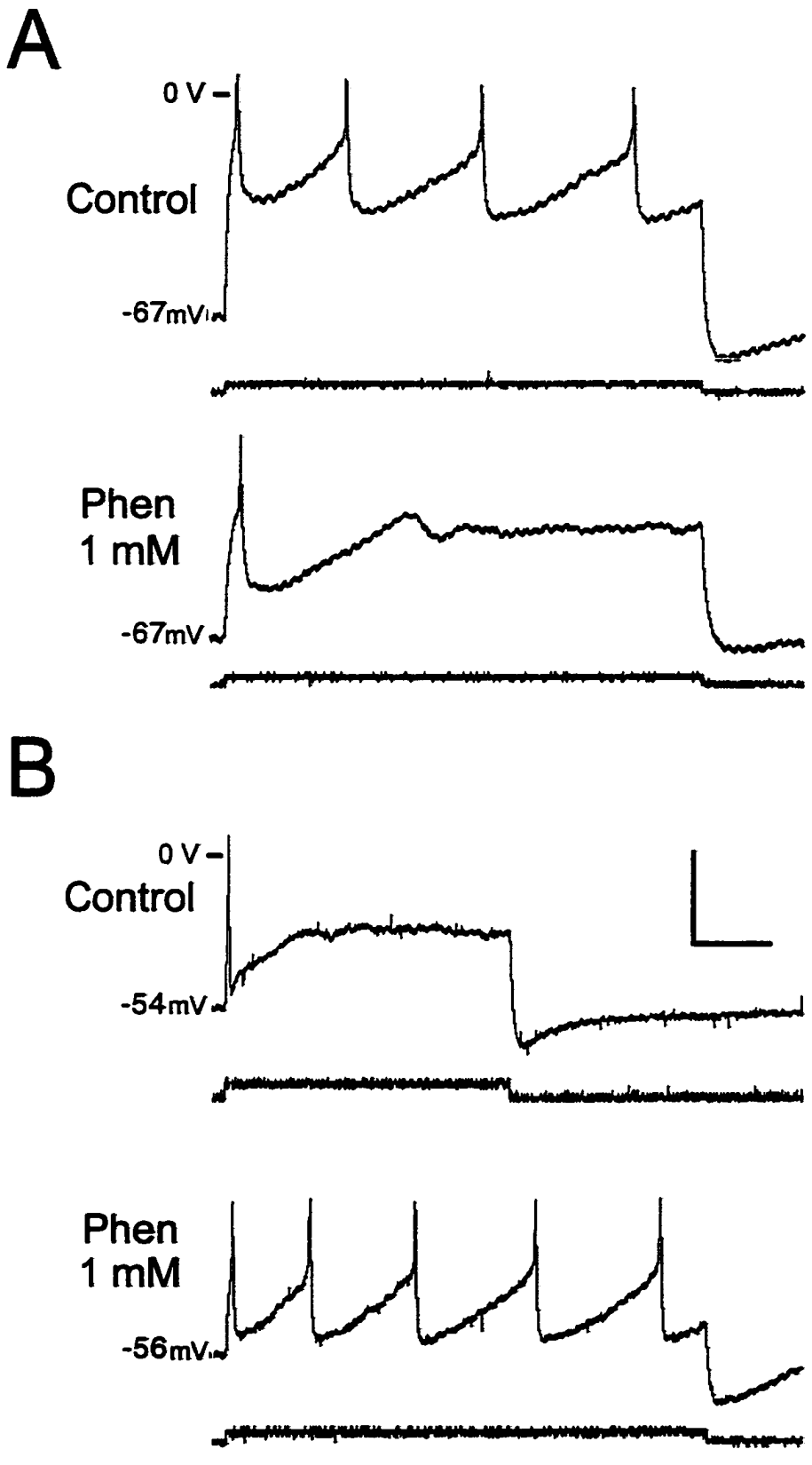
A
0 V
Control
-67mV
Phen
1 mM
-67mV
B
0 V
Control
-54mV
Phen
1 mM
-56mV

Figure 26

difficult due to the amount of time required to test for agonist responses, rinse the tissue, apply the antagonist and retest for agonist responses. The duration of most viable neuron penetrations was between 20 and 40 minutes; in many cases there was not enough time for a complete cycle of agonist-antagonist testing. However, this process was completed on a total of 10 neurons. In the instances when prazosin was applied (at a concentration of 10 μM), it abolished the effect of PHEN on whole cell conductance and membrane potential as shown in the examples in Figure 28. Not all of the cells in this group demonstrated a PHEN-mediated changes in both membrane potential and whole-cell conductance. Four of the cells tested with PHEN (1mM), responded with a mean depolarization of 6 ± 2 mV; this response was abolished in the presence of prazosin. Six of the neurons exhibited a mean increase of 115 ± 1% (n=6) in conductance after the application of PHEN (1mM); in the presence of prazosin, the same dose of PHEN produced no change in conductance.

ß-adrenergic effects

Pressure application of the ß-agonist isoproteronol (ISO) from a pipette with its tip near an impaled neuron resulted in changes in one or more of: resting membrane potential, whole-cell conductance, firing behaviour or synaptic transmission, in 87% of neurons tested. The majority of neurons in this part of the study which did not respond to the application of ISO were also tested with PHEN, and did not respond to that agent either.

Figure 27. PHEN abolished the response of an intracardiac neuron to single-pulse (0.5 ms duration STIM, arrow) stimulation of an interganglionic nerve. In the top trace (control), this stimulus evoked an EPSP which was suprathreshold for AP generation. Approximately 3 min following PHEN (1 mM) application the same nerve stimulation evoked no response. In both traces the stimulation artifact has been truncated for clarity. Vertical bar: 20 mV; horizontal bar: 10 ms.

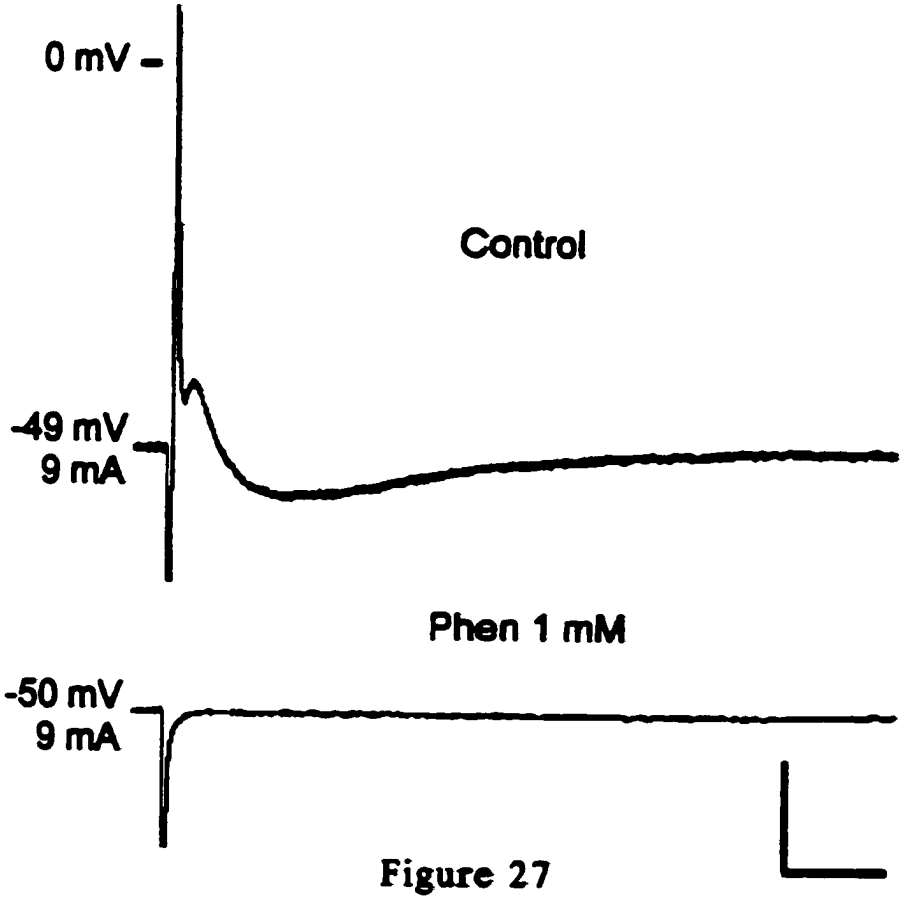

Figure 27

i) Effects on membrane potential

Approximately 67% of the neurons tested showed a change in their resting membrane potential at doses of either 100 μM or 1 mM ISO. Figure 29 presents examples of responses to ISO. Figure 29A illustrates a short-duration, transient depolarization (13 mV) of the membrane potential with concurrent changes in conductance after the application of 100 μM ISO. Figure 29B shows a prolonged depolarization (peak amplitude 20 mV) of membrane potential with the application of 1mM of ISO. A total of 15 neurons of 45 tested displayed depolarization in response to ISO application. Mean values for depolarizing changes in membrane potential are presented in Figure 30. The amplitude of depolarization after the application of 100 μM ISO was not significantly different from that in response to 1 mM ISO.

ISO was also capable of hyperpolarizing neurons. In Figure 29C, a 100 μM dose of ISO induced a hyperpolarization of 11 mV. Data from hyperpolarizing responses are summarized in Figure 30. The mean hyperpolarizing change in membrane potential showed a dose-dependent effect; 1mM ISO evoked a greater hyperpolarizing response than did 100 μM ISO. Some neurons had no membrane potential response to the application of ISO. No response was observed when vehicle alone was applied from the drug delivery pipette.

ii) Effects on membrane conductance

Changes in membrane conductance induced by ISO were estimated as described in the previous section for responses to PHEN. Figure 29A illustrates a short-duration,

Figure 28. Prazosin (10 μM in bath for 5 min) abolished the response of an intracardiac neuron to pressure-applied PHEN (100 mM, 200 ms pulse). Control: the application of PHEN resulted in an decrease in the whole cell conductance as indicated by the increased amplitude of the voltage response (upper trace) to hyperpolarizing current pulses (lower trace). Prazosin abolished the response to a second application of PHEN. Vertical bar: 40 mV and 2 nA; horizontal bar: 6 s.

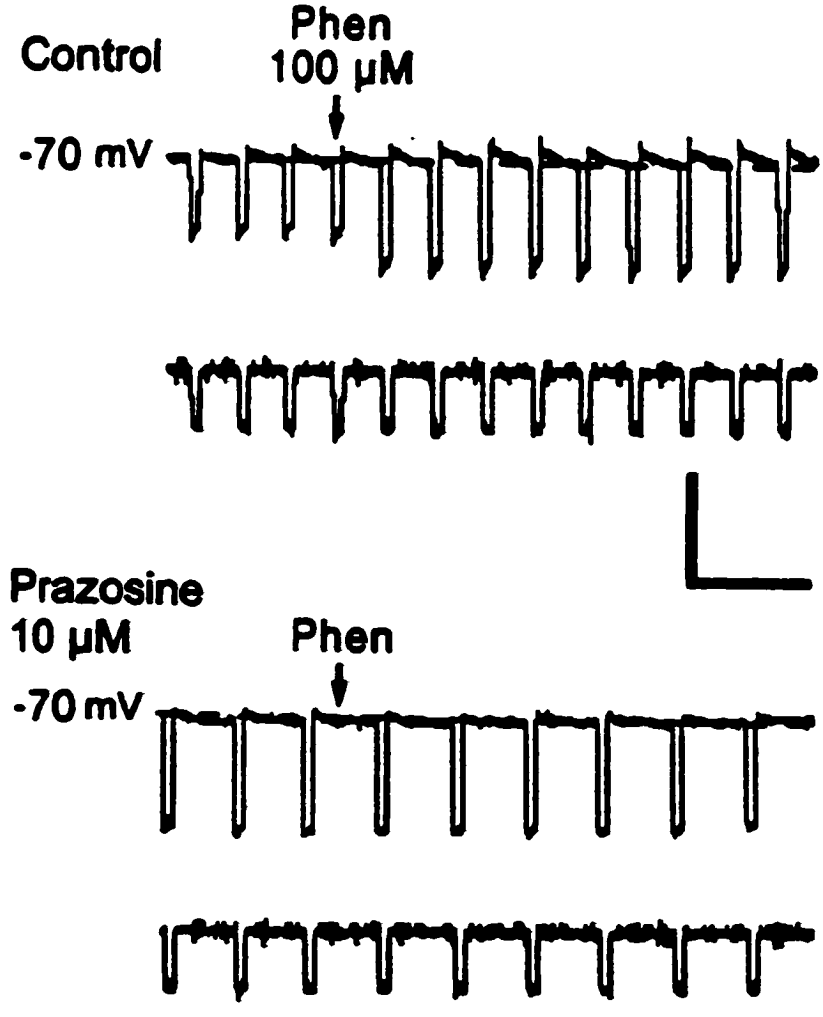

Figure 28

Figure 29. Examples of the effects of isoproteronol (ISO) on whole cell conductance and resting membrane potential in three intracardiac neurons. A: ISO (100 μM, 200 ms pulse) elicited a brief depolarization of the membrane potential and reduction in whole cell conductance. B: ISO (1 mM, 200 ms pulse) produced a prolonged depolarization of membrane potential. C: ISO (1 mM, 200 ms pulse) hyperpolarized membrane potential with no change in conductance. Vertical bar: 40 mV and 2 nA; horizontal bar: 10 s.

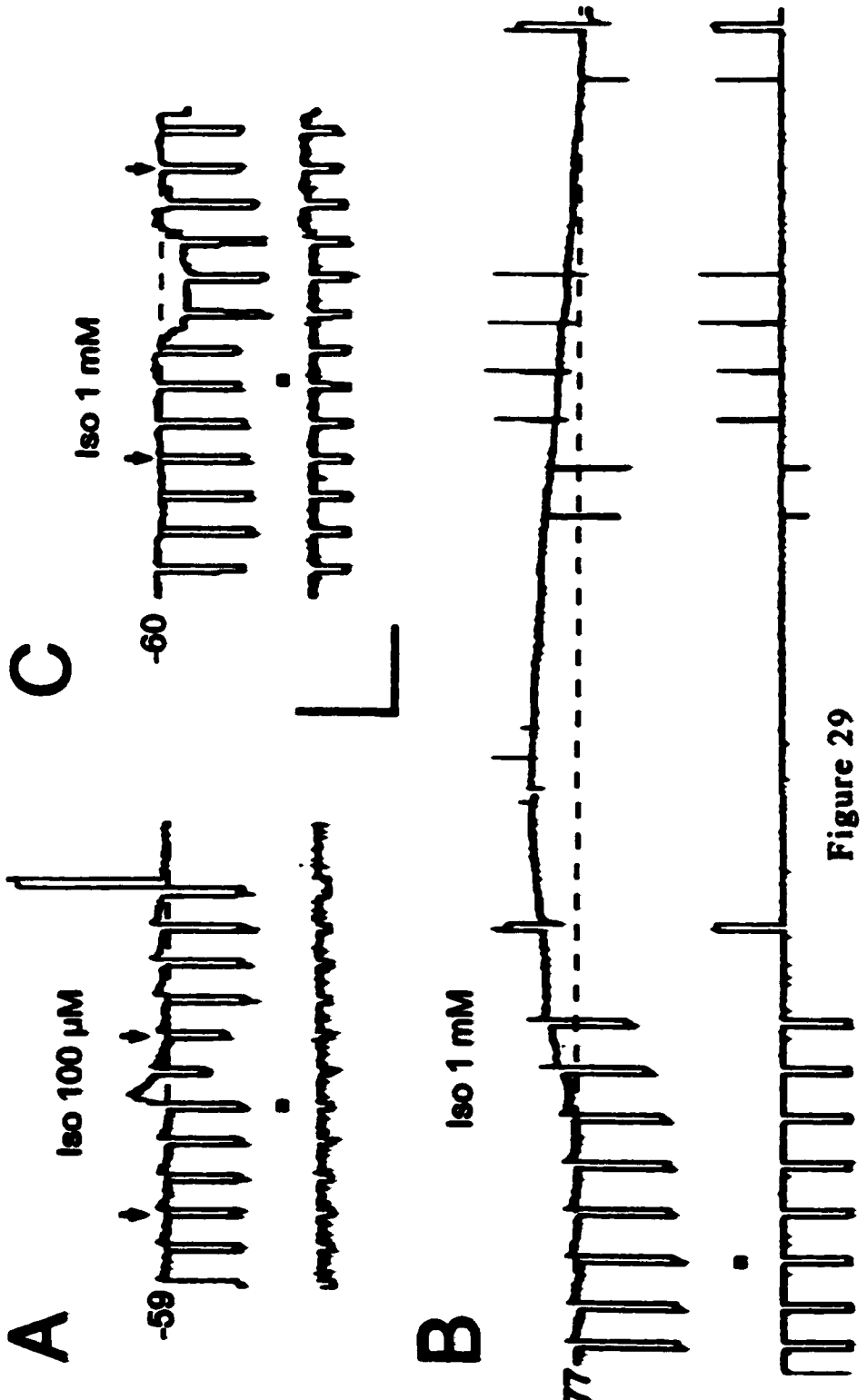

Figure 29

transient depolarization (13 mV) of the membrane potential with a concurrent decrease of 24% in the membrane conductance after the application 100 μM of ISO. In other instances, 100 μM ISO induced no change in membrane conductance while altering the membrane potential (Fig. 29B,C).

A total of 40 (92% of those tested) neurons responded to ISO application with a change in conductance. Only 1 neuron demonstrated a biphasic response to this agent and was excluded from the data set. The mean changes in whole-cell conductance for 100 μM and 1 mM concentrations of ISO are presented in Figure 31. Thirteen neurons showed an ISO-induced increase in conductance while 27 neurons showed a decrease in conductance. These responses did not correlate consistently with neuron type, and analysis of other membrane properties showed no ISO-induced change in these properties.

iii) Effects on firing behaviour

The firing behaviour of intracardiac neurons was altered by ISO. In the example shown in Figure 32, the neuron displayed an accommodating firing pattern in response to a 500 ms depolarizing current pulse from the intracellular electrode. Following a 200 ms pulse of ISO (100 μM), the same neuron displayed phasic firing. This inhibitory effect was the only type of modification of firing behaviour evoked by ISO; no augmentation of firing was observed in this study. No Type I neurons displayed a changes in neuronal firing behaviour after ISO application, and the firing behaviour of Type II neurons, the majority of which were phasic, was also not affected by ISO. However, 18% of the Type

Figure 30. Mean changes in resting membrane potential with the application of ISO at two concentrations (100 μM and 1 mM). Bars represent membrane potential responses for each of three groups of neurons: those neurons that depolarized (designated as a positive displacement from the resting potential), hyperpolarized (designated as a negative displacement from the resting potential) or showed no change in response to the application of ISO. The number of neurons included in each group is indicated in parentheses.

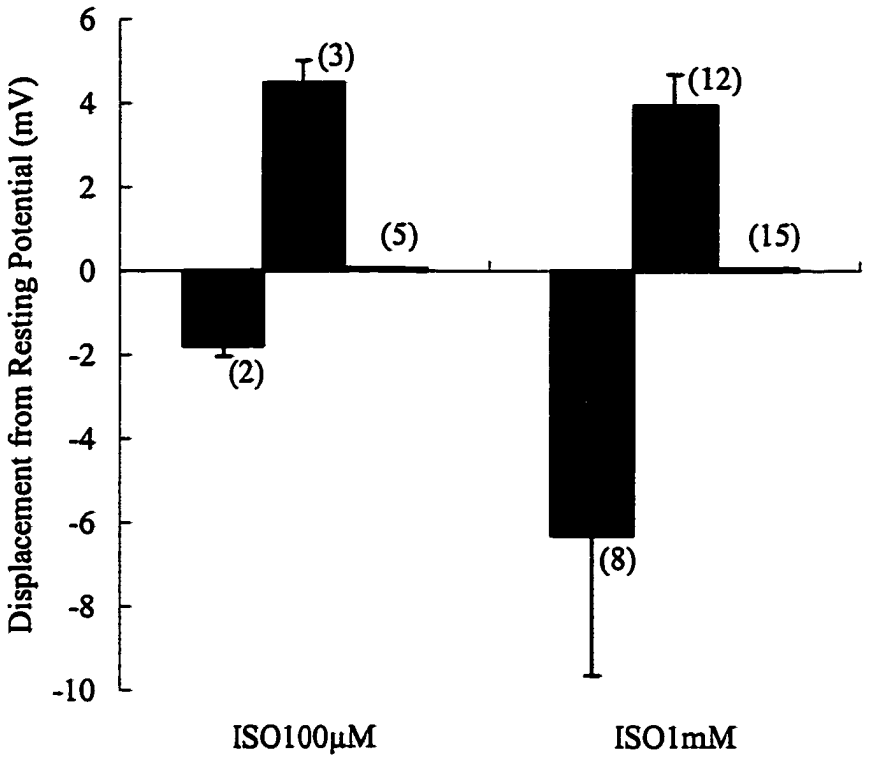
Displacement from Resting Potential (mV)
6
4
2
0
-2
-4
-6
-8
-10
(3)
(5)
(2)
(12)
(15)
(8)
ISO100μM
ISO1mM

Figure 30

III neurons tested showed inhibition of AP discharge with the application of ISO; these neurons were accommodating (Table 7). At the lower dose of 100 μM, ISO was just as effective in altering neuronal excitability as it was the higher dose, unlike the situation for PHEN, which had no effect on neuronal excitability at the lower dose.

iv) Effects on neurotransmission

ISO was capable of attenuating or enhancing the response to orthodromic stimulation of 5 of 7 intracardiac neurons tested. Figure 33 demonstrates the responses of two neurons to interganglionic nerve stimulation before and after the application of ISO. In Figure 33A, the AP was superimposed on a large EPSP. However, a 1 mM concentration of ISO reduced the amplitude of the EPSP, leaving only the AP. Clearly one or more synaptic inputs to this neuron had been blocked by ISO. The neuron illustrated in Figure 33B displayed inhibition of the post-synaptic response to nerve stimulation when a 100 μM concentration of ISO was applied. In this example, ISO apparently increased the threshold for generating an action potential, reducing the safety factor of synaptic transmission. In another neuron, ISO decreased the threshold for generation of an AP or increased the amplitude of the EPSP (Fig. 34). The neuron in this example responded with a fast EPSP but no AP to interganglionic nerve stimulation prior to application of ISO, but the presence of 1 mM ISO facilitated the generation of an AP.

Figure 31. Mean changes in whole cell conductance with the application of ISO at two concentrations (100 μM and 1 mM). Bars represent changes in whole-cell conductance for each of three groups of neurons: those neurons that displayed an increase (positive displacement from the initial conductance value), a decrease (negative displacement from the initial conductance value) or no change (short bar) in response to the application of ISO. The number of neurons included in each group is indicated in parentheses. Asterisk (*) denotes a significant difference in conductance after ISO application.

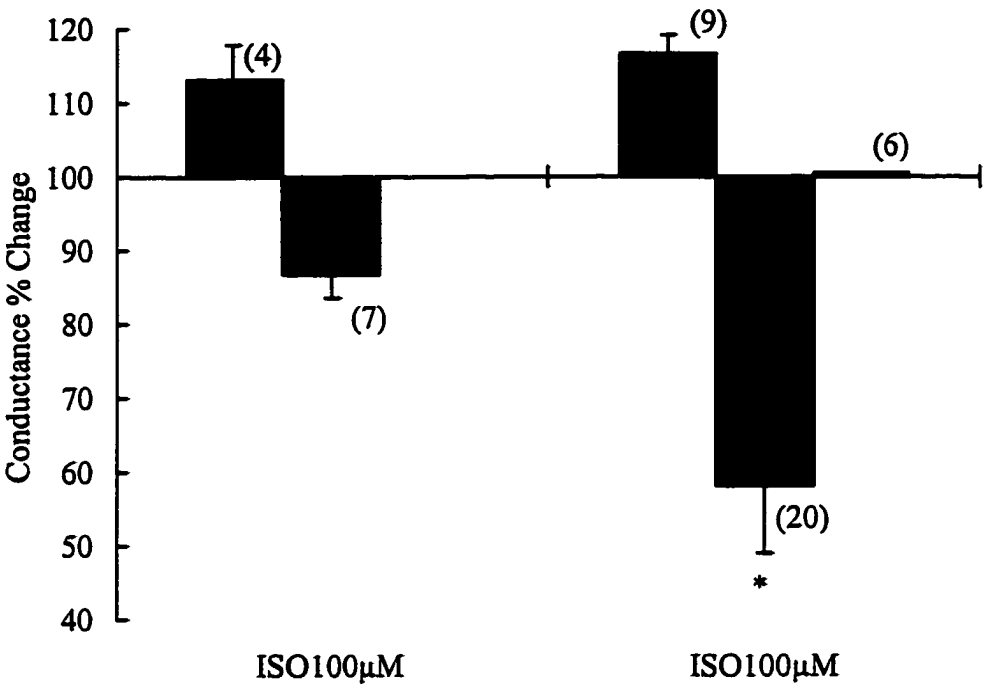
120
110
100
90
80
70
60
50
40
Conductance % Change
(4)
(7)
(9)
(6)
(20)
*
ISO100μM
ISO100μM

Figure 31

Figure 32. ISO-induced modification of firing behaviour. Control: uper panel, neuron fired repetitively in an accommodating pattern during membrane depolarization (500ms current pulse, lower trace). Lower panel: ISO (100 μM) decreased the firing frequency in response to an 800 ms current pulse, inhibiting neuronal excitability. Vertical bar: 30 mV and 0.5 nA; horizontal bar: 100 ms.

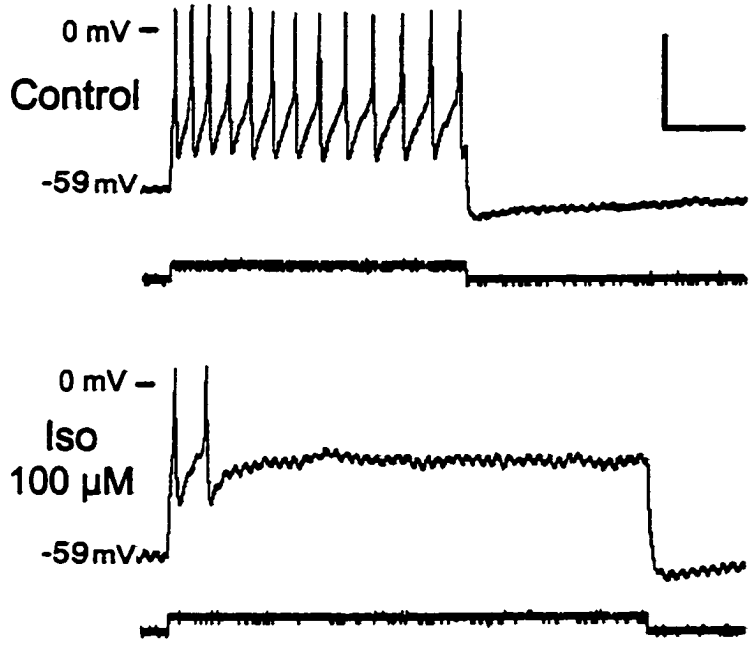

Figure 32

Figure 33. Effects of ISO on postsynaptic responses to interganglionic nerve stimulation (0.5ms duration) in two intracardiac neurons. A: Control (upper panel): stimulation induced an action potential and a late EPSP. Lower panel: the amplitude of the portion of the EPSP remaining after the AP was attenuated following the application of 1 mM ISO while the AP remained unaffected. B: Control: (upper panel) nerve stimulation produced an EPSP which exceeded the threshold for AP generation. Lower panel: ISO (100 μM, 200 ms pulse) eliminated the AP, reducing the EPSP amplitude to a level below threshold for AP generation. Vertical bar: 30 mV; horizontal bar: 10 ms.

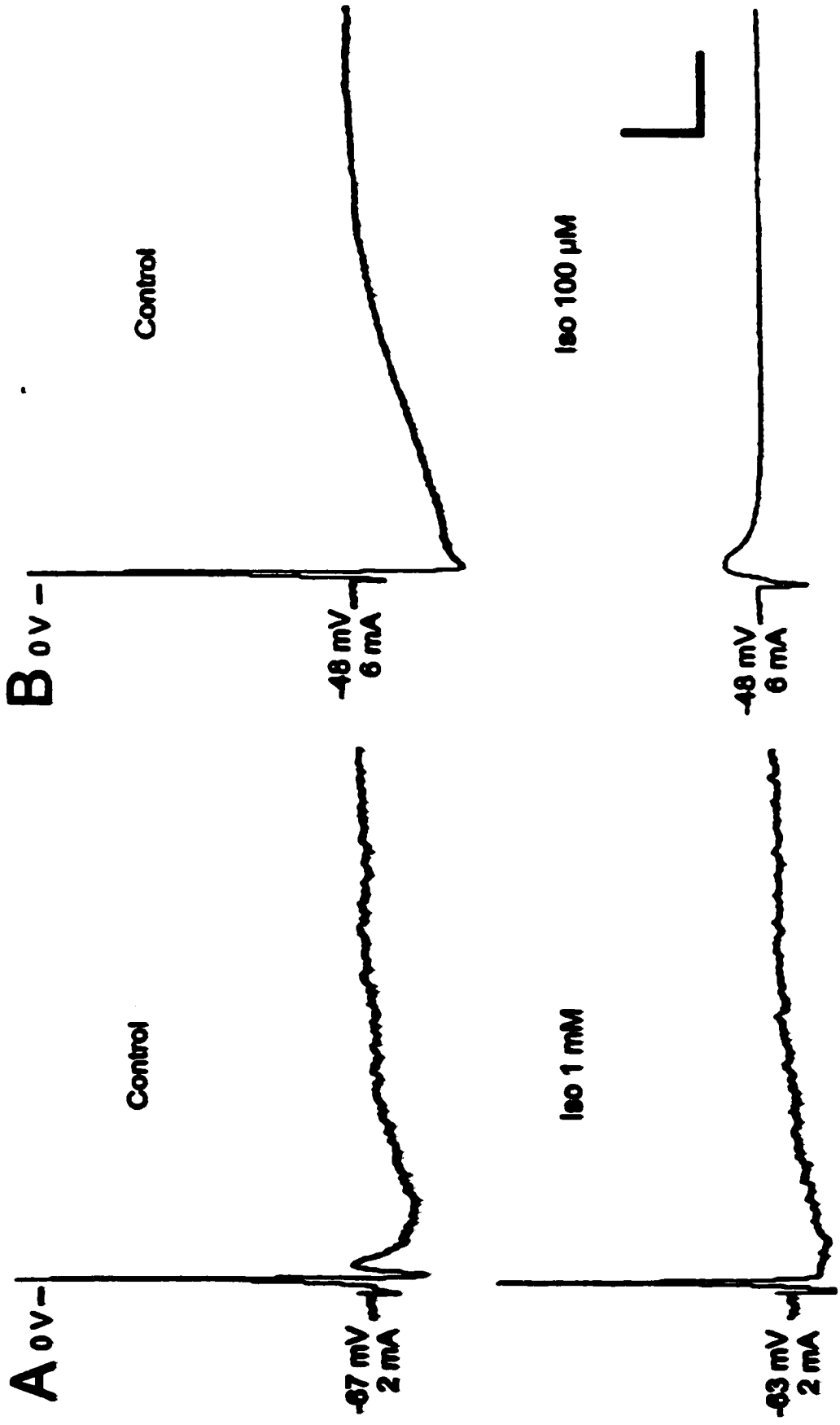
A
0 V
-67 mV
2 mA
Control
Iso 1 mM
-83 mV
2 mA
B
0 V
-48 mV
6 mA
Control
Iso 100 µM
-48 mV
6 mA

Figure 33

Table 8. Time-dependent rectification in the three classes of intracardiac neurons. Rectification was generally observed at hyperpolarizing potentials displaced more than 30 mV from resting membrane potential.

Table 8

		Type I	n	Type II	n	Type III	n
Non-rectifying	RMP	-55 ± 4	7	-54 ± 2	14	-54 ± 4	6
Rectifying	RMP	-49 ± 13	2	-55 ± 2	26	-61 ± 2	23
	onset at:	-85 ± 25		-86 ± 4		-97 ± 3	

v) Effect of timolol

The ß-adrenergic receptor antagonist, timolol, attenuated or eliminated all ISO-induced effects on whole-cell conductance, resting membrane potential and membrane excitability, as shown in Figure 35. In this example, the effect of ISO on membrane potential and conductance were eliminated. Summarizing the effects of timolol on 5 neurons in which 1mM ISO depolarized the membrane potential by an average of 6 ± 3 mV (n=4) or hyperpolarized the membrane potential by -35 mV (n=1), timolol (10 μM) attenuated this response by reducing the ISO-induced depolarization to an average of 1 ± 1 mV and the hyperpolarization to -2 mV. In 11 other neurons in which conductance was effected ISO produced either a mean decrease in conductance of 50 ± 22% (n=5) or a mean increase of 123 ± 12% (n=6). These effects were eliminated, when the tissue was exposed to 10μM timolol. The inhibitory affect of ISO on firing behaviour was also abolished following a 20 min pre-incubation of the tissue in 10 μm timolol

Finally, to test for the specificity of receptor activation by each adrenergic agonist, the inappropriate antagonist was paired with one of the agonists during the physiological experiments. For example, when the α-adrenergic agonist was applied in the presence of the ß-adrenergic receptor antagonist, the response of the neuron did not differ from that of control applications of the α-adrenergic agonist alone. A similar observation was made when the receptor specific agonist and antagonist were reversed. Thus, the results of this study appear to be the consequence of receptor-specific activation.

Figure 34. ISO (1 μM, 200 ms pulse) facilitated the response to interganglionic nerve stimulation. Control (upper panel): maximal nerve stimulation (10 mA, 0.5 ms, artefact truncated) induced an EPSP with an amplitude subthreshold for AP generation. Lower panel: after ISO application (lower panel), nerve stimulation at reduced intensity (4 mA) produced an EPSP which exceeded threshold for AP generation. Vertical bar: 30 mV; horizontal bar: 10 ms.

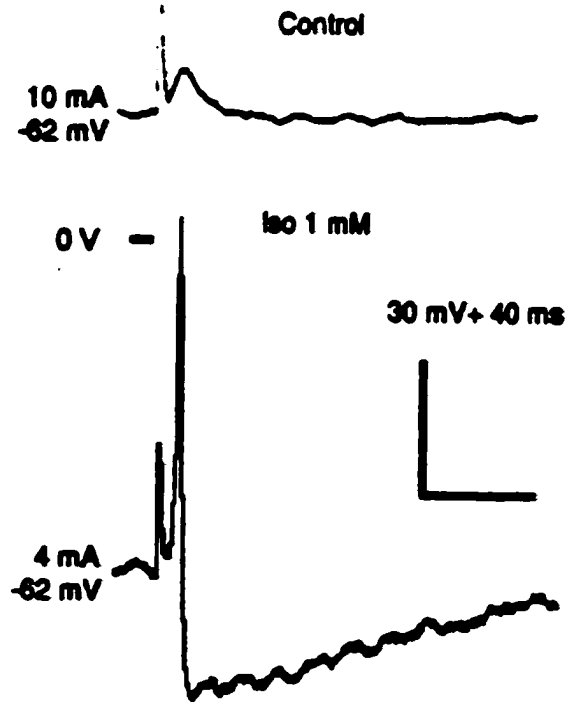

Figure 34

Figure 35. Timolol (10 μM in perfusate for 5 min) abolished the response of intracardiac neuron to locally applied ISO (100 μM, 200 ms pulse). Upper panel (Control): the application of ISO (100 μM) resulted in depolarization of membrane potential and an increase in the whole cell conductance. Lower panel: exposure of the preparation to timolol abolished the response to a second application of isoproteronol. Vertical bar: 30 mV and 2 nA; horizontal bar: 10 s.

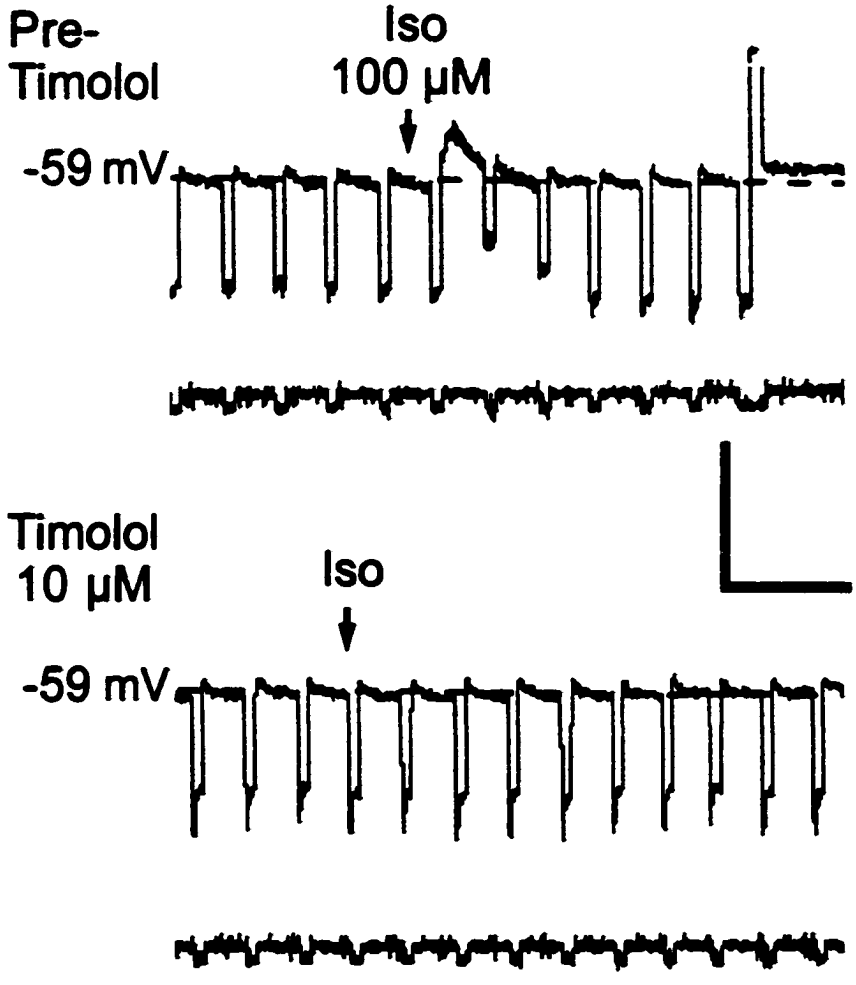

Figure 35

Discussion

The results of this study show that guinea-pig intracardiac neurons form a heterogeneous group. This heterogeneity is evident from several different viewpoints: neurons are morphologically diverse, have different aggregates of basic electrophysiological properties, and can be distinguished by different responses to pharmacological agents. In this study I have classified neurons into categories based on the time course of their AHPs, and have shown that neurons in these classes exhibit other physiological and morphological attributes in common. This classification scheme provides a rational framework for further analysis of the organization of the intracardiac nervous system. Regardless of neuron type, adrenergic agents influenced neuronal behaviour by changing either membrane potential, whole-cell conductance, neuron excitability, or more than one of these factors simultaneously. Most importantly, adrenergically induced changes in these properties may influence neuronal responsiveness to orthodromic stimulation, a possible mechanism for modulating ganglionic neurotransmission within the heart.

Classification of guinea-pig intracardiac neurons

In a variety of autonomic ganglia, it has been suggested that neurons with distinct morphologies and firing behaviours display different physiological characteristics and may be involved in different functional pathways (Cassell *et al.*, 1986; McLachlan and Meckler, 1989; Meckler and McLachlan, 1988). Within the heart, potential pathways for

neural control may include those which integrate sensory input from the myocardium, and those which process inputs from extrinsic parasympathetic and sympathetic inputs from neurons in the thorax or central nervous system. Intracardiac neurons of specific types may also have specific role in regulating different aspects of cardiac function, such as chronotropy or ionotropy, or may specifically innervate different target regions of the heart. For this reason, the characteristics which are selected for the primary classification of neurons into functional types becomes an important consideration, if parallels are to be made with the functions of these neuron types. The current experiments have shown that intracardiac neurons can be classified based on differences in their electrophysiological properties. Under the conditions prevailing in my experiments, I have obtained evidence for three classes of neurons within the intracardiac nervous system. A major assumption in this study was that the properties recorded for each type of neuron represent intrinsic properties of the cell in the absence of external influences other than those imposed by the experimental design (ie. application of adrenergic agents). Of these properties, the time course of the AHP appeared to be the most reliable feature for classification of these neurons, as this property did not appear to be altered by most experimental manipulations. Differences in AHP among neuron types may therefore represent real differences in membrane channel composition. The AHP is an active membrane property exhibited by neurons immediately following the repolarizing phase of the action potential. Hyperpolarization of the membrane is the result of K+ ion efflux through specific channels in the membrane (Hodgkin and Huxley, 1952 summarized in Aidley, 1976; Allen and Burnstock, 1987). As stated above, the time course of the AHP (that is, the time required to reach the peak amplitude and then decay), was relatively invariant

for an individual neuron over the period of the experiments. This classification scheme is somewhat arbitrary, segregating neurons into 3 classes based on one particular physiological property, and then correlating a specific stet of properties with each class. However, the time course of the AHP had three distinct trajectories which did not appear to be part of a continuum.

Other studies have classified intracardiac neurons of guinea-pigs (Allen and Burnstock, 1987; Edwards *et al.*, 1995; Hardwick *et al.*, 1995), pigs (Smith *et al.*, 1992), dogs (Xi *et al.*, 1991a, 1991b, 1991c) by their responses to a prolonged depolarizing current injected through the intracellular recording electrode. This can be interpreted as a measure of neuronal excitability, and the excitability of a neuron can in turn be regarded as an indicator of effectiveness of neuronal function within a specific pathway. Those cells with relatively low excitability, for example phasic neurons, could act as low-pass filters setting an upper limit to the rate of neurotransmission through a pathway. Furthermore, the excitability of a neuron has been considered an important correlate of its position within a functional pathway. Intracellular recordings from the guinea-pig celiac ganglion showed that inputs from peripheral axons preferentially innervated tonic neurons while phasic neurons were innervated by preganglionic axons originating in the central nervous system (Meckler and McLachlan, 1988; McLachlan and Meckler, 1989).

However, evidence is accumulating that the excitability of a neuron is not an immutable property and can shift spontaneously or can be induced to change by the application of exogenous compounds such as catecholamines (both phenomena observed in the present study), muscarinic agonists (Allen and Burnstock, 1990; Smith *et al.*, 1992; Selyanko and Skok, 1992), galanin (Konopka and Parsons, 1989) and neurokinins

(Hardwick *et al.*, 1991). Others have found that neuronal excitability in itself was not predictive of a specific set of membrane characteristics or morphological types (Hardwick *et al.*, 1995). Edwards *et al.* (1995), in an attempt to refine a system of neuron classification, correlated time course of the AHP with the firing properties of guinea-pig intracardiac neurons. Phasic firing neurons had short duration AHPs, while accommodating neurons had prolonged AHPs. These observations contradict those of the present study which have shown that all three classes of neuron include examples of both tonic and phasic neurons with similar AHP profiles. On the other hand, support for the present study comes from recordings made from rat intracardiac neurons; neurons with either long or short AHPs could have phasic or tonic firing properties (Selyanko, 1992). It was because there was some ambiguity in these classification schemes that the method of classification used in the present study was adopted for guinea-pig intracardiac neurons.

In the present study the AHP of Type I neurons had a mean duration of 34 ± 7 ms at 50% of the maximum amplitude and had the smallest amplitude of all three classes of neurons. Neurons with similar AHP duration have been reported, in other studies of guinea-pig atrial neurons. Edwards *et al.* (1995) described S-type intracardiac neurons of the guinea-pig with a mean AHP duration of 30 ± 11 ms that would discharge a single AP upon depolarization of the membrane. Allen and Burnstock (1987) also classified cultured guinea-pig intracardiac neurons based on the duration of the AHP. In their scheme, the M-cells had relatively short duration AHPs, and exhibited repetitive firing upon depolarization of the membrane. This firing behavior was the opposite of S-type neurons recorded in the *in vitro* preparation of Edwards *et al.* (1995). However, the M-

cells of Allen and Burnstock (1987) showed similarities with A-type sympathetic neurons (Blackman and Purves, 1969; Gallego and Eyzaguirre, 1978) and S/type I enteric neurons (Nishi and North, 1973; Hirst *et al.*, 1974). In the pig intracardiac nervous system, neurons with a mean after-hyperpolarization duration of 39 ms had phasic firing properties (Smith, 1997). Contrary to this, canine intracardiac neurons were not segregated into different categories based on the time course of the AHP because no difference in this characteristic was observed between phasic and accommodating neurons. The mean duration of the AHP for canine intracardiac neurons was 67.9 ± 6.7 ms (Xi *et al.*, 1994); this was at a value intermediate to those of the neuron types of the present study.

Type II neurons in this study had a mean AHP duration of 101 ± 5 ms and had either phasic or accommodating responses to prolonged membrane depolarization. The AHP time course of guinea-pig intracardiac neurons (SAH neurons) from the study by Edwards *et al.* (1995) had a qualitatively similar profile to Type II neurons but the mean duration of the AHP reported for SAH neurons was twice that of Type II neurons; furthermore, Edwards *et al.* (1995) stated that these neurons displayed only tonic firing behaviour. These neurons apparently received synaptic inputs from the central nervous system, a different scenario than that observed in guinea-pig celiac ganglia. Tonic neurons in the celiac ganglion receive inputs of peripheral origin rather than from the central nervous system (Meckler and MacLachlan, 1988). In this context, it should also be noted that tonic neurons of the enteric nervous system have short AHP durations relative to phasic neurons. In the pig heart, neurons with a mean AHP duration of 130 ms

fired repetitively (Smith, 1992). Allen and Burnstock (1987) describe an additional type of cultured guinea-pig intracardiac neuron which had prolonged AHPs lasting up to 3 seconds and displayed either phasic (AH_s) or accommodating (AH_m) firing patterns.

Type III neurons of the present study had the longest mean AHP duration (149 ± 7 ms) and the largest mean amplitude (18 ± 1 mV) of the three types. An equal number of these neurons had phasic and accommodating firing patterns. The P-cells of Edwards *et al.* (1995) showed qualitatively similar though slightly longer duration AHPs of 166 ± 22 ms in guinea-pig intracardiac neurons and had only tonic firing properties. AH/type 2 neurons of the enteric nervous system have a prolonged AHP that lasts for seconds and this factor was suggested to be responsible for the phasic firing behaviour of these neurons (Nishi and North, 1973; Hirst *et al.*, 1974). Type III neurons of the present study, share similar attributes with AH_s and AH_m cells of cultured guinea-pig neurons, as described above. The principal current responsible for the AHP in these neuron types appears to be a potassium channel sensitive to intracellular levels of calcium ions. As evidence for this, removal of Ca^{++} ions from the perfusion medium abolished the AHP in guinea-pig neurons while the application of caffeine, which promotes the release of Ca^{++} ions from intracellular stores, prolonged the AHP (Allen and Burnstock, 1987).

It should be noted that the designations of neuron firing patterns as accommodating or tonic are poorly defined and have not been consistently applied in the literature. High firing frequency and constancy or accommodation of the interspike interval for the duration of the depolarizing stimulus are characteristics which identify tonic firing patterns. In a number of previous studies, neurons showing spike frequency accommodation have been designated as tonic. However, in the present study, the term

accommodating refers to repetitively firing neurons which maintained activity for the full duration of an 800 ms depolarizing pulse, and had a relatively low initial firing frequency with a progressive increase in the interspike interval.

Although there was some variation in membrane properties within each class of neuron in the present study, one trend was consistent. The AHP of accommodating neurons was significantly longer than the AHP of phasic neurons. When a neuron displayed a shift from accommodating to phasic firing as a result of the application of an agonist, the duration of the AHP, but not the overall AHP profile would be altered in some neurons. In keeping with this observation, previous studies of intracardiac neurons have shown that intracardiac neurons which are designated as phasic have short duration AHPs relative to those neurons which have accommodating firing patterns (Allen and Burnstock, 1987; Edwards *et al.*, 1995). Intuitively this appears to contradict the theory which proposes that the duration of the after-hyperpolarization has a direct causal relationship to the rate of repetitive firing behaviour in peripheral autonomic neurons (Adams and Harper, 1995). In this view the duration of the after-hyperpolarization determines, in part, the refractory period of the neuron; that is, the period following an AP when no subsequent AP can be generated. Hence, a longer after-hyperpolarization would contribute to a longer refractory period and thus would dictate a lower maximum firing frequency for the neuron. However, this mechanism does not appear to apply to neurons sampled in the present set of experiments, since accommodating neurons had the highest firing frequency yet tended to have the longest AHPs. This observation is supported by other studies of intracardiac neurons (Allen and Burnstock, 1987; Edwards *et al.*, 1995; Smith, 1997). In an attempt to account for this discrepancy, Allan and

Burnstock (1987) suggested the presence of an additional outward current in phasic neurons which may have been responsible for a marked delayed rectification in the current-voltage relationship of AH_s neurons. This outward current could be another K^+ current activated by depolarization of the membrane in a manner similar to the M-current of sympathetic neurons (Brown and Adams, 1980), acting to inhibit rapid AP discharge. A similar suggestion was made for canine intracardiac neurons where the duration of the AHP did not vary between phasic and tonic neurons (Xi *et al.*, 1994). These authors suggested that an additional possibility was that the A-current discussed by Cassel *et al.* (1986) was involved in determining firing behavior. The results of the present study showed that the use of the AHP properties to classify neurons is a reasonable way of approaching the problem of neuronal heterogeneity. However, resolution of the types of membrane channels involved in setting AHP properties was beyond the scope of this thesis.

Physiological properties of the three neuron types

The utility of any classification system for neurons, such as that presented here, depends to some extent upon the degree to which neurons within a class share common properties. Ideally, neurons in any given class should share more similarities than just the primary feature which is used to erect the classes, and this is the case for neurons of the three classes in the present study. Following the format of Table 6, the similarities and differences among properties of the three classes will be discussed in this section, along with previous findings and the functional significance of these properties as applicable.

The resting membrane potential of Type I and II neurons was similar, at approximately -54 mV (Table 6). Type III neurons were significantly more hyperpolarized than the other two types with a resting membrane potential of -59 ± 1 mV. This range of values approximates that of guinea-pig intracardiac neurons in the study by Edwards *et al.* (1995), in which the averages of resting membrane potentials ranged from -49 to -53 mV for their three groups of neurons. The range of values for the resting membrane potential of cultured guinea-pig neurons was greater, from -45 to -76 mV (Allen and Burnstock, 1987). The resting membrane potential of canine intracardiac neurons (Xi *et al.*, 1994) had a range similar to those of cultured guinea-pig neurons but each class of canine neurons had a significantly different potential value. Non-responding cells ("N-type") of the dog had the most hyperpolarized resting potential, averaging -77 mV. Rat (Selyanko, 1992) and pig (Smith *et al.*, 1992) cardiac neurons and rat enteric neurons (Nishi and North, 1973) had similar resting potentials to those of neurons in the present study, averaging at about -52 mV. The values of membrane potential reported here thus fit well within the range of values reported for mammalian intracardiac neurons. It is not clear why the membrane potential of Type III neurons was hyperpolarized relative to the values for Type I and II neurons, but this difference could imply that Type III neurons require more depolarization to reach firing threshold than the other two neuron types. However, membrane potential displacement to reach firing threshold was similar in all other neuron types (Table 6). This means that in absolute terms, the membrane potential for AP firing in Type III neurons was hyperpolarized relative to that for Type I and II neurons.

The mean input resistance of 79 MΩ for Type I neurons was smaller than that of Type II and Type III neurons; Type III neurons had the largest mean input resistance (118 MΩ) of the three classes. The range of mean input resistance observed in guinea-pig neurons of the present study was similar to that reported by Hardwick *et al.* (1995), about one third smaller than those reported by Edwards *et al.* (1995) and only slightly smaller than the mean input resistance of 123 MΩ in cultured guinea-pig neurons (Allen and Burnstock, 1987). Rat cardiac neurons displayed similar input resistances to the present study while those of the dog and pig were smaller. The functional significance of the input resistance can be understood when it is considered in relation to neuronal excitability. A cell with a low input resistance (or, conversely a high whole-cell membrane conductivity) requires a larger current to displace the membrane potential a given amount, than does a cell with higher input resistance. In keeping with this, Type I neurons, which had the lowest input resistance, required a significantly higher-amplitude current pulse from the intracellular recording electrode to initiate an AP than did the other neuron types. Thus, with all other variables being equal, neurons with low resistances and correspondingly high current thresholds may be considered to be less excitable. There is thus evidence that Type I neurons constitute a class of neurons within the heart which require stronger synaptic input drive to produce an output, than the other neuronal types.

The mean time constant of Type I neurons was not significantly different from that of Type II neurons, but time constants of both Type I and Type II neurons were significantly smaller than that of Type III neurons. The time constant of a neuron can

reflect the cell soma size, because time constant is proportional to whole-cell membrane capacitance. Capacitance is greater as the cell surface area increases, so neurons with larger somata or more extensive processes will have larger surface area, greater membrane capacitance and thus potentially longer time constants. For this reason, as part of the present study, I injected some neurons with the intracellular marker tetramethylrhodamine to attempt to correlate electrophysiological properties with somatic morphology. Type I neurons had the shortest time constant, and this was consistent with the result of the one case in which a Type I neuron was successfully filled and photographed. Analysis of the cell volume of this neuron with the confocal microscope showed that it was smaller than that of any of the Type II or Type III neurons that were filled. In keeping with this trend, the longer time constant of Type III neurons corresponded to the largest cell volume of the three classes of neurons. The results of this analysis cannot be conclusive since only six cell were successfully labeled with the intracellular marker after determining their electrophysiological properties. Nevertheless, the data show that there is a trend toward a correlation between cell volume (and thus total membrane capacitance) and time constant, as predicted above. However, a more thorough analysis of this correlation needs to be done.

Other factors must also be considered when comparing cell volumes and time constants, especially between studies in different species. The time constant for pig and canine cardiac neurons was, for example, smaller than that of guinea-pig neurons, yet pig and canine neurons are larger in their long and short axes dimensions than those of guinea-pig, and have considerably more cell processes (F. Smith, unpublished data; Xi *et al.*, 1991). The time constants for the three guinea-pig neuron types reported by Edward

et al. (1995) were nearly identical to the three neuron types of the present study. Rat (Selyanko, 1992), pig (Smith *et al.*, 1992) and canine (Xi *et al.*, 1992) intracardiac neurons have mean time constants of about 5 ms; a value which is smaller than those of guinea-pig neurons. Amphibian (Clark *et al.*, 1990; Roper, 1976) and mammalian sympathetic postganglionic neurons (Blackman and Purves, 1969; Cassell *et al.*, 1986) had time constants in the range of 10 to 44 ms, similar to the range of values of guinea-pig intracardiac neurons.

The threshold voltage for generating an AP was measured as the voltage displacement from resting potential to the point at which an AP was discharged. Threshold voltage was not significantly different among the three classes of intracardiac neurons, averaging 13 ± 1 mV. This value is within the range reported for cultured guinea-pig neurons (Allen and Burnstock, 1987), and *in vitro* preparations of rat (Selyanko, 1992) and pig cardiac neurons (Smith *et al.*, 1992), but is smaller than that of enteric neurons (Meckler and McLachlan, 1988). In contrast, the amount of current required to depolarize the neurons to threshold for generating an AP was significantly higher (156%) for Type I neurons when compared to Type II and III neurons, as discussed above. Edwards *et al.* (1995) do not report any differences in threshold values among their three neuron classes but used similar current pulses ranging from 0.1 to 0.3 nA. The possible relevance of these properties to neuronal function were discussed above in relation to variations in membrane potential among the three neuron types.

The APs produced by direct activation of neurons through the recording electrode had amplitude and duration characteristics consistent with those reported for other autonomic neurons (Nishi and North, 1973; Allen and Burnstock, 1987; Seabrook *et al.*,

1990). Type I neurons showed a significantly longer AP duration when compared with the other two cell types. Amphibian sympathetic postganglionic neurons display a prolonged AP and a reduced AHP 7 days postaxotomy (Smith, 1994). These changes in the AP were attributed to a loss of Ca^{++} conductance in response to cell injury and regeneration. While the prolonged AP of Type I neurons in the present study is not likely the result of cell injury, the differences in Type I AP and AHP duration compared to those of Type II and III neurons may be attributed to reduced Ca^{++} conductance and reduction in the efflux of K^+ ions from Ca^{++} sensitive K^+ channels (Smith, 1994) or may be the result of differences which reflect larger opening times or delayed inactivation of voltage gated sodium channels in this neuron type.

Morphological analysis of identified intracardiac neurons

As mentioned above, six intracardiac neurons of the guinea-pig were successfully filled with TMR-dextran (3000 m.w) via the recording microelectrode as per the method of Carr *et al.* (1994). Similar methods have also been used by other workers to compare the physiological class of a neuron and its structure (Xi *et al.*, 1991; Edwards *et al.*, 1995; Hardwick *et al.*, 1995). This proved to be a difficult procedure in the present study, due to the length of time required to characterize the neuron and then to inject it with the dye. This latter procedure required 15 to 20 min for a reliable fill, while most impaled neurons could be held for 40 min or less. Among the neurons that were successfully injected, cell somata varied in volume from 2,948 μm^3 to 13,213 μm^3. Cell volume appeared to be a more reliable index for comparing morphologically of different neuron types, than

measures the dimensions of long and short cell axes, since some neurons were quite shallow in depth. The confocal microscope allowed complete optical sectioning of the neurons in whole-mount preparations. As described earlier, cell volume correlated with neuron class: the only Type I neuron that was successfully filled had the smallest cell volume, while Type II neurons were of intermediate volume and Type III were the largest cells. These differences in soma sizes are consistent with the trend reported by Edwards *et al.* (1995). However, Edwards *et al.* (1995) also reported the presence of multiple processes attached to the neuronal somata. These were not seen in the present study, nor were extensive processes identified on intracardiac neurons labelled with immunohistochemical reactions in Chapter 2. In the cell filling experiments, all impaled neurons had a single axon which extended to the cut edge of the tissue, in some cases up to 2 mm from the labeled cell soma. These observations are consistent with those of Hardwick *et al.* (1995) who found little or no dendritic arborization in guinea-pig intracardiac neurons; and with those of Cornbrooks *et al.* (1992) and Mawe (1990) in guinea-pig gall bladder neurons. In the present study, short hair-like processes were observed extending from cell somata, often near the axon hillock, similar to the morphology described by Pauza *et al.* (1997). Furthermore, an example of axon bifurcation was noted in the present study.

It is difficult to explain the discrepancies between these studies, but some form of sampling bias may have prevented the observation of extensive neuronal processes in the present study. The cells that were filled in this study may simply not have long processes. Regarding the overall shape of the somata, both Pauza *et al.* (1997) and Edwards *et al.* (1997) report that 61% and 78% of guinea-pig intracardiac neurons,

respectively, were either monopolar or pseudodipolar without extensive processes besides the axon. Methodological differences might also account for the differences observed in cell morphology. For example, each study has used a different intracellular marker including neurobiotin (Hardwick *et al.*, 1995), biocytin (Edwards *et al.*, 1995), Lucifer Yellow CH (Pauza *et al.*, 1997) and TMR-dextran (present study). Although each group of investigators expressed confidence that the dye used was suitable for full elucidation of the complete pattern of neuronal processes, it is possible that the diffusion rate and pattern of each dye varied depending on molecular size, charge and transport factors within the cell. In the present study, after a 20 min injection, TMR-dextran diffused along the axon for more than 2 mm, suggesting sufficient time was provided to fill all processes extending from the cell soma. Therefore, this procedure should have shown dendritic processes if they had been present. An additional consideration is the range in age of the animals that were used in these studies (3 weeks to 4 months old). Although guinea-pig intracardiac nervous systems are believed to be mature by the age of three weeks (Lipp and Rudolph, 1972), developing rat intracardiac neurons are still undergoing considerable growth in cell size and arborization at this time (Selyanko and Skok, 1992). Thus, interpretation of the results of the present study may be confounded by several factors, but it appears that the majority of guinea-pig intracardiac neurons are unipolar or have minimal processes besides the axon.

Synaptic transmission

Commonly, synaptic responses were generated by stimulation of interganglionic nerves which could be clearly identified as attaching to the ganglion from which

recordings were taken. Approximately 35% of guinea-pig intracardiac neurons received one or more synaptic inputs which elicited fast EPSPs. In some cases, the EPSP amplitude was large enough to exceed threshold and generate an AP. In other instances, fast EPSPs never reached threshold for AP firing even when nerve stimulation intensity was maximal. Electrical stimulation of either the right or left vagosympathetic trunks could did not elicit a response from any of the neurons sampled in this part of the study. Contrary to these results, Edwards *et al.* (1995) reported that all of 34 SAH neurons identified in that study received suprathreshold inputs from the vagosympathetic trunk. The other two classes of neurons in that study did not receive any input from the extracardiac vagus nerves. It is not clear why no neuronal responses to vagus nerve stimulation were obtained in the present study. Although unlikely, it is possible that differences in stimulation parameters between the present study and that of Edwards *et al.* (1995) might account for this discrepancy. However, the stimulation parameters of the present study generated compound APs along the vagus nerve, as measured by an extracellular electrode placed on the nerve. Furthermore, stimulation of local interganglionic nerves evoke postsynaptic responses. There may in fact be only a small minority of neurons in the heart with vagal input, and sampling bias in the present study may have excluded those neurons.

In any case, neurons in the isolated preparation used in the present study were activated by orthodromic stimulation via interganglionic nerves (Fig. 20-22). To determine whether APs were generated by transynaptic mechanisms as opposed to antidromic stimulation of the efferent axon of the sampled neuron, the Ca^{++} ion concentration was reduced and the concentration of Mg^{++} ions was increased in the

perfusate. The release of neurotransmitter from vesicles in the presynaptic terminal is dependent on an inward Ca^{++} current at the synaptic bouton (Aidley, 1976). A low concentration of Ca^{++} therefore interferes with normal release of neurotransmitter from the presynaptic terminal, thus demonstrating that these neurons were activated orthodromically and not antidromically by nerve stimulation.

The neuronal response to electrical stimulation of the interganglionic nerves consisted of a fast depolarizing EPSP often accompanied by an AP (Fig. 20). This activity was the result of postsynaptic nicotinic receptor activation, since hexamethonium, a nicotinic channel blocker, abolished all responses to nerve stimulation. Muscarinic cholinergeric receptor subtypes have also been proposed to be present in cultured rat (Fieber and Adams, 1991) and guinea-pig (Allen and Burnstock, 1990) intracardiac neurons. However, hexamethonium-resistant synaptic transmission was not observed in the present study, suggesting that the primary neurotransmitter was ACh, acting at nicotinic post-synaptic receptors. Similar results were found in the canine intracardiac nervous system (Xi *et al.*, 1991) but these findings contradict other intracellular and extracellular studies of canine and porcine intracardiac neurons which reported hexamethonium-independent synaptic mechanisms (Smith *et al.*, 1992; 1999; Huang *et al.*, 1993b). However, in the present study, mecamylamine, a nicotinic receptor antagonist, only reduced the amplitude of EPSPs in two of instances without completely suppressing them (Fig. 22). In contrast to the results with hexamethonium, this would appear to be consistent with reports of incomplete blockade of the fast EPSP in pig intracardiac neurons (Smith *et al.*, 1992) and rat intracardiac neurons (Selyanko and Skok, 1992), which have led to the suggestion that intracardiac neurons receive non-

nicotinic excitatory inputs. However, neither of these previous studies used mecamylamine, so this is still an open question. Non-cholinergic agonists such as adenosine and peptides, including substance P, can depolarize neurons when applied via the perfusate (Fieber and Adams, 1991; Hardwick *et al.*, 1995). Alternatively, Selyanko and Skok (1992) suggested that neurons of different peripheral ganglia vary in their sensitivity to nicotinic blockade so that the potency of a particular drug may vary depending on the ganglion type.

The population of neurons sampled in the present study did not show any inhibitory potentials following nerve stimulation, a finding consistent with other studies in guinea-pig (Edwards *et al.*, 1995; Hardwick *et al.*, 1995), rat (Salyanko and Skok, 1992a; Seabrook *et al.*, 1990), pig (Smith *et al.*, 1992) and dog (Xi *et al.*, 1991).

In some experiments an attempt was made to stimulate extrinsic inputs to the heart originating in the right stellate ganglion, while recording from intracardiac neurons. This ganglion and attached cardiopulmonary nerves were incorporated into 13 of the *in vitro* preparations as outlined in Chapter 3. Electrical stimulation of the stellate ganglion did not appear to influence intracardiac neurons in the cases that were examined (data not presented), even when stellate stimulation was capable of eliciting an increase in the spontaneous contraction rate of the atria in the same preparation. Due to the difficulty in setting this preparation up for recording, and the low probability of finding neurons with appropriate connections to the stellate ganglion, this line of study was not pursued further. The relatively few terminals within a ganglion which labelled positive for catecholamine content following formaldehyde induced fluorescence, would suggest that relatively few neurons in the heart receive direct inputs from the stellate ganglion. Such

inputs may also target highly regional or restricted areas of the atria, none of which were included in the areas sampled during intracellular recording experiments. Therefore, an alternative method of assessing the potential effects of sympathetic input on ganglionic neurotransmission was used. In these experiments, local pressure application of adrenergic agonists and bath application of antagonists was employed to determine the extent to which these agents could modulate intracardiac neuronal properties and activity.

Adrenergic effects on neuronal activity

Both α- and ß-adrenergic receptors have been reported to be present on intracardiac neurons (Adams *et al.*, 1987; Adams and Xu, 1989; Allen and Burnstock, 1987; Saito *et al.*, 1988; Huang *et al.*, 1993). In this study, neuronal responses to the α_1-adrenergic agonist, phenylephrine (PHEN) were analyzed because there has been considerable work on the influence of α_1-adrenergic receptor activation on the heart in general, and more specifically, recent work has suggested that this receptor subtype may be more common among intracardiac neurons than the other α-adrenoceptor subtypes (Wetzel *et al.*,1985). Prazosin was used as a specific α_1-adrenoceptor antagonist.

The general ß-adrenergic receptor agonist isoproterenol was used to determine broad-spectrum ß-adrenoceptor mediated effects on intracardiac neurons, because a number of different subtypes of this receptor have been proposed to be present on the intracardiac neurons (Saito *et al.*, 1988; Huang *et al.*, 1993; Armour, 1997). An important component of the present study was a survey of the range of ß-adrenergic

effects on neurons, so it was felt that a general ß-adrenoceptor agonist such as ISO would be the most appropriate. Likewise, the general ß-adrenoceptor antagonist timolol was used to block broad-spectrum effects of ISO.

As described in the results section, adrenergic agonists applied to the intracardiac nervous system could alter membrane potential, whole-cell conductances and postsynaptic effects of nerve stimulation, and the implications of these effects are discussed below.

α-adrenergic effects on neuronal activity

The majority of intracardiac neurons (91%) tested in this study had some type of response to the application of PHEN. The response to this agent varied from cell to cell, but could involve a combination of changes in membrane potential and conductance, in either direction. Neurons exhibiting an α-adrenoceptor mediated hyperpolarization or depolarization of the membrane potential could also display either an increase or decrease in conductance. The excitability of some neurons was also modulated by α-adrenoceptor activation and this change was, in some cases, accompanied by changes in whole-cell conductance. However, the direction of changes in conductance were not necessarily correlated with changes in neuronal excitability in individual neurons. For example, some neurons showed increased conductance (indicative of an decrease in input resistance) which would imply a decrease in excitability, but these neurons fired more APs when stimulated with long intracellular current pulses, indicating an increase in excitability. A similar observation was made in a previous study of the effects of

substance P on an intracardiac neuron preparation, leading the authors to conclude that in an individual neuron, more than one type of channel could be altered by the peptide (Hardwick *et al.*, 1995). In neurons of the present study which exhibited complex responses to α-adrenoceptor activation, the activity of a number of different membrane channels may have been modulated, each channel being responsible for a different component of the response. Cultured rat and guinea-pig intracardiac neurons have been shown in previous studies to possess adrenergic receptors and to respond to the application of norepinephrine (Adams *et al.*, 1987; Adams and Xu, 1989; Allen and Burnstock, 1987). More specifically, it has been reported that α_2-adrenergic activation resulted in Ca^{++} current inhibition and activation of a small outward K^+ current in cultured rat cardiac neurons (Adams *et al.*, 1987; Xu and Adams, 1993). Similar adrenergic effects on Ca^{++} current were reported for cultured guinea-pig cardiac neurons, along with inhibition of the AHP via the K^+-mediated M-current (Allen and Burnstock, 1987). Studies of α_1-adrenergic effects have suggested that this receptor class has opposing effects to those of α_2-adrenoceptors. Hence, α_1-adrenoceptors have been reported to mediate excitatory responses while α_2-adrenoceptors mediate inhibitory responses (Ruffolo *et al.*, 1991). The excitatory effects of α_1-adrenoceptors were attributed to an influx of Ca^{++} from either extracellular or intracellular sources, acting to increase the Ca^{++} concentration within the cell. Membrane depolarization and increased excitability was a common response to PHEN administration in the study of Ruffolo *et al.* (1991). This variety of responses is supported by results of the present study. On the other hand, the α_1-receptor apparently mediated the inhibition of acetylcholine release

from rat atria during transmural stimulation (Wetzel *et al.*, 1985) suggesting that α_1-adrenoceptors situated on intracardiac postganglionic neurons suppressed the release of ACh. However, such an inhibitory role is believed to be more common for α_2-receptors which are typically considered responsible for reduction of ACh release from presynaptic terminals (Haass *et al.*, 1993).

The latency and time course of inhibitory responses to PHEN in the present study were shorter than those reported in previous studies. Many of the effects attributed to α-adrenergic agonist application only occurred after prolonged exposure to the agonist (from seconds to minutes) (Tsurusaki *et al.*, 1990; Meel *et al.*, 1990), whereas the effects of PHEN in the present study were the result of brief, 200 to 500 ms pulses, delivered from a nearby micropipette. Thus, differences in experimental methods must be considered when comparing the responses of intracardiac neurons to α-adrenergic agonists. In any case, the results of this study show that intracardiac neurons in the guinea-pig heart possess complex responses to a single type of α-agonist, which presumably acted via multiple intracellular signaling pathways to alter characteristics of several membrane channel populations. These results raise further questions about the nature of the channels involved, and the overall influences of neurons with particular channel complements on control of cardiac function. In addition, the position of the micropipette may have introduced variability in the responses of the intrinsic cardiac neurons to adrenergic agonists. Adrenergic agonists released from a position closer to the recording electrode and the impaled neuron may have produced a more rapid and localized response while release of the agonist from a more distant position might

activate a number of neurons within the vicinity which could have influenced the behaviour of the impaled neuron. This possibility could have been addressed by substituting the normal perfusate with a solution containing a reduced concentration of Ca^{++} to inhibit neurotransmission through the release of neurotransmitter, thereby removing any influence of neighboring neurons. This method was not, however, employed for this purpose in the present study.

All of the effects observed following exposure of guinea-pig intracardiac neurons to PHEN were abolished following a 10-15 min exposure to the α_1-adrenergic receptor antagonist, prazosin. The effectiveness with which the antagonist blocked PHEN lends further support to the argument that α_1-adrenergic receptors were specifically activated by this agonist. However, it is possible that some α_2-adrenoceptors may have contributed to the resulting behavioral changes of the neurons due to receptor cross-activation. Canine stellate ganglia (Satoh *et al.*, 1989) and rabbit urinary bladder (Tsurusaki *et al.*, 1990) have both been shown to possess predominantly α_2-receptors, which have been shown to be responsible for inhibition of ganglionic neurotransmission. However the extent of PHEN influence on α_2-receptors which might include concentration-dependent inhibition, was not explored in the present study.

In the experiments reported here, α_1-adrenergic receptors inhibited synaptic neurotransmission to some of the cells tested; neurotransmission was never facilitated by activation of this receptor type. The current threshold for generation of an AP by nerve stimulation was increased in some cases, while in others even maximal stimulus intensity would not elicit an AP from neurons which, previous to PHEN exposure, showed

consistent AP responses to nerve stimulation. Furthermore, the fast EPSP generated by interganglionic nerve stimulation was completely abolished in some neurons. Consistent with these observations, epinephrine and norepinephrine were observed to reduce the fast EPSP evoked by supramaximal stimulation of preganlgionic nerve fibers synapsing on neurons in the urinary bladder of rabbits (Tsurusaki *et al.*, 1990). Conversely, NE potentiated the postsynaptic effects of nerve stimulation in pig intracardiac neurons (Smith *et al.*, 1992). Whether the observed changes from these latter studies resulted from specific activation of α-adrenergic receptors was not determined.

The evidence presented in this study would suggest that the responses of neurons to α_1-adrenergic receptor activation are complex it is clear that α_1-receptor agonists can influence the basic properties of neurons, as well as their firing pattern and responses to nerve stimulation. Hence, α_1-adrenegic receptors have a wide range of potential modulatory effects on neuronal function and neurotransmission in intracardiac ganglia.

ß-adrenergic effects on neuronal activity

The ß-adrenergic agonist isoproterenol (ISO) is equipotent in activating different subtypes of this receptor (Anderson, 1972). Thus, in using this agonist, no attempt was made to separate the effects of activating different ß-adrenoceptor subpopulations. ISO had effects on one or more properties of 88% of neurons tested in this study. Collectively, responses to ISO included changes in membrane potential, whole-cell conductance, neuronal excitability and modulation of neurotransmission, with some neurons expressing complex mixtures of several of these responses. Again, as with

responses to PHEN, responses to ISO varied from cell to cell. A given response, such as change in membrane potential, could occur as a hyperpolarization or a depolarization. Overall, no consistent patterns of correlation among ISO-induced effects emerged from this study. In cells displaying concurrent changes in conductance and excitability, the directions of these responses were not correlated. For example, one relatively common mixture of responses was concurrent changes in conductance and firing behaviour. It might be expected that, in neurons with this combination of responses, the direction of the conductance change would augment the change in firing behaviour. This was not usually the case; a more common observation was that conductance was increased in neurons in which ISO induced an increase in number of APs fired during depolarizing current injection. The high degree of variability in responses of single intracardiac neurons to ISO reported here supports the results of a previous study of the effects of this agent on canine intracardiac neurons. Huang *et al.* (1993) reported increases or decreases in the activity of extracellularly recorded intracardiac neurons following the application of ISO in the beating heart *in situ*. That ß-adrenergic receptors are present on intracardiac neurons has been confirmed by studies of binding patterns of radiolabelled ligands. In rat intracardiac ganglia, there was a high concentration of [^{125}I] iodocyanopindolol binding sites on neuronal somata (Saito *et al.*, 1988). Further more, these authors determined that intracardiac neurons expressed mainly the $ß_2$-adrenergic receptor subtype and myocytes expressed $ß_1$-adrenergic receptors.

ISO had the capacity to either facilitate or inhibit neurotransmission in the present study of guinea-pig intracardiac neurons. These effects were not necessarily coincident with an "appropriate" agonist-induced change in membrane potential or, again,

conductance. In previous studies of autonomic neurons, such ß-adrenergic facilitation and inhibition of neuronal activity have been reported. ß-adrenergic agents increased the spontaneous activity of canine intrathoracic ganglion neurons involved in cardiac regulation (Butler *et al.*, 1990b). These agonists also inhibited synaptic transmission in sympathetic and parasympathetic ganglia of several other mammalian species (deGroat and Booth, 1980; Nakamura *et al.*, 1984; Akasu *et al.*, 1985; Nishi, 1986). Cat and rabbit sympathetic superior cervical ganglia also displayed inhibition after application of norepinephrine (Kushiku *et al.*, 1980; Satoh *et al.*, 1989). This evidence supports the contention that catecholamines may play a role in modulating synaptic transmission within mammalian cardiac ganglia (Smith *et al.*, 1992; Huang *et al.*, 1993) as in the sympathetic ganglia (Kushiku *et al.*, 1980; Satoh *et al.*, 1989).

The general ß-adrenergic antagonist timolol (Goodman *et al.*, 1990) was used to confirm that neuronal responses evoked by ISO were specifically ß-adrenergic. All responses to ISO application were blocked by the presence of timolol in the perfusate, as shown in Figures 34 and 35. Of particular interest is the novel effect of membrane depolarization observed in many instances which appeared to be the result of specific β–receptor binding.

The results of this section of the study show that guinea-pig intracardiac neurons display complex mixtures of responses to both α- and ß-adrenergic activation, but the specific receptor subtypes involved remain largely unknown at the level of single neurons. However, on the basis of evidence presented here and in previous studies, it is very likely that subtle modulation of specific neuronal properties by endogenously

released or circulating catecholamines could have very powerful consequences for the processing of information by the entire intracardiac nervous system.

The data presented in Chapter 2 of this thesis has shown the occurrence of both TH-immunoreactivity and formaldehyde induced fluorescence of catecholamines in morphologically similar terminals within intracardiac ganglia. These terminals may, therefore, be a source of catecholamines in addition to circulating hormones within the intracardiac nervous system (Baluk and Gabella, 1990; Steele *et al.*, 1994 and 1996; Mawe *et al.*, 1996; Leger *et al.*, 1999). In Chapter 4, I have shown that adrenergic agents are capable of modulating the behaviour of intracardiac neurons. It is therefore possible that, in regions of the heart where sympathetic terminals are present in ganglia, inputs from this arm of the autonomic nervous system can regulate ganglionic neurotransmission.

Conclusions

In summary, the guinea-pig intracardiac neurons show a great deal of diversity in morphology, electrophysiological properties and responses to the application of α- and ß-adrenergic agents. In the first part of this study, these neurons were classified into categories based on the time course of the AHP; these classes of neurons were shown to have common physiological and morphological attributes. This classification scheme provides a foundation for further analysis of the roles of these neurons in the intracardiac nervous system. In the second part of this study, it was demonstrated that local application of adrenergic agents influenced the behaviour of some intracardiac neurons

by alternating membrane potential, whole-cell conductance or neuron excitability, or some combination of these factors. Adrenergic agonists also were capable of facilitating or inhibiting responses to synaptic input. Thus, it is possible that adrenergically induced changes in neuronal properties and responses to activation may modulate ganglionic neurotransmission in the heart.

Chapter 5: General Discussion

The classical view of the role of neurons in intracardiac ganglia is that these neurons are simple relays which transmit signals from the central nervous system to the myocardium. However, the complexity of the intracardiac neurons system has only begun to be appreciated in the past few decades. It has been suggested that the purpose of this complex intracardiac network is to provide the flexibility to respond rapidly and appropriately to the prevailing conditions and short-term demands for maintaining cardiac output. In support of this point of view, Lipsitz *et al.* (1997), working in the maturing pig heart proposed that the increasing complexity in the variation of the interbeat interval with time after birth, was correlated with an increasing complexity of connections and interactions within the developing intracardiac neural network. The primary site of interaction between sympathetic and parasympathetic nervous systems within the heart has conventionally been considered to be at the neuromuscular junction and these interactions are thought to be mediated by the combined influences of transmitter and modulator substances released by both sympathetic and parasympathetic terminals (Loffelholz and Pappano, 1985). Both sympathetic modulation of parasympathetic neurotransmitter release from presynaptic terminals and the converse of this have been described (Levy, 1990; Potter and Ulman, 1994; and see Fig. 1 of Chapter 1). However, it is only recently that the intracardiac ganglia have been recognized as another potential site for sympathetic and parasympathetic interaction. In order for the sympathetic system to influence the parasympathetic system, or *vice versa*, coactivation of both systems would be required. Coactivation of sympathetic and parasympathetic extrinsic nerves to the heart has in fact been observed in certain physiological conditions, such as during periods of increased atrial filling when sympathetic output is increased

to elevate stroke volume and heart rate (Koizumi, *et al.*, 1990; Koizumi and Kollai, 1992). Under this condition, the parasympathetic system is activated presumably to limit sympathetically mediated overdrive of heart rate so that the efficiency of ventricular ejection is not reduced. A similar kind of sympathetic-parasympathetic convergence has also been described in prevertebral ganglia innervating the pelvic organs. Such convergence is a key factor in regulating pelvic organ function during changes in relative activity of the two autonomic limbs (Crowcroft and Szurszewski, 1971; de Groat and Saum, 1972; Janig and McLachlan, 1987; de Groat and Booth, 1993). Sympathetic terminals situated adjacent to neurons within pelvic ganglia are ideally positioned to modulate the activity of these neurons.

The work reported in this thesis has provided anatomical evidence for adrenergic terminals near intracardiac neurons, and pharmacological and physiological evidence for adrenergic modulation of intracardiac neuronal activity. The two neuronal characteristics of greatest functional consequences that were influenced by exogenous application of adrenergic agents are neuronal excitability, that is, the pattern of AP firing when neurons are activated, and synaptic neurotransmission. In terms of neurotransmission through intracardiac ganglia, for example, a phasic neuron may act as low-pass filters, reducing the frequency of ganglionic output in response to even very high levels of synaptic drive. In the present study, both α- and ß-adrenergic agents could alter neuronal excitability. Adrenergically-mediated inhibition of neurotransmission would obviously impede signal transmission requiring greater levels of synaptic activity before a response could be elicited, when sympathetic inputs were active. Conversely, adrenergic agents also increased the sensitivity of some neurons to low levels of stimulation, showing that, in some pathways in the intracardiac ganglia, elevated sympathetic input could augment neuronal activity at the level of individual neurons. Both inhibition and

facilitation of ongoing ganglionic neuronal activity by sympathetic inputs would be highly selective, depending upon the specific targeting of particular neurons by sympathetic terminals. That the experiments in this study might mimic the effects of catecholamine release from endogenous sympathetic terminals is supported by anatomical data which show positive immunoreactivity for TH, an adrenergic marker, and histochemical reactivity for catecholamines, in terminals surrounding individual intracardiac neurons.

Alterations in the overall autonomic control of the heart may play a role in disease states such as myocardial infarction, hypertension, and cardiac arrhythmia. Loss of blood supply or modified afferent input to the intracardiac neurons may drastically alter the function of, or even incapacitate the intracardiac neural network (Huang *et al.*, 1993). In support of this idea, it was discovered that electrical or chemical modification of intracardiac neuronal activity could generate cardiac arrhythmias (Cardinal *et al.*, 1992; Huang *et al.*, 1991). Disruptions in the autonomic nervous system have also been shown to contribute to, and to accompany, heart failure (Snow, 1989; Packer, 1990; Packer, 1993). In fact, the intracardiac nervous system will continue to influence cardiodynamics even in the absence of input from the central nervous system (Ardell *et al.*, 1991; Murphy *et al.*, 1994a; Murphy *et al.*, 1994b). It has been suggested that some responses elicited in transplanted hearts may be due to the influence that intrinsic cardiac neurons exert on the heart (Horackova and Armour, 1995). These observations on the importance of the intracardiac nervous system have important implications concerning the development of future pharmacotherapies.

In the cardiac autonomic nervous system, our understanding of control of the heart by the sympathetic and parasympathetic branches is still poor. For example, some physiological evidence has suggested that stimulation of the right stellate ganglion has a greater effect on heart

rate than does stimulation of the left stellate ganglion (Myano *et al.*, 1998). Others would disagree with such a lateralization of function. In the parasympathetic nervous system, Blinder *et al.* (1998) have shown that the ventrolateral nucleus ambiguus of the cat brain stem has two distinct populations of neurons; one which projects to intracardiac ganglia innervating the sinoatrial node and another which projects to ganglia innervating the atrioventricular node. Not only are these two areas on the heart anatomically separated but they are functionally differentiated as well. The SA node functions as the principal pacemaker of the heart, while the AV node is normally responsible for signal conduction from the atria to the ventricles to ensure coordinated contraction of the four chambers and only functions secondarily as a pacemaker. Earlier studies in the canine by Randall and co-workers (Fee *et al.*, 1987; O'Toole *et al.*, 1986; Randall and Armour, 1994; Randall *et al.*, 1986) and by Dickerson (1998) and in the cat (Gatti *et al.*, 1997; Gatti *et al.*, 1995) have proposed that vagal control of rate, AV conduction and myocardial contractility are mediated by anatomically separate and physiologically independent intracardiac ganglia. Again, evidence from other studies does not support such conclusions of precise anatomical separation of neurons involved in these control pathways. Electrical and chemical stimulation of areas in the heart far removed from those ganglia circumscribed by Ardell and colleagues as rate control centers (Butler *et al.*, 1990a, b), could alter rate, suggesting that neural networks in the heart are highly distributed (Armour, 1994).

Despite the results of the work presented here, it is still not possible to determine the control pathway (or pathways) in which a particular, physiologically identified neuron might function. However, it is clear from this work that the function of a given neuron can be altered, depending upon the surrounding milieu of neurotransmitters and neuromodulators. A prominent example of this is the observation that some intracardiac neurons could be transformed from

phasic to accommodating, and *visa versa,* by adrenergic agonists in the present study. At the level of individual peripheral autonomic neurons, studies proposing schemes of classification based on firing behaviour have suggested that phasic neurons receive input from the central nervous system while tonic neurons receive input from the periphery. However, if the firing behaviour of a neuron receiving a particular type of synaptic input can be altered by neuromodulators, a good correlation between innervation of these neurons and their firing patterns may not be possible. The classification of neurons based on the time course of the AHP, as used in the present study, is an improvement on classification schemes based on firing properties, since AHP characteristics were relatively unchanged by manipulation in the present study. It seems improbable that specific types of intracardiac neurons are dedicated to specific functional pathways, instead, it is more likely that all types of neuron are found in each pathway. The behaviour of a neuron would thus be determined by the requirements of its role within a particular pathway. Furthermore, neurons with similar cellular properties could perform different functions depending on their patterns of connectivity (ie. input patterns and output projection pathways) or exposure to neurochemicals. Thus, interneurons may function differently than efferent neurons or sensory neurons both as a result of their intrinsic properties and responses to neurochemicals, as well as their anatomical connections. However, corroborating evidence for this assertion is lacking in the literature, at present.

Future studies must involve identification of intracardiac neurons involved in a particular functional pathway, such as regulation of heart rate by the SA node. Once particular neurons or specific ganglia are identified within this pathway, the process of characterizing their neuronal behaviour, synaptic inputs and output projections could be undertaken. The *in vitro* preparation developed in this thesis is ideal for continuing such studies because the atria, including the

functioning SA node, its neural plexus and extrinsic cardiac nerves innervation, can be studied as a functional unit.

Literature Cited

Adams, D. J., Fieber, L. A., and Konishi, S. (1987). Neurotransmitter action and modulation of a calcium conductance in rat cultured parasympathetic cardiac neurones. *J. Physiol.Lond.* **394**, 153P.

Adams, J. A. and Harper, A. A. (1995). Electrophysiological properties of autonomic ganglion neurons. In "The Autonomic Nervous System Vol.6 :Autonomic Ganglia" (E. M. McLachlan, Ed). Harwood Academic Publishers, Reading U.K., pp. 153-212.

Adams, P. R. and Koch, C. (1990). Peripheral ganglia. In "The Sympathetic Organization of the Brain" (G. M. Shepherd, Ed) 3rd edn.. Oxford University Press, NY,Oxford, pp. 67-87.

Ahren, B., Bottcher, G., Kowalyk, S., Dunning, B. B., Sundler, F., and Taborsky, G. J. (1990). Galanin is colocalized with noradrenaline and neuropeptide Y in dog pancreas and celiac ganglion. *Cell Tissue Res.* **261**, 49-58.

Aidley, D. J. (1976). "The Physiology of Excitable Cells", Cambridge University Press, London.

Akasu, T., Gallagher, J. P., Nakamura, T., Shinnick-Gallagher, P., and Yoshimura, M. (1985). Noradrenaline hyperpolarization and depolarization in cat vesical parasympathetic neurones. *J. Physiol. Lond.* **361**, 165-184.

Allen, T. G. J. and Burnstock, G. (1987). Intracellular studies of the electrophysiological properties of cultured intracardiac neurones of the guinea-pig. *J. Physiol. Lond.* **388**, 349-366.

Allen, T. G. J. and Burnstock, G. (1990). M1 and M2 muscarinic receptors mediate excitation and inhibition of guinea-pig intracardiac neurones in culture. *J. Physiol. Lond.* **422**, 463-480.

Allen, T. G. J., Hassall, C. J. S., and Burnstock, G. (1994). Mammalian intrinsic cardiac neurones in cell culture. In "Neurocardiology" (J. A. Armour and J. L. Ardell, Eds) Oxford University Press, New York.

Amory, D.W. and West,T.C. (1962). Chronotropic response following direct electrical stimulation of the isolated sinoatrial node: a pharmacological evaluation. *J. Pharmacol. Exp. Ther.* **137**, 14-23.

Anderson, R. H. (1972). The disposition, morphology and innervation of cardiac specialized tissue in the guinea-pig. *J. Anat.* **111**, 453-468.

Ardell, J. L. (1994). Structure and function of mammalian intrinsic cardiac neurons. In "Neurocardiology" (J. A. Armour and J. L. Ardell, Eds). Oxford University Press, Oxford, pp. 95-114.

Ardell, J. L., Butler, C. K., Smith, F. M., Hopkins, D. A., and Armour, J. A. (1991). Activity of in vivo atrial and ventricular neurons in chronically decentralized canine hearts. *Am. J. Physiol.* **260**, H713-H721.

Armour, J. A. (1994). Peripheral autonomic neuronal interactions in cardiac regulation. In "Neurocardiology" (J. A. Armour and J. L. Ardell, Eds) Oxford University Press, New York.

Armour, J. A. (1997). Intrinsic cardiac neurons involved in cardiac regulation possess $alpha_1$-, $alpha_2$-, $beta_1$- and $beta_2$-adrenoceptors. *Can. J. Cardiol.* **13**, 277-284.

Armour, J. A. and Ardell, J. L. (1994). "Neurocardiology", Oxford University Press, New York.

Armour, J. A. and Hopkins, D. A. (1984). Anatomy of the extrinsic efferent autonomic nerves and ganglia innervating the mammalian heart. In "Nervous Control of Cardiovascular Function" (W. C. Randall, Ed). Oxford University Press, New York, pp. 20-45.

Armour, J. A. and Hopkins, D. A. (1990). Activity of canine in situ left atrial ganglion neurons. *Am. J. Physiol.* **259**, H1207-H1215.

Armour, J. A., Huang, M. H., and Smith, F. M. (1993). Peptidergic modulation of in situ canine intrinsic cardiac neurons. *Peptides* **14**, 191-202.

Armour, J. A. and Randall, W. C. (1985). Rebound cardiovascular responses following stimulation of canine vagosympatheic complexes or cardiopulmonary nerves. *Can. J. Physiol. Pharmacol.* **63**, 1122-1132.

Armour, J. A., Yuan, B. X., and Butler, C. K. (1990). Cardiac responses elicited by peptides administered to canine intrinsic cardiac neurons. *Peptides* **11**, 753-761.

Baluk, P. and Gabella, G. (1990). Some parasympathetic neurons in the guinea-pig heart express aspects of the catecholaminergic phenotype in vivo. *Cell Tiss. Res.* **261**, 275-285.

Baumgarten, H. G. and Lange, W. (1969). Extrinsic adrenergic innervation of the extrahepatic biliary duct system in guinea-pigs, cats and rhesus monkeys. *Z. Zellforsch. Mikrosk. Anat.* **100**, 606-615.

Berne, R. M. and Levy, M. N. (1983). The autonomic nervous system and its control. In "Physiology". C.V.Mosby Co., St. Louis, pp. 314-335.

Biscoe, T. J. (1971). Carotid body: structure and function. *Physiol. Rev.* **51**, 437-495.

Blackman, J. G., Crowcroft, P. J., Devine, C. E., Holman, M. E., and Yonemura, K. (1969). Transmission from preganglionic fibres in the hypogastric nerve to peripheral ganglia of male guinea-pigs. *J. Physiol. Lond.* **201**, 723-743.

Blackman, J. G. and Purves, R. D. (1969). Intracellular recordings from ganglia of the thoracic sympathetic chain of the guinea-pig. *J. Physiol. Lond.* **203**, 173-198.

Blinder, K. J., Gatti, P. J., Johnson, T. A., Lauenstein, J. -M., Coleman, W. P., Gray, A. L., and Massari, V. J. (1998). Ultrastructural circuitry of cardiorespiratory reflexes: There is a monosynaptic path between the nucleus of the solitary tract and vagal preganglionic motoneurons controlling atrioventricular conduction in the cat. *Brain Res.* **785**, 143-157.

Blinks, J. R. (1966). Field stimulation as a means of effecting the graded release of autonomic transmitters in isolated heart muscle. *J. Pharmacol. Exp. Ther.* **151**, 221-235.

Bojsen-Moller, F. and Tranum-Jensen, J. (1971). Whole-mount demonstration of choinesterase-containing nerves in the right atrial wall, nodal tissue, and atrioventricular bundle of the pig heart. *J. Anat.* **108**, 375-386.

Bornstein, J. C., Furness, J. B., and Costa, M. (1989). An electrophysiological comparison of substance P-immunoreactive neurons with other neurons in the guinea pig submucous plexus. *J. Auton. Nerv. Syst.* **26**, 113.

Bowden, J. J. and Gibbins, I. L. (1992). Vasoactive intestinal peptide and neuropeptide Y coexist in non-noradrenergic sympathetic neurons to guinea pig trachea. *J. Auton. Nerv. Syst.* **38**, 1-20.

Brown, D. A. and Adams, P. R. (1980). Muscarinic suppression of a novel voltage-sensitive K+ current in a vertebrate neurone. *Nature* **283**, 673-676.

Buller, J. R. and Rossi, M. L. (1993). Immunocytochemistry on paraffin wax Golgi-Cox impregnated central nervous tissue. *Funct. Neurol.* **8**, 135-151.

Burkholder, T., Chambers, M., Hotmire, K., Wurster, R. D., Moody, S., and Randall, W. C. (1992). Gross and microscopic anatomy of the vagal innervation of the rat heart. *Anat. Rec.* **232**, 444-452.

Burnstock, G. and Costa, M. (1975). General organization and functions of adrenergic nerves. In "Adrenergic Neurons: Their organization, function, and development in the peripheral nervous system" (G. Burnstock and M. Costa, Eds). Chapman and Hall, London, pp. 4-42.

Butler, C. K., Smith, F. M., Cardinal, R., Murphy, D. A., Hopkins, D. A., and Armour, J. A. (1990a). Cardiac responses to electrical stimulation of discrete loci in canine atrial and ventricular ganglionated plexi. *Am.J.Physiol.* **259**, H1365-H1373.

Butler, C. K., Smith, F. M., Nicholson, J., and Armour, J. A. (1990b). Cardiac effects induced by chemically activated neurons in canine intrathoracic ganglia. *Am. J. Physiol.* **259**, H1108-H1117.

Calaresu, F. R. and St.Louis, A. J. (1967). Topography and numerical distribution of intracardiac ganglion cells in the cat. *J. Comp. Neurol.* **131(1)**, 55-66.

Campbell, G. D., Edwards, F. R., Hirst, G. D. S., and O'Shea, J. E. (1989). Effects of vagal stimulation and applied acetylcholine on pacemaker potentials in the guinea-pig heart. *J. Physiol.* **415**, 57-68.

Cannon, W. B. (1939). "The wisdom of the body", W.W.Norton, New York.

Cardinal, R., Scherlag, B. J., Vermeulen, M., and Armour, J. A. (1992). Distinct epicardial activation patterns of idioventricular rhythms and sympathetically-induced ventricular tachycardias in dogs with atrioventricular block. *PACE* **15**, 1300-1316.

Carr, P. A., Noga, B. R., Nance, D. M., and Jordan, L. M. (1994). Intracellular labeling of cat spinal neurons using a tetramethylrhodamine-dextran amine conjugate. *Brain Res. Bull.* **34**, 447-451.

Cassell, J. F., Clark, A. L., and McLachlan, E. M. (1986). Characteristics of phasic and tonic sympathetic ganglion cells of the guinea-pig. *J. Physiol. Lond.* **372**, 457-483.

Cheng, Z., Powley, T. L., Schwaber, J. S., and Doyle, F. J.,III (1997a). A laser confocal microscopic study of vagal afferent innervation of rat aortic arch: Chemoreceptors as well as baroreceptors. *J. Auton. Nerv. Syst.* **67**, 1-14.

Cheng, Z., Powley, T. L., Schwaber, J. S., and Doyle, F. J.,III (1997b). Vagal afferent innervation of the atria of the rat heart reconstructed with confocal microscopy. *J. Comp. Neurol.* **381**, 1-17.

Chow, L. T. -c., Chow, S. S. -m., Anderson, R. H., and Gosling, J. A. (1993). Innervation of the human cardiac conduction system at birth. *Br. Heart J.* **69**, 430-435.

Clark, R. B., Tse, A., and Giles, W. R. (1990). Electrophysiology of parasympathetic neurones isolated from the interatrial septum of bull-frog heart. *J. Physiol. Lond.* **427**, 89-125.

Cornbrooks, E. B., Pouliot, W. A., and Mawe, G. M. (1992). Structure of neurons and ganglia of the guinea pig gallbladder: Light and electron microscopic studies. *J. Comp. Neurol.* **317**, 31-44.

Crick, S. J., Wharton, J., Sheppard, M. N., Royston, D., Yacoub, M. H., Anderson, R. H., and Polak, J. M. (1994). Innervation of the human cardiac conduction system. A quantitative immunohistochemical and histochemical study. *Circulation* **89**, 1697-1708.

Crowcroft, P. J. and Szurszewski, J. H. (1971). A study of the inferior mesenteric and pelvic ganglia of guinea-pigs with intracellular electrodes. *J. Physiol. Lond.* **219**, 421-441.

Cuello, A. C., Priestley, J. V., and Matthews, M. R. (1982). Localization of substance P in neuronal pathways. *Ciba Found. Symp.* 55-83.

Dail, W. G. (1976). Histochemical and fine structure studies of SIF cells in the major pelvic ganglion of the rat. In "SIF cells, structure and function of the small intensely fluorescent sympathetic cells" (O. Eranko, Ed). Fogarty International Center Proceedings No. 30, Washington, D.C., pp. 8-18.

Dail, W. G., Evan, A. P., and Eason, H. R. (1975). The major ganglion in the pelvic plexus of the male rat: A histochemical and ultrastructural study. *Cell Tiss. Res.* **159**, 49-62.

Dalsgaard, C. -J., Hökfelt, T., Elfvin, L. -G., Skirboll, L., and Emson, P. (1982). Substance P-containing primary sensory neurons projecting to the inferior mesenteric ganglion: Evidence from combined retrograde tracing and immunohistochemistry. *Neuroscience* **7(3)**, 647-654.

Dalsgaard, C. J., Franco-Cereceda, A., Saria, A., Lundberg, J. M., Theodorsson-Norheim, E., and Hökfelt, T. (1986). Distribution and origin of substance P- and neuropeptide Y-immunoreactive nerves in the guinea-pig heart. *Cell Tissue Res.* **243**, 477-485.

De Groat, W. C. and Booth, A. M. (1980). Inhibition and facilitation in parasympathetic ganglia of the urinary bladder. *Fed. Proc.* **39**, 2990-2996.

De Groat, W. C., Booth, A. M., and Krier, J. (1979). Interaction between sacral parasympathetic and lumbar sympathetic inputs to pelvic ganglia. In "Integrative Functions of the Autonomic Nervous System" (C. McC. Brooks, K. Koizumi, and A. Sato, Eds). University of Tokyo Press, Tokyo, pp. 234-245.

De Groat, W. C. and Saum, W. R. (1972). Sympathetic inhibition of the urinary bladder and of pelvic ganglionic transmission in the cat. *J. Physiol. Lond.* **220**, 297-314.

Dey, R. D., Altemus, J. B., Rodd, A., Mayer, B., Said, S. I., and Coburn, R. F. (1996). Neurochemical characterization of intrinsic neurons in ferret tracheal plexus. *Am. J. Respir. Cell Mol. Biol* **14**, 207-216.

Dogiel, A. S. (1899). Uber den bau der ganglien in den geflechten de darmes and der gallenblase des menschen und der saugetiere. *Arch. Anat. Physiol. Leipzig., Anat. Abtr.* **1899**, 130-158. See Wood *et al.* 1994.

Eckenstein, F. and Sofroniew, M. V. (1983). Identification of central cholinergic neurons containing both choline acetyltransferase and acetylcholinesterase and of central neurons containing only acetylcholinesterase. *J. Neurosci.* **3**, 2286-2291.

Edwards, F. R., Hirst, G. D. S., Klemm, M. F., and Steele, P. A. (1995). Different types of ganglion cell in the cardiac plexus of guinea-pigs. *J.Physiol.Lond.* **486**, 453-471.

Ehinger,B., Falck,B., Persson,H., and Sporrong, B. (1968). Adrenergic and cholinesterase-containing neurons of the heart. *Histochimie* **16**, 197-205.

Ellison, J. P. and Hibbs, R. G. (1974). Catecholamine-containing cells of the guinea pig heart: An ultrastructural study. *J. Mol. Cell. Cardiol.* **6**, 17-26.

Ellison, J. P. and Hibbs, R. G. (1976). An ultrastructural study of mammalian cardiac ganglia. *J. Mol. Cell. Cardiol.* **8**, 89-101.

Fee, J. D., Randall, W. C., Wurster, R. D., and Ardell, J. L. (1987). Selective ganglionic blockade of vagal inputs to sinoatrial and/or atrioventricular regions. *J. Pharmacol. Exp. Ther.* **242**, 1006-1012.

Fibiger,H.C. (1982). The organization and some projections of cholinergic neurons of the mammalian forebrain. *Brain Res.Rev.* **4**, 327-388.

Fieber, L. A. and Adams, D. J. (1991). Acetylcholine-evoked currents in cultured neurones dissociated from rat parasympathetic cardiac ganglia. *J. Physiol. Lond.* **434**, 215-237.

Flavahan, N. A. and McGrath, J. C. (1982). alpha 1-adrenoceptor activation can increase heart rate directly or decrease it indirectly through parasympathetic activation. *Br. J. Pharmacol.* **77**, 319-328.

Fu, C., Jasani, B., Vujanic, G. M., Leadbeatter, S., Berry, P. J., and Knight, B. H. (1994). The immunocytochemical demonstration of a relative lack of nerve fibres in the atrioventricular node and bundle of His in the sudden infant death syndrome (SIDS). *Forensic Science International* **66**, 175-185.

Furness, J. B. and Bornstein, J. C. (1995). The enteric nervous system and its extrinsic connections. In "Enteric Nervous System" (T. Yamada, Ed) pp. 2-24. JB Lippincott Company, Philadelphia.

Furness, J. B. and Costa, M. (1987). "The Enteric Nervous System", Churchill Livingstone, Edinburgh.

Furness, J. B., Costa, M., and Eckenstein, F. (1983). Neurones localized with antibodies against choline acetyltransferase in the enteric nervous system. *Neurosci. Lett.* **40**, 105-109.

Furness, J. B., Costa, M., and Keast, J. R. (1984). Choline acetyltransferase-and peptide immunoreactivity of submucous neurons in the small intestine of the guinea-pig. *Cell Tissue Res.* **237**, 329-336.

Furness, J. B., Johnson, P. J., Pompolo, S., and Bornstein, J. C. (1995). Evidence that enteric motility reflexes can be initiated through entirely intrinsic mechanisms in the guinea-pig small intestine. *Neurogastroenterl. Mot.* **7**, 89-96.

Furukawa, Y., Martin, P., and Levy, M. N. (1990). AV junctional rhythm induced by sympathetic-parasympathetic imbalance in dog hearts. *Am. J. Physiol.* **259**, H839-H842.

Gallego, R. and Eyzaguirre, C. (1978). Membrane and action potential characteristics of A and C nodose ganglion cells studied in whole ganglia and in tissue slices. *J. Neurophysiol.* **41**, 1217-1232.

Gatti, P. J., Johnson, T. A., McKenzie, J., Lauenstein, J. M., Gray, A., and Massari, V. J. (1997). Vagal control of left ventricular contractility is selectively mediated by a cranioventricular intercardiac ganglion in the cat. *J. Auton. Nerv. Syst.* **66**, 138-144.

Gatti, P. J., Johnson, T. A., Phan, P., Jordan, I. K.,III, Coleman, W., and Massari, V. J. (1995). The physiological and anatomical demonstration of functionally selective parasympathetic ganglia located in discrete fat pads on the feline myocardium. *J. Auton. Nerv. Syst.* **51**, 255-259.

Gordon, L., Polak, J. M., Moscoso, G. J., Smith, A., Kuhn, D. M., and Wharton, J. (1993). Development of the peptidergic innervation of human heart. *J. Anat.* **183**, 131-140.

Gulbenkian, S., Saetrum Opgaard, O., Barroso, C. P., Wharton, J., Polak, J. M., and Edvinsson, L. (1994). The innervation of guinea pig epicardial coronary veins: immunohistochemistry, ultrastructure and vasomotility. *J. Auton. Nerv. Syst.* **47**, 201-212.

Gulbenkian, S., Saetrum Opgaard, O., Ekman, R., Costa Andrade, N., Wharton, J., Polak, J. M., Queiroz e Melo, M., and Edvinsson, L. (1993). Peptidergic innervation of human epicardial coronary arteries. *Circ. Res.* **73**, 579-588.

Gulbenkian, S., Wharton, J., and Polak, J. M. (1987). The visualisation of cardiovascular innervation in the guinea pig using an antiserum to protein gene product 9.5 (PGP 9.5). *J. Auton. Nerv. Syst.* **18**, 235-247.

Gurnett, C. A., Whiteis, C. A., Pardini, B. J., and Schmid, P. G.,Jr. (1993). Norepinephrine release from guinea pig cardiac sympathetic nerves is insensitive to ryanodine under physiological conditions. *Brain Res.* **612**, 238-242.

Hamberger, B. and Norberg, K. A. (1965a). Adrenergic synaptic terminals and nerve cells in bladder ganglia of the cat. *Int. J. Neuropharm.* **4**, 41-45.

Hamberger, B. and Norberg, K. A. (1965b). Studies on some systems of adrenergic synaptic terminals in the abdominal ganglia of the cat. *Acta Physiol. Scand.* **654**, 235-242.

Hancock, J. C., Hoover, D. B., and Hougland, M. W. (1987). Distribution of muscarinic receptors and acetylcholinesterase in the rat heart. *J. Auton. Nerv. Syst.* **19**, 59-66.

Hardwick, J. C., Mawe, G. M., and Parsons, R. L. (1995). Evidence for afferent fiber innervation of parasympathetic neurons of the guinea-pig cardiac ganglion. *J. Auton. Nerv. Syst.* **53**, 166-174.

Heym, C., Klimaschewski, L., Borghini, N., and Fischer-Colbrie, R. (1994). Immunohistochemistry of small intensely fluorescent (SIF) cells and of SIF cell-associated nerve fibers in the rat superior cervical ganglion. *Microsc. Res. Tech.* **29**, 143-150.

Hirst, G. D. S., Holman, M. E., and Spence, I. (1974). Two types of neurones in the myenteric plexus of duodenum in the guinea-pig. *J. Physiol. Lond.* **236**, 303-326.

Hirst, G. D. S. and McKirdy, H. C. (1974). A nervous mechanism for descending inhibition in guinea-pig small intestine. *J. Physiol. Lond.* **238**, 129-143.

Horackova, M. and Armour, J. A. (1995). Role of peripheral autonomic neurones in maintaining adequate cardiac function. *Cardiovasc. Res.* **30**, 326-335.

Horackova, M., Croll, R. P., Hopkins, D. A., Losier, A. M., and Armour, J. A. (1996). Morphological and immunohistochemical properties of primary long-term cultures of adult guinea-pig ventricular cardiomyocytes with peripheral cardiac neurons. *Tissue and Cell* **28**, 411-425.

Horackova, M., Huang, M. H., Armour, J. A., Hopkins, D. A., and Mapplebeck, C. (1993). Cocultures of adult ventricular myocytes with stellate ganglia or intrinsic cardiac neurones from guinea pigs: spontaneous activity and pharmacological properties. *Cardiovasc. Res.* **27**, 1101-1108.

Howe, A., Morgan, M., and Pack, R. J. (1978). A comparison of the ultrastructure of the abdominal vagal paraganglia and similar tissues in the rat. *J. Physiol. Lond.* **275**, 34-35P.

Huang, M. -H., Ardell, J. L., Hanna, B. D., Wolf, S. G., and Armour, J. A. (1993a). Effects of transient coronary artery occlusion on canine intrinsic cardiac neuronal activity [see comments]. *Integr. Physiol. Behav. Sci.* **28**, 5-21.

Huang, M. H., Smith, F. M., and Armour, J. A. (1993b). Amino acids modify activity of canine intrinsic cardiac neurons involved in cardiac regulation. *Am. J. Physiol.* **264**, H1275-H1282.

Huang, M. H., Sylvén, C., Pelleg, A., Smith, F. M., and Armour, J. A. (1993c). Modulation of in situ canine intrinsic cardiac neuronal activity by locally applied adenosine, ATP, or analogues. *Am. J. Physiol.* **265**, R914-R922.

Jacobowitz, D. (1967). Histochemical studies of the relationship of chromaffin cells and adrenergic nerve fibers to the cardiac ganglia of several species. *J. Pharmacol. Exp. Ther.* **158**, 227-240.

Jacobowitz, D. M. and Palkovits, M. (1974). Topographic atlas of catecholamine and acetylcholinesterase-containing neurons in the brain. *J. Comp. Neurol.* **157**, 13-28.

Janes, R. D., Brandys, J. C., Hopkins, D. A., Johnstone, D. E., Murphy, D. A., and Armour, J. A. (1986). Anatomy of human extrinsic cardiac nerves and ganglia. *Am. J. Cardiol.* **57**, 299-309.

Jänig, W. and McLachlan, E. M. (1987). Organization of lumbar spinal outflow to distal colon and pelvic organs. *Physiol. Rev.* **67**, 1332-1404.

Jänig, W. and McLachlan, E. M. (1992). Specialized functional pathways are the building blocks of the autonomic nervous system. *J. Auton. Nerv. Syst.* **41**, 3-14.

Keast, J. R., Kawatani, M., and DeGroat, W. C. (1990). Sympathetic modulation of cholinergic transmission in cat vesical ganglia is mediated by α- and β_2-adrenoceptors. *Am. J. Physiol.* **258**, R44-R50.

Keast, J. R., Luckensmeyer, G. B., and Schemann, M. (1995). All pelvic neurons in male rats contain immunoreactivity for the synthetic enzymes of either noradrenaline or acetylcholine. *Neuroscience Letters* **196**, 209-212.

King, B. F., Love, J. A., and Szurszewski, J. H. (1989). Intracellular recordings from pancreatic ganglia of the cat. *J. Physiol. Lond.* **419**, 379-403.

King, T. S. and Coakley, J. B. (1958). The intrinsic nerve cells of the cardiac atria of mammals and man. *J. Anat.* **92(3)**, 353-376.

Kirchgessner, A. L. and Gershon, M. D. (1988). Identification of vagal and submucosal inputs to the myenteric plexus by retrograde and anterograde transport. In "Nerves and the Gastrointestinal Tract" (M. V. Singer and H. Goebell, Eds). MTP Press, Lancaster, pp. 69-78.

Kirchgessner, A. L., Tamir, H., and Gershon, M. D. (1992). Identification and stimulation by serotonin of intrinsic sensory neurons of the submucosal plexus of the guinea pig gut: activity-induced expression of Fos immunoreactivity. *J. Neurosci.* **12**, 235-249.

Kobayashi, R. M., Brownstein, M., Saavedra, J. M., and Palkovits, M. (1975). Choline acetyltransferase content in discrete regions of the rat brain stem. *J. Neurochem.* **24**, 637-640.

Koelle, G. B. (1963). Cytological distributions and physiological functions of cholinesterases. In "Handbuch der experimentellen Pharmakology. Ergla UManungswerk" (O. Eichler and A. Farah, Eds) 15th edn. pp. 187-298. Springer-Verlag, Heidelberg.

Koizumi, K. and Kollai, M. (1992). Multiple modes of operation of cardiac autonomic control: development of the ideas from Cannon and Brooks to the present. *J. Auton. Nerv. Syst.* **41**, 19-30.

Koizumi, K., Terui, N., Kollai, M., and Brooks, C. MC. (1982). Functional significance of coactivation of vagal and sympathetic cardiac nerves. *Proc. Natl. Acad. Sci. USA* **79**, 2116-2120.

Konopka, L. M. and Parsons, R. L. (1989). Characteristics of the galanin-induced depolarization of mudpuppy parasympathetic postganglionic neurons. *Neurosci. Lett.* **99**, 142-146.

Kriebel, R. M., Angel, A., and Parsons, R. L. (1991). Biogenic amine localization in cardiac ganglion intrinsic neurons: electron microscopic histochemistry of SIF cells. *Brain Res. Bull.* **27**, 175-179.

Kuhar, M. J. (1976). The anatomy of cholinergic neurons. In "Biology of Cholinergic Function" (A. M. Goldberg and I. Hanin, Eds). Raven Press, New York, pp. 3-27.

Kunze, W. A. A., Bornstein, J. C., and Furness, J. B. (1995). Identification of sensory nerve cells in a peripheral organ (the intestine) of a mammal. *Neurosci.* **66**, 1-4.

Kushiku, K., Furukawa, T., Ichimasa, S., and Kamiya, H-o. (1980). Negative chronotropic effect of catacholamines on adrenergic receptors in the cardiac ganglia in the spinal dog. *J. Cardiovasc. Pharmacol.* **2**, 857-866.

Leger, J., Croll, R. P., and Smith, F. M. (1999). Regional distribution and extrinsic innervation of intrinsic cardiac neurons in the guinea pig. *J. Comp. Neurol.* **407**, 303-317.

Levy, M. N. (1990). Autonomic interactions in cardiac control. *Ann. N. Y. Acad. Sci.* **601**, 209-221.

Levy, M. N., Ng, M., Martin, P., and Zieske, H. (1966). Sympathetic and parasympathetic interactions upon the left ventricle of the dog. *Circ. Res.* **19**, 5-10.

Lipp, J. M. and Rudolph, A. M. (1972). Sympathetic nerve development in the rat and guinea-pig heart. *Biol. Neonate* **21**, 76-82.

Lipsitz, L. A., Pincus, S. M., Morin, R. J., Tong, S., Eberle, L. P., and Gootman, P. M. (1997). Preliminary evidence for the evolution of complexity of heart rate dynamics during autonomic maturation in neonatal swine. *J. Auton. Nerv. Syst.* **65**, 1-9.

Loffelholz, K. and Pappano, A. J. (1985). The parasympathetic neuroeffector junction of the heart. *Pharmacol. Rev.* **37**, 1-24.

Marron, K., Wharton, J., Sheppard, M. N., Gulbenkian, S., Royston, D., Yacoub, M. H., Anderson, R. H., and Polak, J. M. (1994). Human endocardial innervation and its relationship to the endothelium: an immunohistochemical, histochemical, and quantitative study. *Cardiovasc. Res.* **28**, 1490-1499.

Mawe, G. M. (1990). Intracellular recording from neurones of the guinea-pig gall-bladder. *J. Physiol. Lond.* **429**, 323-338.

Mawe, G. M. (1993). Noradrenaline as a presynaptic inhibitory neurotransmitter in ganglia of the guinea-pig gall-bladder. *J. Physiol. Lond.* **461**, 387-402.

Mawe, G. M. and Gershon, M. D. (1989). Structure, afferent innervation, and transmitter content of ganglia of the guinea pig gallbladder: relationship to the enteric nervous system. *J. Comp. Neurol.* **283**, 374-390.

Mawe, G. M., Talmage, E. K., Lee, K. P., and Parsons, R. L. (1996). Expression of choline acetyltransferase immunoreactivity in guinea pig cardiac ganglia. *Cell Tissue Res.* **285**, 281-286.

McGrath, J. C., Brown, C. M., and Wilson, V. G. (1991). -adrenergic receptors. In "Receptor Data for Biological Experiments; A guide to drug sensitivity" (H. N. Doods and J. C. A. Van Meel, Eds). Ellis Horwood, New York, London, pp. 13-208.

McKibben, J. S. and Getty, R. (1969). Innervation of heart of domesticated animals: horse. *Am. J. Vet. Res.* **30**, 193-202.

McLachlan, E. M. and Meckler, R. L. (1989). Characteristics of synaptic input to three classes of sympathetic neurone in the coeliac ganglion of the guinea-pig. *J. Physiol. Lond.* **415**, 109-129.

Meckler, R. L. and McLachlan, E. M. (1988). Axons of peripheral origin preferentially synapse with tonic neurones in the guinea pig coeliac ganglion. *Neurosci. Lett.* **86**, 189-194.

Miyano, H., Nakayama, Y., Shishido, T., Inagaki, M., Kawada, T., Sato, T., Miyashita, H., Sugimachi, M., Alexander, J., Jr., and Sunagawa, K. (1998). Dynamic sympathetic regulation of left ventricular contractibility studied in the isolated canine heart. *Am. J. Physiol.* **275**, H400-H408.

Molist, P., Rodriguez Moldes, I., and Anadon, R. (1993). Organization of catecholaminergic systems in the hypothalamus of two elasmobranch species, Raja undulata and Scyliorhinus canicula. A histofluorescence and immunohistochemical study. *Brain Behav. Evol.* **41**, 290-302.

Moravec, J. and Moravec, M. (1987). Intrinsic nerve plexus of mammalian heart: morphological basis of cardiac rhythmical activity? *Int. Rev. Cytol.* **106**, 89-148.

Moravec, M., Courtalon, A., and Moravec, J. (1986). Intrinsic neurosecretory neurons of the rat heart atrioventricular junction: possibility of local neuromuscular feed back loops. *J. Mol. Cell. Cardiol.* **18**, 357-367.

Moravec, M. and Moravec, J. (1984). Intrinsic innervation of the atrioventricular junction of the rat heart. *Am. J. Anat.* **171**, 307-319.

Moravec, M. and Moravec, J. (1989). Adrenergic neurons and short proprioceptive feedback loops involved in the integration of cardiac function in the rat. *Cell Tiss. Res.* **258**, 381-385.

Moravec, M., Moravec, J., and Forsgren, S. (1990). Catecholaminergic and peptidergic nerve components of intramural ganglia in the rat heart. An immunohistochemical study. *Cell Tiss. Res.* **262**, 315-327.

Murphy, D. A., O'Blenes, S., Hanna, B. D., and Armour, J. A. (1994). Capacity of intrinsic cardiac neurons to modify the acutely autotransplanted mammalian heart. *J. Heart Lung Transplant.* **13**, 847-856.

Nakamura, T., Yoshimura, M., Shinnick-Gallagher, P., Gallagher, J. P., and Akasu, T. (1984). $_2$ and $_1$-adrenoceptors mediate opposing actions on parasympathetic neurons. *Brain Res.* **323**, 349-353.

Neel, D. S. and Parsons, R. L. (1986). Anatomical evidence for the interaction of sympathetic and parasympathetic neurons in the cardiac ganglion of *Necturus*. *J. Auton. Nerv. Syst.* **15**, 297-308.

Nishi, S. (1986). Electrophysiological properties of sympathetic neurons. In "Autonomic and Enteric Ganglia" (A. G. Karczmar, K. Koketsu, and S. Nishi, Eds) pp. 79-106.

Nishi, S. and North, R. A. (1973). Intracellular recording from the myenteric plexus of the guinea-pig ileum. *J. Physiol. Lond.* **231**, 471-491.

O'Toole, M. F., Ardell, J. L., and Randall, W. C. (1986). Functional interdependence of discrete vagal projections to SA and AV nodes. *Am. J. Physiol.* **251**, H398-H404.

Olmez, E., Guc, M. O., and Ilhan, M. (1995). Inhibitory muscarinic cholinoceptors on postganglionic sympathetic nerves in the guinea pig isolated atrium are of the M_3 subtype. *Pharmacology* **51**, 112-117.

Opthof, T., deJonge, B., Mackaay, A. J. C., Bleeker, W. K., Masson-Pevet, M., Jongsma, H. J., and Bouman, L. N. (1985). Functional and morphological organization of the guinea-pig

sinoatrial node compared with the rabbit sinoatrial node. *J. Mol. Cell. Cardiol.* **17**, 549-564.

Packer, M. (1993). How should physicians view heart failure? The philosophical and physiological evolution of three conceptual models of the disease. *Am. J. Cardiol.* **71**, 3C-11C.

Pardini, B. J., Patel, K. P., Schmid, P. G., and Lund, D. D. (1987). Location, distribution and projections of intracardiac ganglion cells in the rat. *J. Auton. Nerv. Syst.* **20**, 91-101.

Pauza, D. H., Skripkiene, G., Skripka, V., Pauziene, N., and Stropus, R. (1997). Morphological study of neurons in the nerve plexus on heart base of rats and guinea pigs. *J. Auton. Nerv. Syst.* **62**, 1-12.

Pirola, F. T. and Potter, E. K. (1990). Vagal action on atrioventricular conduction and its inhibition by sympathetic stimulation and neuropeptide Y in anaesthetised dogs. *J. Auton. Nerv. Syst.* **31**, 1-12.

Potter, E. K. and Ulman, L. G. (1994). Neuropeptides in sympathetic nerves affect vagal regulation of the heart. *NIPS* **9**, 174-177.

Randall, D. C. and Brown, D. R. (1994). Autonomic nervous control of cardiovascular function in the awake animal. In "Neurocardiology" (J. A. Armour and J. L. Ardell, Eds) pp. 343-363. Oxford University Press, Oxford.

Randall, W. C. (1994). Efferent sympathetic innervation of the heart. In "Neurocardiology" (J. A. Armour and J. L. Ardell, Eds). Oxford University Press, Oxford, pp. 77-94.

Randall, W. C. and Ardell, J. L. (1985). Differential innervation of the heart. In "Cardiac Electrophysiology and Arrhythmias". Grune & Stratton, pp. 137-144.

Randall, W. C. and Ardell, J. L. (1988). Functional anatomy of the cardiac efferent innervation. In "Neurocardiology" (H. E. Kulbertus and G. Franck, Eds) pp. 3-24. Futura Pub. Comp., Mount Kisco, NY.

Randall, W. C., Ardell, J. L., and Becker, D. M. (1985). Differential responses accompanying sequential stimulation and ablation of vagal branches to dog heart. *Am. J. Physiol.* **249**, H133-H140.

Randall, W. C., Armour, J. A., Geis, W. P., and Lippincott, D. B. (1972). Regional cardiac distribution of the sympathetic nerves. *Fed. Proc.* **31**, 1199-1208.

Randall, W. C., Armour, J. A., Randall, D. C., and Smith, O. A. (1971). Functional anatomy of the cardiac nerves in the baboon. *Anat. Rec.* **170**, 183-198.

Randall, W. C., Milosavljevic, M., Wurster, R. D., Geis, G. S., and Ardell, J. L. (1986). Selective vagal innervation of the heart. *Ann. Clin. Lab. Sci.* **16**, 198-208.

Rende, M., Giambanco, I., Buratta, M., and Tonali, P. (1995). Axotomy induces a different modulation of both low-affinity nerve growth factor receptor and choline acetyltransferase between adult rat spinal and brainstem motoneurons. *J. Comp. Neurol.* **363**, 249-263.

Roberts, L. A., Slocum, G. R., and Riley, D. A. (1989). Morphological study of the innervation pattern of the rabbit sinoatrial node. *Am. J. Anat.* **185**, 74-88.

Roper, S. (1976). The acetylcholine sensitivity of the surface membrane of multiply-innervated parasympathetic ganglion cells in the mudpuppy before and after partial denervation. *J. Physiol. Lond.* **254**, 455-473.

Roskoski, R.,Jr., Mayer, H. E., and Schmid, P. G. (1974). Choline acetyltransferase activity in guinea-pig heart *in vitro*. *J. Neurochem.* **23**, 1197-1200.

Rueff, A. and Dray, A. (1993). Sensitization of peripheral afferent fibres in the in vitro neonatal rat spinal cord-tail by bradykinin and prostaglandins. *Neuroscience* **54**, 527-535.

Ruffolo, R. R.,Jr., Nichols, A. J., Stadel, J. M., and Hieble, J. P. (1991). Structure and function of β-adrenoceptors. *Pharmacological Rev.* **43**, 475-505.

Saito, A., Kimura, S., and Goto, K. (1986). Calcitonin gene-related peptide as potential neurotransmitter in guinea pig right atrium. *Am. J. Physiol.* **250**, H693-H698.

Saito, K., Potter, W. Z., and Saavedra, J. M. (1988). Quantitative autoradiography of β-adrenoceptors in the cardiac vagus ganglia of the rat. *Eur. J. Pharmacol.* **153**, 289-293.

Sann, H., McCarthy, P. W., Schemann, M., Jurzak, M., Poethke, R., and Pierau, F. -K. (1995). Choline acetyltransferase-immunoreactive neurones in a prevertebral sympathetic ganglion, the inferior mesenteric ganglion. *J. Auton. Nerv. Syst.* **54**, 195-205.

Satoh, K., Armstrong, D. M., and Fibiger, H. C. (1983). A comparison of the distribution of central cholinergic neurons as demonstrated by acetylcholinesterase pharmacohistochemistry and choline acetyltransferase immunohistochemistry. *Brain Res. Bull.* **11**, 693-720.

Satoh, Y., Kohli, J. D., and Goldberg, L. I. (1989). Effects of *alpha* adrenoceptor and dopamine receptor agonists and antagonists on ganglionic transmission. *J. Pharmacol. Exp. Ther.* **251**, 253-257.

Schemann, M., Schaaf, C., and Mäder, M. (1995). Neurochemical coding of enteric neurons in the guinea pig stomach. *J. Comp. Neurol.* **353**, 161-178.

Seabrook, G. R., Fieber, L. A., and Adams, D. J. (1990). Neurotransmission in neonatal rat cardiac ganglion in situ. *Am. J. Physiol.* **259**, H997-H1005.

Selyanko, A. A. (1992a). Membrane properties and firing characteristics of rat cardiac neurones in vitro. *J. Auton. Nerv. Syst.* **39**, 181-190.

Selyanko, A. A. and Skok, V. I. (1992b). Acetylcholine receptors in rat cardiac neurones. *J. Auton. Nerv. Syst.* **40**, 33-48.

Selyanko, A. A. and Skok, V. I. (1992c). Synaptic transmission in rat cardiac neurones. *J. Auton. Nerv. Syst.* **39**, 191-200.

Sisk, D. B. (1976). Physiology. In "The Biology of the Guinea-Pig" (J. E. Wagner and P. J. Manning, Eds) pp. 73-85. Academic Press, New York.

Slavikova, J., Goldstein, M., and Dahlström, A. (1993). The postnatal development of tyrosine hydroxylase immunoreactive nerves in rat atrium, studied with immunofluorescence and confocal laser scanning microscopy. *J. Auton. Nerv. Syst.* **43**, 159-170.

Smith, F. M. (1999). Extrinsic inputs to intrinsic neurons in the porcine heart in vitro. *Am. J. Physiol.* **276**, R455-R467.

Smith, F. M., Hopkins, D. A., and Armour, J. A. (1992). Electrophysiological properties of in vitro intrinsic cardiac neurons in the pig (*Sus scrofa*). *Brain Res. Bull.* **28**, 715-725.

Smith, P. A. (1994). Amphibian sympathetic ganglia: an owner's and operator's manual. *Prog. Neurobiol.* **43**, 439-510.

Smith, T. K., Bornstein, J. C., and Furness, J. B. (1990). Distension-evoked ascendiing and descending reflexes in circular muscle of guinea pig ileum: an intracellular study. *J. Auton. Nerv. Syst.* **29**, 203-215.

Smith, T. K., Bornstein, J. C., and Furness, J. B. (1991). Interactions between reflexes evoked by distension and mucosal stimulation: electrophysiological studies of guinea-pig ileum. *J. Auton. Nerv. Syst.* **34**, 69-75.

Smith, T. K. and Furness, J. B. (1988). Reflex changes in muscle activity elicited by stroking the mucosa: and electrophysiological analysis in the isolated gyinea-pig. *J. Auton. Nerv. Syst.* **25**, 205-212.

Steele, P. A. and Choate, J. K. (1994). Innervation of the pacemaker in guinea-pig sinoatrial node. *J. Auton. Nerv. Syst.* **47**, 177-187.

Steele, P. A., Gibbins, I. L., and Morris, J. L. (1996). Projections of intrinsic cardiac neurons to different targets in the guinea-pig heart. *J. Auton. Nerv. Syst.* **56**, 191-200.

Steele, P. A., Gibbins, I. L., Morris, J. L., and Mayer, B. (1994). Multiple populations of neuropeptide-containing intrinsic neurons in the guinea-pig heart. *Neuroscience* **62**, 241-250.

Suburo, A. M., Gibson, S. J., Moscoso, G., Terenghi, G., and Polak, J. M. (1992). Transient expression of neuropeptide Y and its C-flanking peptide immunoreactivities in the spinal cord and ganglia of human embryos and fetuses. *Neuroscience* **46**, 571-584.

Talmage, E. K., Pouliot, W. A., Schemann, M., and Mawe, G. M. (1996). Structure and chemical coding of human, canine and opossum gallbladder ganglia. *Cell Tiss. Res.* **284**, 289-302.

Tay, S. S. W., Wong, W. C., and Ling, E. A. (1984). An ultrastructural study of the neuronal changes in the cardiac ganglia of the monkey *(Macaca fascicularis)* following unilateral vagotomy. *J. Anat.* **138**, 67-80.

Thompson, R. J., Doran, J. F., Jackson, P., Dhillon, A. P., and Rode, J. (1983). PGP 9.5--a new marker for vertebrate neurons and neuroendocrine cells. *Brain Res.* **278**, 224-228.

Trendelenburg, A. -U., Limberger, N., and Starke, K. (1995). Subclassification of presynaptic $_2$-adrenoceptors: $_{2D}$-autoreceptors in guinea-pig atria and brain. *Naunyn-Schmiedeberg's Arch. Pharmacol.* **352**, 49-57.

Trowern, A. R., Laight, R., MacLean, N., and Mann, D. A. (1996). Detection of neuron-specific protein gene product (PGP) 9.5 in the rat and zebrafish using anti-human PGP 9.5 antibodies. *Neurosci. Lett.* **210**, 21-24.

Tsurusaki, M., Yoshida, M., Akasu, T., and Nagatsu, I. (1990). $_2$-adrenoceptors mediate the inhibition of cholinergic transmission in parasympathetic ganglia of the rabbit urinary bladder. *Synapse* **5**, 233-240.

Van Meel, J. C. A., De Jonge, A., Timmermans, P. B. M. W. M., and van Zwieten, P. A. (1981). Selectivity of some *alpha* adrenoceptor agonists for peripheral *alpha*-1 and *alpha*-2 adrenoceptors in the normotensive rat. *J. Pharmacol. Exp. Ther.* **219**, 760-767.

Wang, H. -S. and McKinnon, D. (1995). Potassium currents in rat prevertebral and paravertebral sympathetic neurones: Control of firing properties. *J. Physiol. Lond.* **485**, 319-335.

Wells, D. G. and Mawe, G. M. (1994). Sympathetic input to ganglia of the guinea pig sphincter of Oddi. *Am.J.Physiol.***266**, G1162-G1169.

Wetzel, G. T. and Brown, J. H. (1985a). Presynaptic modulation of acetylcholine release from cardiac parasympathetic neurons. *Am. J. Physiol.* **248**, H33-H39.

Wetzel, G. T., Goldstein, D., and Brown, J. H. (1985b). Acetylcholine release from rat atria can be regulated through an $_1$-adrenergic receptor. *Circ. Res.* **56**, 763-766.

Wood, J. and Garthwaite, J. (1994). Models of the diffusional spread of nitric oxide: implications for neural nitric oxide signalling and its pharmacological properties. *Neuropharmacol.* **33**, 1235-1244.

Wood, J. D. (1981). Intrinsic neural control of intestinal motility. *Annu. Rev. Physiol.* **43**, 33-51.

Wood, J. D. (1994). Application of classification schemes to the enteric nervous system. *J. Auton. Nerv. Syst.* **48**, 17-19.

Wurster, R. D., Xi, X., Webber, M., and Randall, W. C. (1990). Morphological organization of ganglion cells and small intensely fluorescent (SIF) cells of the canine intracardiac ganglia. *Neurosci. Abstr.* **16**, 860. (Abstract)

Xi, M. C., Woody, C. D., and Gruen, E. (1994). Identification of short latency auditory responsive neurons in the cat dentate nucleus. *Neuroreport.* **5**, 1567-1570.

Xi, X., Randall, W. C., and Wurster, R. D. (1991a). Morphology of intracellularly labeled canine intracardiac ganglion cells. *J. Comp. Neurol.* **313**, 1-7.

Xi, X., Randall, W. C., and Wurster, R. D. (1991b). Intracellular recording of spontaneous activity of canine intracardiac ganglion cells. *Neurosci. Lett.* **128**, 129-132.

Xi, X., Randall, W. C., and Wurster, R. D. (1990). Excitatory and inhibitory synaptic transmissions on canine intracardiac ganglion cells. *Neurosci. Abstr.* **16**, 675. (Abstract)

Xi, X., Randall, W. C., and Wurster, R. D. (1994). Electrophysiological properties of canine cardiac ganglion cell types. *J. Auton. Nerv. Syst.* **47**, 69-74.

Xi, X., Thomas, J. X., Jr., Randall, W. C., and Wurster, R. D. (1991c). Intracellular recordings from canine intracardiac ganglion cells. *J. Auton. Nerv. Syst.* **32**, 177-182.

Xu, Z. -J. and Adams, D. J. (1993). Adrenergic modulation of ionic currents in cultured parasympathetic neurons from rat intracardiac ganglia. *J. Neurophysiol.* **69**, 1060-1070.

Yasunaga, K. and Nosaka, S. (1979). Cardiac sympathetic nerves in rats: anatomical and functional features. *Jpn. J. Physiol.* **29**, 691-705.

Yuan, B. -X., Ardell, J. L., Hopkins, D. A., Losier, A. M., and Armour, J. A. (1994). Gross and microscopic anatomy of the canine intrinsic cardiac nervous system. *Anat. Rec.* **239**, 75-87.

Zar, J. H. (1984). "Biostatistical Analysis", 2nd edn. Prentice-Hall, Englewood Cliffs, N.J..

Author's Index